AN ABSTRACT OF THE THESIS OF

William Wiley Evans IV for the degree of Master of Science in Oceanography

presented on June 23, 2006.

Title: Impact of Tropical Instability Waves on Nutrient and Chlorophyll Distributions in the Equatorial Pacific

Abstract approved:

_____

Peter G. Strutton

Tropical instability waves (TIWs) are prominent seasonal features in both the equatorial Pacific and Atlantic Oceans. This work quantifies their role in modulating the distributions of nutrients and phytoplankton biomass. Using an eight year record of biannual ship observations along the Tropical Atmosphere Ocean (TAO) buoy array, cruise sections crossing TIWs were identified. Both a case study approach of individual TIWs and a first attempt at calculating their average effect on mixed layer properties were performed.

Examination of individual TIWs demonstrates that their effect on nutrient and chlorophyll distributions is a function of the TIW intensity. Both strong and weak TIWs drive elevated nutrient concentrations directly on the equator, but strong TIWs possess enhanced recirculation which advects nutrient- and chlorophyll-poor waters from adjacent to the upwelling zone equatorward. This

decreases nutrient concentrations from approximately 2°N to 8°N. Weak TIWs retain elevated nutrient concentrations in this latitudinal band due to less recirculation in TIW vortices, permitting chlorophyll increases.

These differences between strong and weak TIWs were only observed north of the equator. Less recirculation was observed in TIW vortices south of the equator. This resulted in nutrient enhancements from TIWs along the southern portions of the cruise sections, especially in the eastern Pacific. The differences between northern and southern TIW dynamics suggest strong differences in TIW modulated carbon cycling between the two hemispheres.

Seasonal modification of the equatorial currents also influences the extent to which TIWs alter nutrient and chlorophyll distributions. TIWs observed during boreal winter demonstrated enhanced nutrient and chlorophyll concentrations north of the equator. This resulted from the water mass north of the upwelling zone containing elevated nutrient and chlorophyll concentrations due to a shallow thermocline. Thermocline shoaling in boreal winter is the result of a slowing in the South Equatorial Current and North Equatorial Countercurrent caused by the seasonal decrease in westward trade wind velocities. These results suggest that there is a synergistic effect from TIWs and the seasonal shoaling of the thermocline which may be important for carbon cycling north of the equator.

Composites of average mixed layer nutrient concentrations show TIW-induced nutrient enhancement on and south of the equator along most of the TAO lines, but no subsequent increase in mixed layer chlorophyll. This is likely due to the lag time between nutrient enhancement and biomass increase and/or

chlorophyll increases in unsampled portions of the vortex. Regions of elevated chlorophyll concentrations were observed in SeaWiFS composites in unsampled portions of TIWs, which suggests that TIW induced lateral transport of nutrients may be driving important episodic export events south of the equator.

Impact of Tropical Instability Waves on Nutrient and Chlorophyll Distributions in the Equatorial Pacific

by
William Wiley Evans IV

A THESIS

submitted to

Oregon State University

in partial fulfillment of
the requirements for the
degree of

Master of Science

Presented June 23, 2006
Commencement June 2007

Master of Science thesis of William Wiley Evans IV
presented on June 23, 2006.

APPROVED:

Major Professor, representing Oceanography

Dean of the College of Oceanic and Atmospheric Sciences

Dean of the Graduate School

I understand that my thesis will become part of the permanent collection of Oregon State University libraries. My signature below authorizes release of my thesis to any reader upon request.

William Wiley Evans IV, Author

ACKNOWLEDGEMENTS

I extend my sincere thanks to Pete for giving me this opportunity and supporting a large part of my work on tropical instability waves in the equatorial Pacific. He has been an outstanding advisor, mentor and friend. He has challenged my understanding on every level; from the seemingly simple process of acquiring data, to data management and processing, to the use of data in addressing questions about the ocean. Thank you so much Pete and I look forward to continuing to work with you in the future.

I thank my thesis committee: Pat Wheeler, Murray Levine and George Boehlert. Conversations with all of them tremendously improved the quality of this thesis. I would particularly like to thank Pat for all her thorough comments on my writing. I feel like my writing ability has progressed greatly in constructing this thesis.

My wife was a central component in enabling the completion of this thesis. Her love, devotion, tolerance, understanding and level headedness is the rudder of my life; keeping me on course with the wind on my back. Clear skies and fair winds for you and me Maya, always.

Lastly, I thank my parents and particularly my father. The rocky road I traveled before landing in the field of oceanography left many doubts in their minds. Thank you both for your patience and love.

This work was supported by NASA Headquarters under the Earth System Science Fellowship Grant NNG05GQ34H.

TABLE OF CONTENTS

TABLE OF CONTENTS (CONTINUED)

LIST OF FIGURES

LIST OF FIGURES (CONTINUED)

LIST OF FIGURES (CONTINUED)

LIST OF FIGURES (CONTINUED)

LIST OF APPENDIX FIGURES

LIST OF APPENDIX FIGURES (CONTINUED)

LIST OF APPENDIX FIGURES (CONTINUED)

LIST OF APPENDIX FIGURES (CONTINUED)

LIST OF APPENDIX FIGURES (CONTINUED)

LIST OF APPENDIX FIGURES (CONTINUED)

LIST OF APPENDIX FIGURES (CONTINUED)

Impact of Tropical Instability Waves on Nutrient and Chlorophyll Distributions in the Equatorial Pacific

1 Introduction

The equatorial oceans are of significant scientific interest because they are centers of intense coupling between the ocean and atmosphere. This is particularly true for the equatorial Pacific, because changes in this region impact global climate through atmospheric teleconnections (Bjerknes, 1969). Certain intra-annual scales of physical variability are fairly predictable in space and time, making this region an excellent candidate for studying the chemical and biological responses to these physical alterations. Processes at these timescales may dominate the variability in the export flux of organic carbon (Dunne *et al*., 2000) so it is important to understand how the factors driving organic carbon export change in accordance with the physical variability. This work will address the impacts of physical variability due to tropical instability waves (TIWs) on the temporal and spatial distributions of nutrients and chlorophyll.

1.1 Oceanography of the equatorial Pacific

The equatorial Pacific current system consists of a series of zonal currents which are largely forced by the trade winds that blow from the northeast in the northern hemisphere and the southeast in the southern hemisphere (Philander, 1990). The southeast trade winds cross the equator and travel as far as 10°N, where they converge with the northeast trade winds in a region known to mariners as the Doldrums. Here the surface winds are light and most of the flow

in the atmosphere is directed upward which generates a region of persistent cloud cover known as the Intertropical Convergence Zone (ITCZ).

In each hemisphere the trade winds are always stronger during fall and winter months. This seasonal cycling drives the migration of the ITCZ north in the boreal summer and south in the boreal winter. The waxing and waning in the strength of the trade winds also drives seasonal variability in the strength of the zonal currents (Philander, 1990).

The wind-driven zonal currents (the North Equatorial Current (NEC) and the South Equatorial Current (SEC)) are westward flowing and are the equatorward branches of the subtropical gyres. These currents tend to elevate sea surface height in the western portion of the basin, known as the western warm pool, causing a zonal pressure gradient to exist between the western and eastern portions of the basin. This zonal pressure gradient is the driving force for the eastward flowing Equatorial Undercurrent (EUC) (Tomczak and Godfrey, 2003).

The NEC is centered at approximately 15°N with a typical velocity of 0.3 m s^{-1} (Tomczak and Godfrey, 2003). The SEC straddles the equator with the core of its northern limb at 2°N and the core of its southern limb at 4°S (Johnson *et al.*, 2001). Both currents are seasonally modified by changes in the speed of the trade winds, with each flowing strongest during their respective hemisphere's winter. A typical velocity for the SEC is on the order of 0.6 m s^{-1}, with the southern limb being significantly slower (Tomczak and Godfrey, 2003).

The eastward flowing currents are situated where either the Coriolis force or wind stress is minimized. The curl of the wind stress over the Pacific drives the NECC (Munk, 1950), which is positioned in the region of atmospheric convergence described earlier as the Doldrums. In this area wind stress is at a minimum and NECC's typical velocities are near 0.4 m s^{-1} (Tomczak and Godfrey, 2003). On the equator the Coriolis force is zero, so the EUC travels down the pressure gradient applied by the sea level difference across the basin. The EUC flows at depth, away from the influence of wind stress, with a typical eastward velocity of 1.5 m s^{-1} (Tomczak and Godfrey, 2003). The core of the EUC is near 200 m in the western portion of the Pacific basin and rises to 40 m or shallower in the east.

A South Equatorial Countercurrent (SECC) has been observed in the southern hemisphere (Wyrtki and Kilonsky, 1984) although it appears highly variable and is not resolved in calculations of integrated transport (Kessler and Taft, 1987). It is not clear whether the SECC consists of one or many cores (Kessler and Taft, 1987) or how far east it extends (Eldin, 1983). There is evidence for a convergent boundary existing in the shear zone between the SECC and the SEC near the dateline (Eldin and Rodier, 2003), but the strength of convergence is clearly less than that occurring along the basin in the northern hemisphere between the NECC and the SEC.

The winds that force the zonal currents also drive a net Ekman flow of water poleward, causing a divergence of surface water at the equator, and upwelling of cooler, nutrient rich, high CO_2 waters from below. This is called the

equatorial cold tongue (Wyrtki, 1981) and can extend from the coast of South America across the International Dateline - one quarter of the earth's equatorial circumference.

Vertical velocities associated with the region of upwelling on the equator are significantly smaller than the horizontal velocities in the region. Direct measurement of *w* is very difficult and most estimates are derived from vertically integrating the continuity equation to a depth below the EUC core (Weisberg and Qiao, 2000; Johnson *et al.*, 2001; Halpern *et al.* 1989) or from calculating Ekman divergence in meridional volume transports (Wyrtki, 1981). The estimates provided by these methods range from approximately 0.3 to 2 m d^{-1}.

In the northern hemisphere cooler upwelled water is advected poleward by Ekman dynamics where it converges with warmer water and subducts to join the main thermocline waters. Due to the east-west tilt of the thermocline near the equator, the flow in the thermocline is in geostrophic balance and is directed equatorward. This flow then joins the water upwelled to the surface near the EUC core. Through this process, a meridional overturning cell is established within the upper 100 meters in the northern hemisphere between 10°N and the equator (Wyrtki and Kilonsky, 1984; Johnson and McPhaden, 1999).

Equatorward flow in the thermocline is also present in the southern hemisphere, though a region of convergence in the surface waters is less clearly defined, so the presence of a recirculating cell is not apparent. Some work suggests that there is stronger poleward flow in the surface layer in the northern hemisphere with stronger equatorward flow in the thermocline south of the

equator (Johnson *et al.*, 2001). As has been suggested, this imbalance in meridional circulation likely provides some connectivity between the thermocline waters in both hemispheres. It also suggests that perhaps a majority of the macronutrients supplied to the surface from Ekman divergence at the equator are derived from the thermocline waters of the southern hemisphere.

Due to upwelling, the equatorial Pacific is a distinct region where biological rates are elevated relative to the adjacent oligotrophic subtropical gyres. Changes to the physical environment described above alter these rates. The timescales of physical variability vary from diurnal to interannual (El Niño Southern Oscillation; ENSO) and interdecadal (Pacific Decadal Oscillation; PDO). In order to quantify the global significance of carbon fluxes in the equatorial Pacific, we must develop a strong understanding of the biological responses to physical forcing on all timescales. This work addresses the effects of physical variability due to TIWs on nutrient and phytoplankton distributions in the equatorial Pacific.

1.2 Biogeochemical significance of the equatorial Pacific

The tropical Pacific Ocean plays a key role in global carbon cycling. The tongue of cool upwelled water spans approximately one quarter of the earth's circumference (Wyrtki, 1981). This upwelled water has a higher partial pressure of CO_2 compared to the air above it, and so CO_2 outgases to the atmosphere at a rate of ~10^{15} gC yr^{-1} (Feely *et al.*, 1999). Consequently, this region represents the dominant oceanic source of carbon dioxide to the atmosphere.

Upwelling also supplies the surface ocean with macronutrients (nitrate, silicic acid and phosphate), but chlorophyll and primary production remain low due to a combination of iron limitation and grazing control (Landry *et al*., 1997) as well as possible silicon limitation of diatoms (Dugdale *et al*., 1995). This condition of a low standing stock of phytoplankton biomass even in the presence of excess nutrients characterizes the region as a high-nutrient-low-chlorophyll (HNLC) area. Despite this relatively low productivity, the equatorial Pacific may account for approximately ~21 % of global new production due to the vastness of the region (Chavez and Toggweiler, 1995).

The US Joint Global Ocean Flux Study in the equatorial Pacific (JGOFS-EqPac) set out to gain an understanding of how physical processes controlled the flux of carbon and related elements between the atmosphere, the surface ocean and the deep ocean in this HNLC region. Survey and time series cruises were conducted during a boreal spring El Niño period and a boreal fall non-El Niño period. Results showed that the region experiences strong temporal variability between El Niño and La Niña conditions in the magnitude of primary productivity and phytoplankton biomass (Barber *et al.,* 1996), phytoplankton growth rates and microzooplankton grazing (Landry *et al.,* 1995), mesozooplankton grazing (Dam *et al.*, 1995), particulate organic carbon export (Murray *et al.*, 1996) and air-sea CO_2 flux (Feely *et al.*, 1995). TIWs also emerged as a dominant source of physical, chemical and biological variability in the region (Foley *et al*., 1997; Barber *et al.,* 1996).

1.3 Tropical instability waves

1.3.1 The physics

TIWs become fully developed when the trade winds in the equatorial regions are at their maximum, which begins around May in the Atlantic and spans only a few months. In the Pacific Ocean the season of high TIW activity is substantially longer, beginning by approximately June and lasting as late as the following March. Seasonally amplified trade winds strengthen the currents on, and adjacent to, the equator, which generates strong zonal shear between the eastward flowing NECC and EUC, and the opposing westward flowing SEC (Philander, 1990). This current shear develops instabilities which spawn trains of anticyclonic vortices (Kennan and Flament, 2000) that are present on both sides of the equator and propagate westward with phase speeds of ~50 km d^{-1} (Qiao and Weisberg, 1995). Without the trade winds driving the enhancement of the equatorial currents, TIW activity is minimized, so they are weak or absent during El Niño.

TIW vortices induce strong meridional velocity perturbations, as well as undulations in the sea surface temperature (SST) and chlorophyll fronts. Perturbations in meridional velocity are almost fifty percent larger in the northern hemisphere (Chelton *et al*., 2000). The period, zonal wavelength and meridional amplitude of these features, as observed from both acoustic Doppler current profilers (Qiao and Weisberg, 1995) and satellite tracked drifters (Flament *et al*., 1996), are on the order of ~30 days, ~1500 km and ~500 km, respectively.

Recent work by Chelton *et al.* (2001) describes significant differences between northern and southern hemisphere TIW phase speeds. Northern TIWs are approximately 50 percent faster than southern TIWs, though southern TIWs show an increased phase speed in the later part of the year. Differences in circulation also exist in the south. Inspection of SST spatial patterns suggests the presence of both anticyclonic and cyclonic circulations in the southern TIWs (Legeckis *et al.,* 2004).

An order of magnitude increase in the normal rate of equatorial upwelling has been documented within TIWs (Weisberg and Qiao, 2000; Kennan and Flament, 2000). Evidence also exists in the northern hemisphere for enhanced subduction of freshly upwelled cool surface water along convergent boundaries with warmer water north of the equator (Yoder et al., 1994; Flament et al., 1996). Consequently, areas of enhanced upwelling and downwelling are spatially segregated within individual TIW vortices (Kennan and Flament, 2000), as illustrated schematically in figure 1.

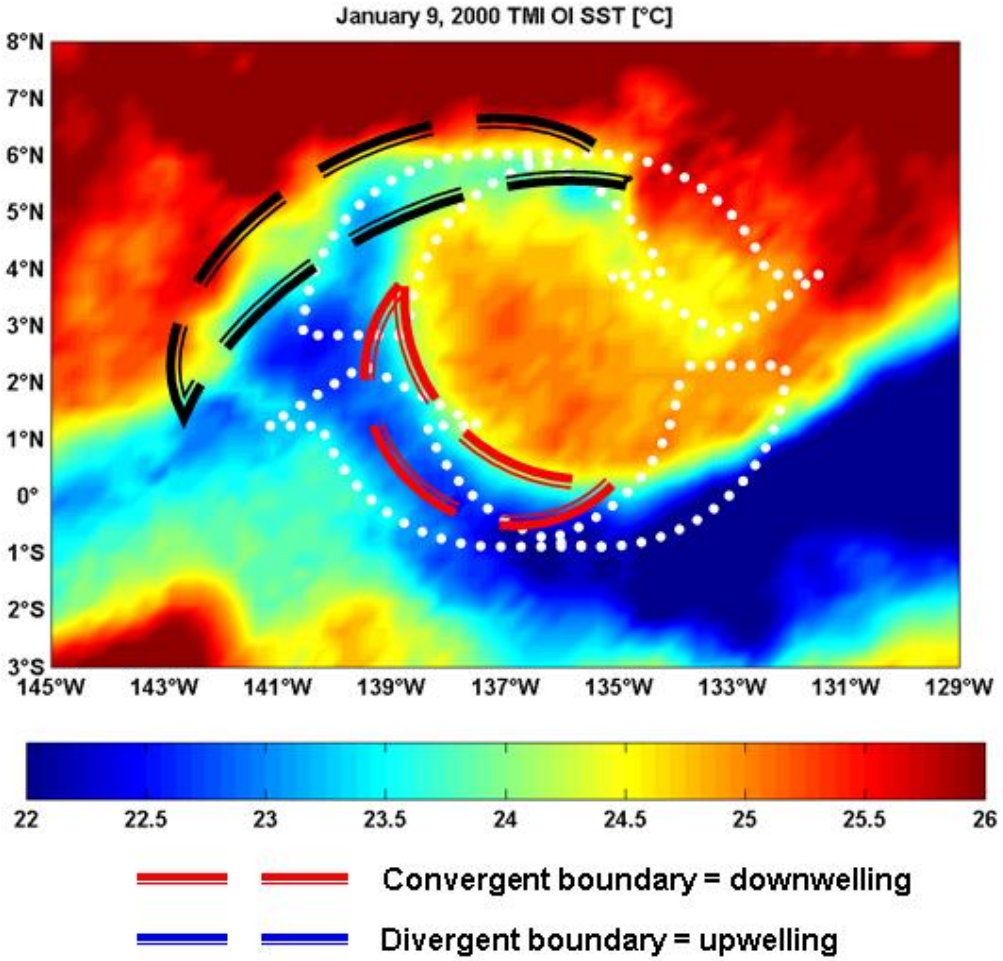

Figure 1: A TIW indicated by microwave sea surface temperature (°C) from January 9th 2000. Areas of enhanced downwelling along convergent boundaries are encircled in black dashes while areas of enhanced upwelling along divergent boundaries are encircled in red dashes. The TIW vortex is imbedded in the cusp of the SST front, represented by white dotted arrows (after figs. 14a and 15 in Kennan and Flament, 2000).

1.3.2 Biogeochemical significance of TIWs

Stimulation of primary production by mesoscale eddies has been identified as a critically important phenomenon in other ecosystems such as the Sargasso Sea (McGillicuddy *et al.,* 1998). TIWs in the tropical Pacific and Atlantic Oceans could be considered analogs of these features and are somewhat predictable in space and time, making them an ideal candidate for studying the effects of

transient features on oceanic carbon cycling. TIWs produce strong anomalies in sea-surface temperature and chlorophyll concentrations through their dramatic impact on upper ocean circulation (Yoder et al., 1994; Chelton et al., 2000; Strutton et al., 2001). Their persistence, particularly in the Pacific where these signals are the strongest, has stimulated interest in their role in shaping both surface ocean ecology and chemical processes related to carbon cycling.

Documented TIW effects on surface ocean biology include the concentration and subduction of parcels of high chlorophyll water (Yoder et al., 1994; Archer et al,. 1997; Strutton et al., 2001) and enhanced zooplankton and micronekton populations in association with TIW vortices (Flament et al., 1996; Menkes et al., 2002). Some work during the JGOFS-EqPac program showed an increase in nutrients near the equator from TIW-enhanced upwelling; with an increase in primary production analogous to an iron addition experiment (see figs.12 and 13 in Barber *et al.*, 1996). Therefore, enhanced vertical advection from TIW activity is perhaps important in modulating processes associated with carbon cycling.

In contrast to the conclusions presented by Barber *et al*. (1996), a study in October-November of 1996 that focused on the western extension of the equatorial cold tongue documented relative decreases in nutrients at the equator caused by TIWs (Eldin and Rodier, 2003). This study illustrated that there are both ‘enrichment and impoverishment’ phases of TIW vortices, but it was not clear how the alternating nutrient phases impacted the food web structure of the region.

The perspective of TIWs as ‘natural iron addition experiments’ (Barber *et al.*, 1996) from the JGOFS era has further been brought into question through a modeling study conducted by Gorgues *et al*. (2005). In this work it was determined that the TIW-enhanced horizontal advection was a principle factor in reducing iron concentrations on the equator by 10%. The reduced iron concentrations resulted in decreases in chlorophyll concentrations (10%) and new production (10%).

Given that TIWs are persistent and potentially important features of the equatorial Pacific and Atlantic oceans, it is important to develop our understanding of their effects on the processes that control the production and fate of organic carbon. TIWs have been identified as a primary modulator in determining the variability in carbon export fluxes (Dunne *et al.,* 2000), primary production and nutrient fluxes (Murray *et al*., 1994). However, Gorgues *et al.* (2005) suggested that TIWs may have an adverse effect on phytoplankton biomass and new production. It is important to resolve these contradictory views as a proper understanding of the role of TIWs directly impacts our ability to model the biogeochemical processes shaped by these features.

The equatorial Pacific represents the ideal setting to address this issue as the Tropical Atmosphere Ocean (TAO) mooring array has been in place for more than a decade (McPhaden *et al.,* 1998) with cruises consistently servicing each mooring line twice per year. This provides an excellent opportunity to employ a retrospective analysis of TIW impacts on the distributions of nutrients and phytoplankton biomass in the Pacific.

1.4 Research objectives

The central goal of this research was to investigate the impact of TIWs on the processes governing carbon cycling in the equatorial Pacific; namely changes in the distributions of nutrients and chlorophyll (chlorophyll *a*; as a proxy for phytoplankton biomass). This investigation was conducted by analysis of hydrographic, chemical and biological property distributions from TAO maintenance cruises that transited through TIWs. This project encompassed a retrospective analysis of TIW seasons from 1998 to 2004 and addressed three central research questions:

(1) How much do nutrient concentrations change in response to TIWs?

(2) How do TIWs impact the level of phytoplankton biomass through the alteration of the surface nutrient fields?

(3) How does the impact on nutrients and chlorophyll change as a function of latitude and longitude?

1.5 Overview of the results and significance

In contrast to the JGOFS view of TIWs as natural iron fertilizers (Barber *et al.,* 1996), it appears that strong TIWs reduce nutrient and chlorophyll concentrations in the region between 8°N and 8°S. This is the result of nutrient- and chlorophyll-poor waters being advected toward the equator in the recirculating flow of a TIW vortex. This effect is not as apparent in weak TIWs

that contain elevated nutrient concentrations which permits chlorophyll to increase before subduction to the north.

There is a substantial difference in the impact from northern and southern hemisphere TIWs. South of the equator the recirculating flow of a TIW vortex is less pronounced. This facilitates nutrient enhancement, though there were few observations of corresponding chlorophyll increases above climatological concentrations. This is likely due to the lag time between nutrient addition and chlorophyll increase; or the nutrient enhancement could have lead to chlorophyll increases in unsampled portions of the vortex. The nutrient enhancements observed during this study are most likely responsible for the reported observations of phytoplankton blooms in the frontal waters east of the Marquesas Islands (Legeckis *et al*., 2004) as well as the apparent increase in SeaWiFS climatological monthly chlorophyll south of the equator during boreal fall (fig. 43; top panel).

This apparent difference in the circulation of a TIW vortex between the northern and southern hemispheres may result in substantial differences in the processes governing carbon cycling on the two hemispheres. Archer *et al*. (1997) discussed the possibility of a ‘leak’ in the biological pump in the northern hemisphere associated with a TIW wave front, whereby upwelled nutrients are subducted at the convergent boundary of the wave front before they are consumed. South of the equator there is little evidence of convergence east of the dateline since flow in the SECC is low and variable (Eldin, 1983; Kessler and Taft, 1987), so possibly no ‘leak’ of nutrients occurs there.

In combination with the varying effect on nutrient and chlorophyll distributions from TIW intensity is the seasonal modulation of the thermocline. Reduced SEC and NECC velocities near the end of the TIW season shoal the trough in the thermocline near 5°N (Kessler and Taft, 1987; fig. 2). This shoaling of the thermocline trough below the SEC/NECC convergence zone is likely a major factor determining the levels of nutrients available to the phytoplankton in the region between the equator and 10°N. TIWs identified during boreal winter contained greater quantities of nutrients and chlorophyll over larger portions of the water column, even though they appeared less intense than boreal fall TIWs.

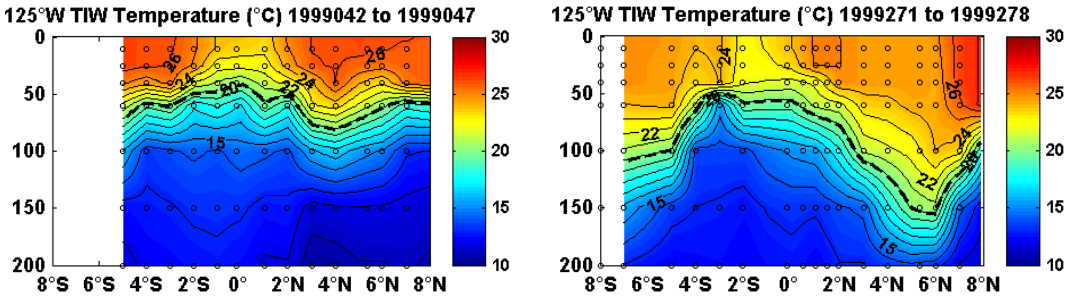

Figure 2: Latitude/depth temperature (°C) sections from the 125°W TAO line from February 1999 (left panel) and September 1999 (right panel). The thermocline is represented by the 20°C isotherm which is highlighted as a black dashed line. The difference in the thermocline depth near ~5°N between the two seasons is the result of seasonal variation in the SEC and NECC current velocities (Kessler and Taft, 1987).

TIW composites for the TAO lines demonstrate nutrient enhancement on and south of the equator, with averages from 8°S to 8°N showing nutrient enhancement present along the entire basin, while chlorophyll concentrations remain below climatological values. Recent modeling efforts (Gorgues *et al*., 2005; Shi *et al*., 2006) identify the importance of enhanced meridional advection on carbon cycling north of the equator, but the analysis presented here describes evidence for the importance of the southern hemisphere where the reduced

convergence of water masses may enhance the utilization of nutrients supplied by TIW-enhanced upwelling and horizontal advection.

This thesis helps to reconcile the differences in results from recent modeling studies (Gorgues *et al*., 2005) and past field programs (Barber *et al*., 1996), and illustrates significant differences between strong and weak TIWs. Both strong and weak TIWs show evidence of nutrient enhancement from enhanced upwelling right on the equator, but strong TIWs possess enhanced horizontal recirculation which advects nutrient and chlorophyll poor waters toward the equator from the adjacent surface waters. This decreases nutrient concentrations and reduces the levels of phytoplankton biomass. Southern TIWs are different and have generated interesting questions that point to the significance of episodic nutrient additions in the southern hemisphere.

2 Methods

2.1 TAO cruise observations

Chlorophyll, temperature, salinity and nutrients (phosphate, silicic acid, nitrate and nitrite) have been sampled on Tropical Atmosphere Ocean (TAO; McPhaden *et al.*, 1998) mooring array maintenance cruises since 1997. The spatial and temporal coverage of these observations is excellent, including 300 stations and two complete basin-crossings per year. These cruise observations were used to establish both climatological means for chlorophyll and nutrients, and mean mixed layer composites from cruise sections that had been identified as crossing a TIW. Note that the term 'composite' is used for the mean from multiple cruises through TIWs, while the term 'climatology' is used for the mean of multiple cruises indicative of neutral ENSO conditions. The cruise observations were also used to compare individual TIW cruise sections in order to understand the role of vortex intensity in shaping the biological and chemical fields.

The cruises occupied the TAO mooring lines along 95°W, 110°W, 125°W, 140°W, 155°W, 170°W, 180°W and 165°E. Figure 3 shows the positions of all stations in the database of TAO cruises. Samples were taken at every degree of latitude from 8°N to 8°S, except between 3°N and 3°S where samples were taken every half degree. Water was drawn from Niskin bottles on a rosette from depths of ~5, 10, 25, 40, 60, 100, 150 and 200 meters. Chlorophyll concentrations were determined at sea using the fluorometric method (Holm-Hansen *et al*., 1965) with a Turner Designs 10-AU field fluorometer. Samples (500 mL) were collected from each depth and filtered through 0.7 μm Whatman

GFF glass fiber filters at a vacuum pressure of <20 kPa. Filters were then placed in 10 mL of 90% acetone and stored at -20°C for 24 to 72 h to allow the pigment to be extracted by the solvent. Nutrient samples were frozen and sent to the Monterey Bay Aquarium Research Institute (MBARI) to be analyzed on an Alpkem Rapid Flow Analyzer (Sakamoto *et al*., 1990). Temperature and salinity profiles were collected by the conductivity temperature depth (CTD) package. Post-cruise processing was performed by Kristene McTaggart and Greg Johnson at NOAA's Pacific Marine Environmental Laboratory (PMEL), Seattle. Mixed layer depths were calculated from the CTD temperature profiles as the depth on the profile where temperatures were 0.5°C less than the surface temperature (Levitus, 1982). Ship-based ADCP data, processed and provided by Eric Firing and Jules Hummon at the University of Hawaii, were also obtained for comparison of velocities along particular TIW cruise sections.

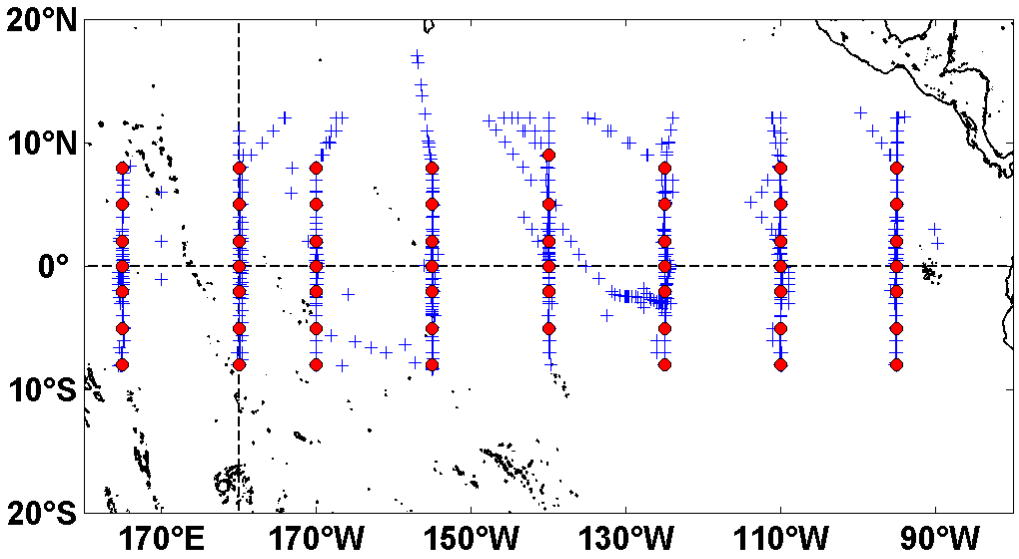

Figure 3: Station locations of TAO cruise observations from 1997-2004. Stations follow each TAO line with approximately 1° spacing. Mooring positions are depicted as red circles; cruise stations as blue plus symbols.

2.2 TAO cruise climatology

The climatological nutrient (silicic acid, phosphate and nitrate), chlorophyll, temperature and salinity distributions were calculated for each TAO mooring line. The cruise data included stations conducted after January 1998 using the following scheme to remove periods of intense ENSO variability.

The Multivariate El Niño Southern Oscillation Index (MEI; Wolter and Timlin, 1999) calculates the ENSO phase by incorporating sea level pressure, zonal and meridional wind, sea surface temperature, surface air temperature and total cloudiness. This robust estimator of ENSO phase takes into account the coupled ocean-atmosphere system, in contrast to the historically used Southern Oscillation Index, which relies wholly on the atmospheric component of the ENSO phenomenon. By definition the MEI has a mean of 0 and a standard deviation of 1. Positive MEI values indicate El Niño conditions while negative values indicate La Niña conditions.

Using this index, months of ship-board observations from time periods when the MEI exceeded ±0.5 were excluded. This exclusion was necessary as the relatively short observational record contained both strong El Niño and La Niña periods. Excluding these periods minimized biases in the calculation of the climatological distributions of nutrients and chlorophyll. Figure 4 depicts the months of data used in calculating the climatology for each TAO line.

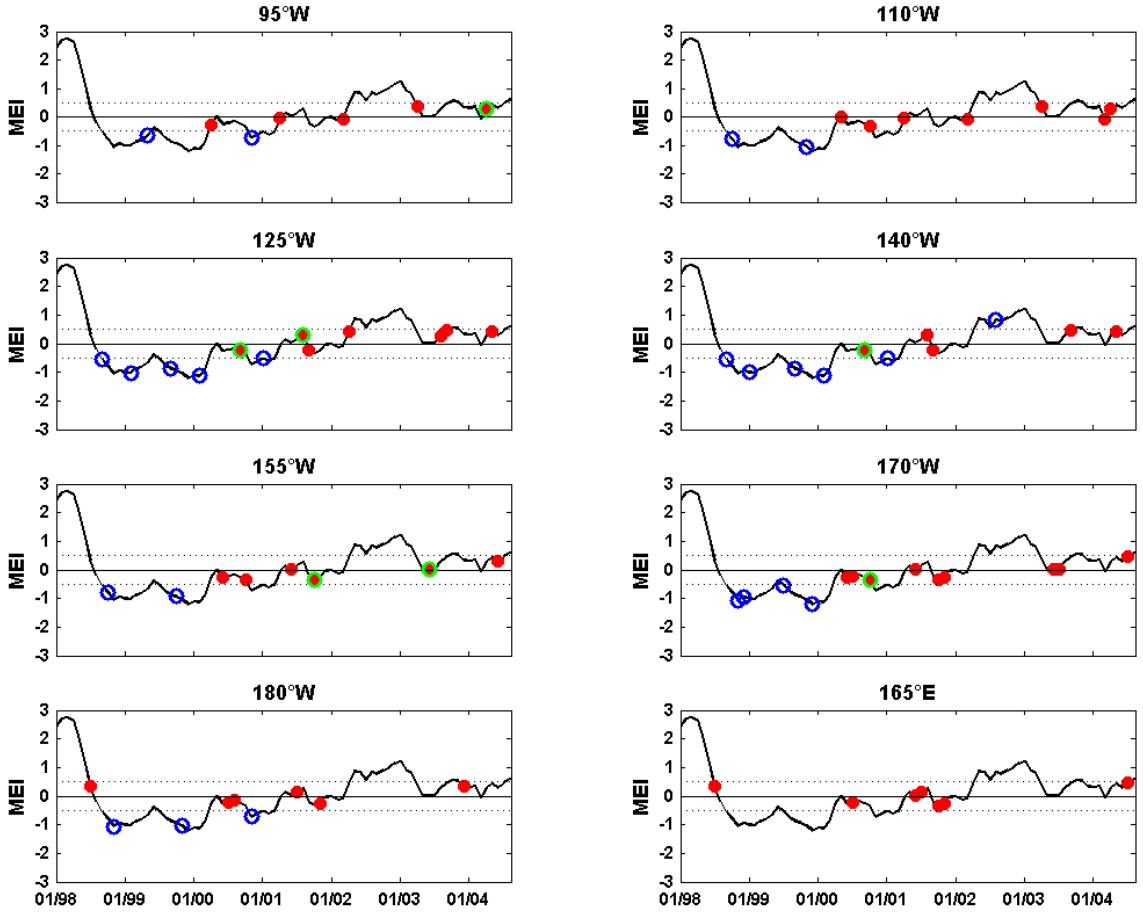

Figure 4: Red filled circles indicate the months used in the climatology calculation for each TAO line. Blue open circles are months where TIWs were crossed by cruises along each TAO line (discussed in section 2.4). Dashed line represents MEI = 0.5. Seven cruises in the climatology crossed TIWs, and are represented as the red filled circles with a green edge.

The reason for depicting the months of data rather than the number of cruises for each TAO line is because cruises may transcend a single month. Since the MEI is a value representative of an entire month, it is important to illustrate that a single cruise could possess two MEI values. Figure 5 illustrates the number of individual stations for each TAO line climatology that were sampled during weak El Niño (0<MEI<=0.5) or weak La Niña (-0.5<=MEI<0) conditions, with the average for each TAO line shown in the upper right corner of the figure. For most TAO lines this strategy leaves approximately equal numbers

of stations for either period, although the 125°W line shows a slight bias toward El Niño conditions.

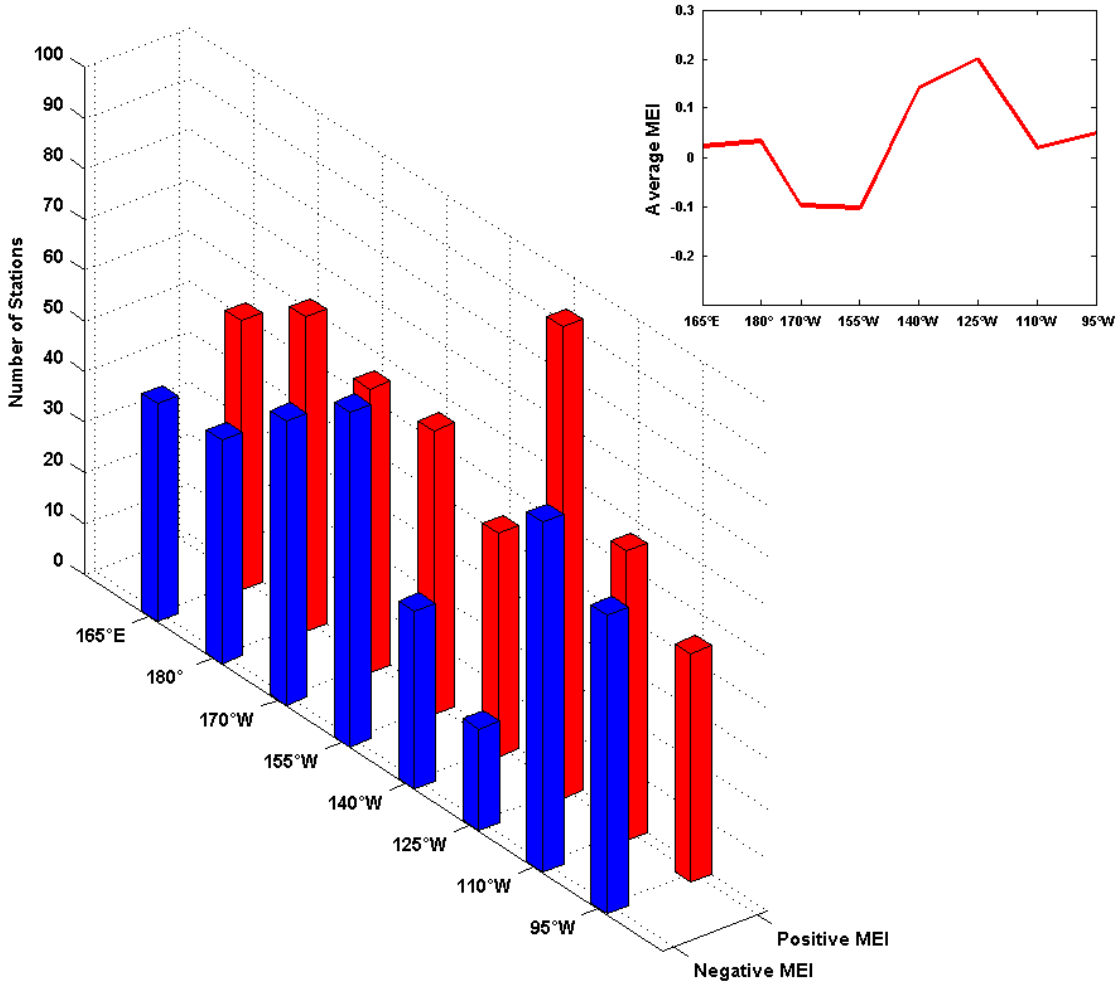

Figure 5: The MEI properties of stations used in calculating climatologies for each TAO line. The red columns are stations which reside on the positive side of the MEI curve (weak El Niño conditions). The blue columns are stations which reside on the negative side of the MEI curve (weak La Niña conditions). The line graph in the upper corner shows the mean MEI for stations used in the climatology.

Individual cruises along each line were identified and sections were produced using linear interpolation to grid data onto 0.1° latitude by 1 m depth grids from 8°S to 8°N, from the surface to 200 m. The grids were then stacked into a three dimensional array and an average grid was computed representing

the climatological mean for all the cruise sections from January 1998 to August 2004.

Quality control by visual inspection was necessary to remove occasional bad data. Silicic acid and nitrate concentrations greater than 40 mmol m^{-3}, chlorophyll concentrations in excess of 2 mg m^{-3} and any negative nutrient or chlorophyll concentrations were discarded. A total of 11 cruise sections were identified as containing aberrant data using these criteria.

A general comparison was conducted with the Levitus94 nitrate climatology (also known as the World Ocean Atlas 1994; http://ingrid.ldeo.columbia.edu/SOURCES/.LEVITUS94) to determine differences between the TAO climatologies and other available climatological data. TAO line climatological nitrate agreed well with Levitus94 nitrate with the exception of more spatial details in the TAO nutricline topography associated patterns of convergence and divergence in the zonal currents.

2.3 TMI/SST

Three microwave optimal interpolation (OI) products are supplied by Remote Sensing Systems (www.remss.com) at daily 0.25° resolution with either tropical or global coverage. The microwave OI SST product that is the primary tool for this study is derived from observations made principally by NASA's Tropical Rainfall Measuring Mission (TRMM) satellite. The microwave imager (TMI) onboard is fairly accurate (+/- 0.5 °C; Wentz 1998, reported in Chelton *et al.*, 2001) and has the capability to collect SST measurements through clouds.

TMI coverage spans approximately 40°N to 40°S and requires nearly 2 days for a complete view of the coverage area. The optimal interpolation (OI) scheme (Reynolds and Smith, 1994) produces daily images which span the entire coverage area. Daily TMI OI products are available from January 1998 to the present.

2.4 TIW cruise identification

Using all cruise data from October 1997 to August 2004, CTD stations from all the TAO cruises were plotted on their corresponding 3 day running mean TMI/SST field. For the first day of cruise stations, the TMI/SST data used was for this day and the two previous. The assumption applied here was that the SST field does not change significantly within a 3 day period. In this way cruise stations could be plotted with the changing SST field over the time taken to sample an entire line, which is approximately 7-9 days. This strategy allowed cruises to be identified that crossed TIW SST fronts. Cruises which crossed through the cusp-like undulation of a TIW SST frontal extension were considered as crossing a TIW. All TIW cruises where identified in this way, irrespective of hemisphere or intensity. Figure 6 depicts a cruise line which occurred in February 2000 along the 140°W TAO line that was identified crossing TIWs in both hemispheres using this strategy.

Cruises that crossed TIWs and were present in the TAO climatology were not included in the analysis of TIWs. That is, they were not used in calculating TIW composites, nor were they considered in the analysis that compared TIWs from different years and seasons. Seven cruises in the climatology crossed

TIWs. Figure 4 shows the months where TIWs were crossed by TAO cruises and the months of data used in constructing the TAO climatology. This slight contamination of the climatology by TIWs was a point of discussion through the writing of this thesis. It shows that TIWs are persistent and prevalent features of the equatorial Pacific and removing them from a climatology is very difficult. Future work will focus on resolving this issue.

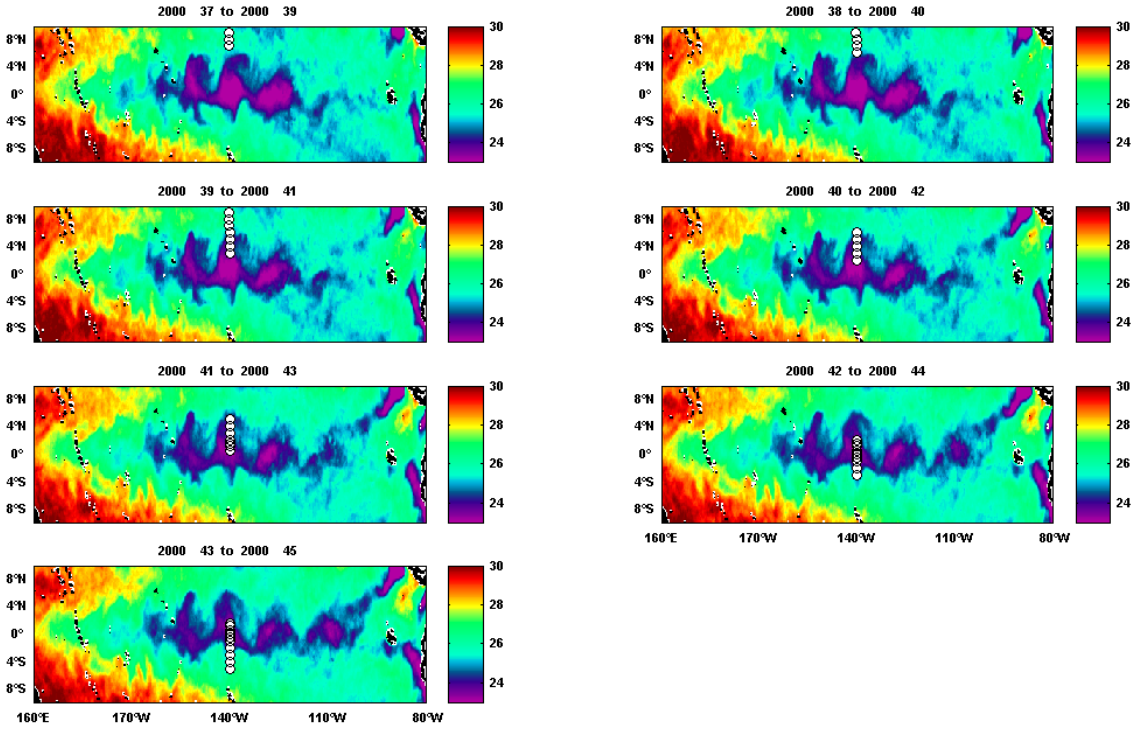

Figure 6: 3 day running mean of microwave SST (°C) for a TAO maintenance cruise along the 140°W line in February 2000. Stations for the corresponding 3 day periods are marked as white circles. This figure demonstrates a cruise which crossed an intense TIW SST front in the northern hemisphere and a weaker TIW SST front in the southern hemisphere. Date is presented as Julian day.

2.5 Auxiliary data

Cruise sections alone do not provide the spatial and temporal coverage to fully resolve the effect of TIWs on nutrient distributions and phytoplankton responses. It is important to employ observations made at numerous temporal

and spatial scales in order to provide the complete picture of TIW effects on the biology and chemistry of the region. This was the impetus for combining the satellite microwave SST and ship-based acoustic Doppler current profiler (ADCP) measurements with mooring observations of thermocline variability and chlorophyll measurements from the Sea-Viewing Wide Field-of-view Sensor (SeaWiFS). This method of combining techniques that cover differing spatial and temporal scales has proven to be powerful in resolving physical-biological coupling in the equatorial Pacific (Strutton and Chavez, 2004).

The depth of the 20°C isotherm is used as a proxy for the depth of the mid-thermocline (Kessler and Taft, 1987). This parameter was used to investigate the differences in thermocline topography between select TIW cruise periods. Thermocline data were obtained as 5 day average values from the TAO moorings along the 125°W, 140°W and 155°W lines from the TAO array website (http://www.pmel.noaa.gov/tao/disdel/disdel-v58.html) for the period from July 1998 to April 2001.

Daily SeaWiFS level 3 chlorophyll data were collected as standard mapped images with 9 km resolution from the NASA's Distributed Active Archive Center (DAAC; http://oceancolor.gsfc.nasa.gov/). The SeaWiFS chlorophyll was used in combination with the microwave SST data to examine the spatial relationship between SST and chlorophyll for select cruises that had been identified as crossing TIWs. A SeaWiFS chlorophyll animation was also constructed for the period from July 1999 to May 2000 to examine the seasonal effect of thermocline and zonal current variability. Lastly, monthly climatological SeaWiFS chlorophyll

data were downloaded from the DAAC level 3 browser to develop a better understanding of the effects of TIWs on the mean chlorophyll distributions along the equator.

2.6 TIW cruise and composite/climatology comparisons

Incorporating the ancillary data mentioned above, cruise comparisons were conducted for selected cruise sections along the 125°W, 140°W and 155°W TAO lines. Cruises were selected for comparison along each line based on either crossing TIWs during nearly the same month in different years, or in the same hemisphere during different seasons. This allowed differences in the effect from TIWs of varying intensity, as well as seasonal modification of the TIW impact on nutrient and chlorophyll distributions to be determined. A total of eight cruises were selected for comparison; two during boreal fall on the 155°W TAO line, two during boreal winter on the 140°W TAO line, and four during boreal fall and winter on the 125°W and 140°W TAO lines.

These comparisons incorporated microwave SST and SeaWiFS chlorophyll to gain a large scale perspective of the dynamics on the equator at the time of the cruise. The 20-50 m shipboard ADCP current velocities were averaged and plotted with their CTD station positions on the mean SST field for the cruise period (~8 d). Cruise comparisons of chlorophyll, nutrients, temperature and salinity anomalies coupled with 20°C isotherm depth from both the TAO moorings and the CTD profiles provided the framework for understanding the impacts of TIW vortex intensity and seasonal thermocline variability on chlorophyll and nutrient distributions.

All cruises identified as crossing TIWs for each TAO line were then compiled to create a composite of mean mixed layer (ML) nutrients and chlorophyll representative of the TIW impact on the upper water column. Nutrient and chlorophyll concentrations from the CTD stations were linearly interpolated to every meter from the surface to 200 m. The concentrations were then averaged over the mixed layer depth recorded for the CTD station based on the 0.5°C temperature criterion (Levitus, 1982). Average concentrations were then binned into 2.5° latitude boxes from 10°S to 10°N. It was assumed that the samples came from normal distributions with unknown and unequal variances. Average ML nutrients and chlorophyll from the CTD stations used for constructing the TAO climatology were produced in the same manner. The averages from the climatology and the TIW composite were then compared using two-tailed *t*-tests to determine latitudinal trends in TIW impacts along each TAO line. Lastly, the longitudinal trend in TIW impacts was examined by comparing mean ML nutrient and chlorophyll concentrations from all the CTD stations within 8.5° of latitude from the equator.

3 Results

3.1 TAO line climatologies

Climatological chlorophyll, temperature, salinity and nutrient latitude/depth sections are presented for each line from 95°W to 165°E and for an equatorial zonal section in Appendix A (pg. 95). Some general trends appear clearly in the TAO line climatology. The thermocline shoaling from west to east results in higher nutrient concentrations at shallower depths in the eastern portions of the basin. Spreading of isotherms in the thermocline is indicative of the EUC (Wyrtki and Kilonsky, 1984**;** Tomczak and Godfrey, 2003; fig. 7) and is evident between 30 and 70 m on the eastern sections, increasing in depth towards the west to about 150 m.

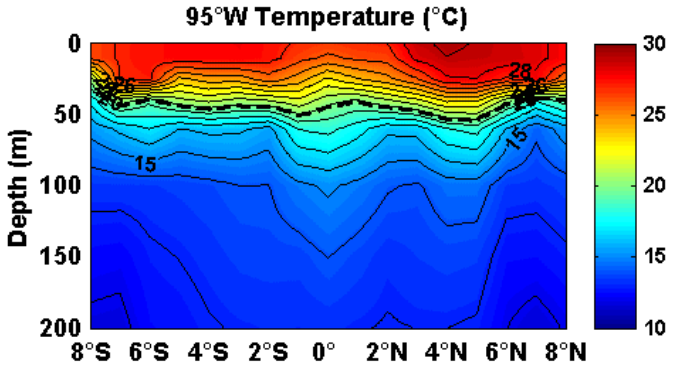

Figure 7: Climatological temperature (°C) section for the 95°W TAO line. The isotherms on the equator appear to be spreading apart as a result of mixing in the EUC (Tomczak and Godfrey, 2003).

The topography of the thermocline in the central equatorial Pacific (125°W and 140°W; fig. 8) depicts the patterns of convergence and divergence in the zonal currents (Kessler and Taft, 1983). The thermocline ridge centered at 0° is associated with the equatorial divergence. A trough appears between 4°N and

6°N where a convergent boundary exists between the northern branch of the SEC and the NECC. North of the trough another ridge associated with a region of divergence between the NECC and the NEC. South of the equator the depth of the thermocline gradually increases, showing little evidence of the ridge/trough topography seen north of the equator. On the 165°E and 180° lines the 22°C to 26°C isotherms rise up toward the surface as a slight ridge, but the 20°C isotherm does not. This is indicative of the SECC which is more persistent west of the dateline (Philander, 1990).

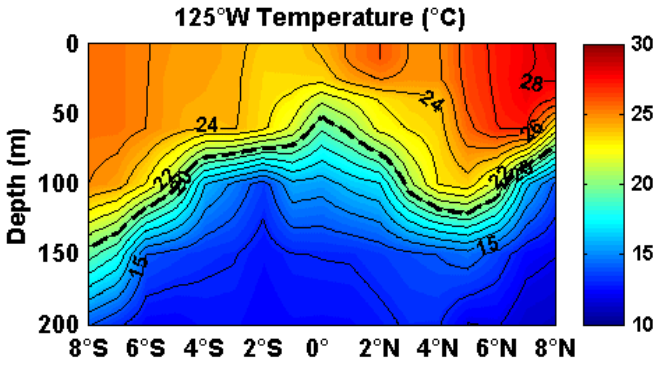

Figure 8: The characteristics of the thermocline topography discussed above are clearly demonstrated in the climatological temperature (°C) section for the 125°W TAO line.

The intrusion of South Pacific Tropical Water (Johnson *et al.*, 2000; SPTW salinity >35.2) is the major salinity feature in the climatology and becomes evident on the 110°W TAO line (fig. 9), expanding and deepening toward the west. The appearance of this high salinity feature reflects two important processes, the high evaporation rates occurring in the South Pacific Gyre and the equatorward motion in the thermocline (Johnson *et al.*, 2001). Salinity minima are associated with regions of high precipitation, such as the ITCZ. This low salinity signal is transported by the NECC (Wyrtki and Kilonsky, 1984) which appears in

eastern sections, but abates in the central Pacific appearing again on the 165°E TAO line. The SECC also carries a low salinity signal that appears in the 165°E and 180° sections.

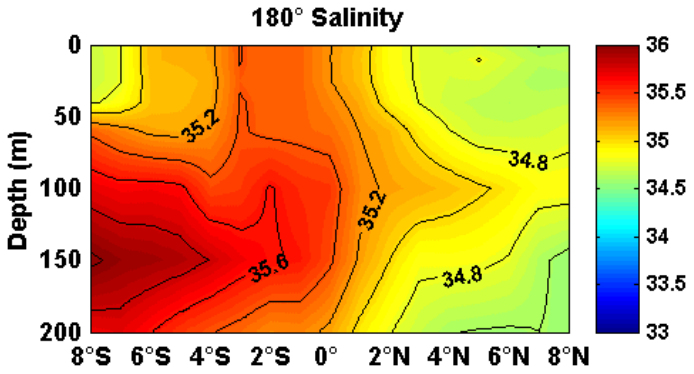

Figure 9: Intrusion of SPTW is evident in the climatological salinity section for 180°. Salinity minima at the surface are associated with the NECC and SECC.

Chlorophyll concentrations generally increase toward the east, concomitant with the shoaling nutricline (thermocline). Highest chlorophyll values occur in the region of equatorial divergence, between 2°N and 2°S along each TAO line. The eastern TAO lines show elevated chlorophyll extending as far as 8°N, particularly on the 95°W TAO line which is associated with elevated primary production occurring in the Costa Rican Cold Dome (Pennington *et al*., 2006). This pattern of elevated chlorophyll north of the equator abates towards the west, where at 170°W elevated chlorophyll is centered directly on the equator. An increase in chlorophyll is apparent west of the dateline and has been noticed in other climatologies for the region (Chavez and Barber, 1991).

3.1.1 Levitus94 annual nitrate comparison

The comparison with Levitus94 climatological nitrate is shown in Appendix B (pg. 100). The TAO climatological nitrate compared well with Levitus94, except

that the TAO data reflected more spatial details associated with the zonal currents that drive the thermocline topography discussed earlier (fig. 10). TAO nitrate concentrations were higher at depth on either side of the equator across all lines. Regions where the TAO climatology appeared lower than the Levitus94 data are in the upper 100 meters in the region north of approximately 2°N for lines east of 140°W, and west of this line where the entire upper water column becomes slightly impoverished. Also the spreading of the nitrate isopleths on the equator which is caused by mixing in the EUC (Wyrtki and Kilonsky, 1984) did not appear in the Levitus94 dataset, and resulted in a region of lower nitrate concentration in the TAO climatology centered at 0°. The Levitus94 climatology does not capture these characteristics namely because it consists of fewer data points with heavy smoothing.

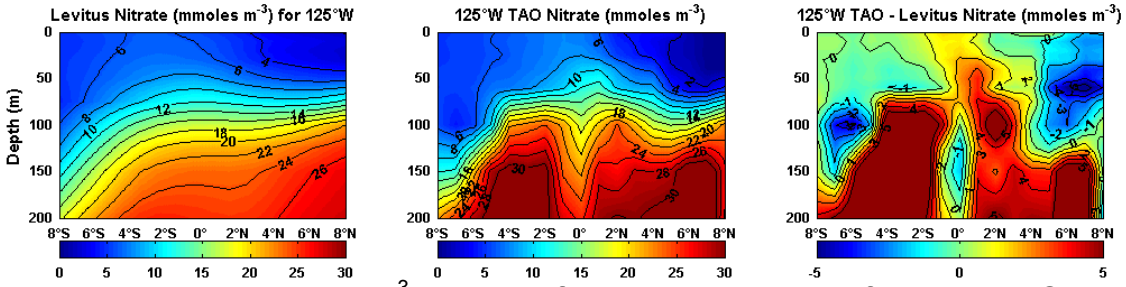

Figure 10: Nitrate (mmol m^{-3}) sections from the Levitus94 (left panel), TAO climatologies (middle panel) and the difference (TAO - Levitus94; right panel).

3.2 TIW sections

The number of cruises in the TAO climatology and that crossed TIWs are summarized in Table 1. The number of cruises that crossed TIWs on each TAO line increases from the east toward the central Pacific and then decreases in the western portion of the basin. This trend reflects the development of TIWs along the equator. Their growth initiates as small perturbations west of the Galapagos

Islands, becoming fully developed in the central Pacific then abating toward the western Pacific (Chelton *et al*., 2000). They rarely appear in microwave SST west of 180°. No cruises were identified crossing TIWs along the 165°E TAO line.

Table 1: The number of TAO cruises in the climatology for each line with the number of cruises that crossed TIWs.

line	# of cruises in climatology	# of cruises identified crossing TIWs
95°W	5	2
110°W	6	2
125°W	5	5
140°W	4	6
155°W	5	2
170°W	5	4
180°	5	3
total	35	24

The lack of TIWs identified in the west Pacific may in fact represent a deficiency in this analysis. Chelton *et al.* (2000) mention that the lack of an SST gradient does not necessarily imply a lack of TIWs. TIWs require shear to be generated (Qiao and Weisberg, 1995) and the lack of an SST gradient means that using SST to detect TIWs may be problematic in certain regions of the equatorial ocean (*i.e.* the west Pacific or Indian Oceans). The following sections briefly describe the cruises that crossed TIWs and their latitude/depth anomaly sections. The nitrate anomaly sections are presented in this discussion as representative of macro-nutrient concentrations, since nitrate, phosphate and silicic acid trend to covary. The reader should refer to Appendix C (pg. 102) for the CTD station/SST maps, latitude/depth sections and anomalies from the TAO climatology for each cruise.

3.2.1 95°W TIW cruises

Two 95°W TAO cruises crossed TIWs in the northern hemisphere. The first cruise was in May 1999 and crossed a moderately developed TIW during a period of decreased upwelling conditions. The second cruise crossed a TIW in November 2000 that appeared only as a slight undulation in the SST front north of the equator, although during enhanced upwelling conditions. The greater spatial extent of cooler SSTs during the November 2000 TAO cruise period is indicative of the seasonal maximum in upwelling that occurs during boreal fall.

The anomaly sections (fig. 11; App. C, pg. 104, figs. 60 and 61) illustrate large regions of the water column below 50 m where nutrient concentrations were substantially lower than climatological values. Regions of nutrient enhancement appear in the upper 50 m south of the equator for both cruises, as well as in the vicinity of the thermocline ridge near 8°N. It should be noted that while the May 1999 TAO cruise crossed a more developed TIW, neither cruise crossed substantially well developed TIWs relative to TIWs crossed on TAO lines further west.

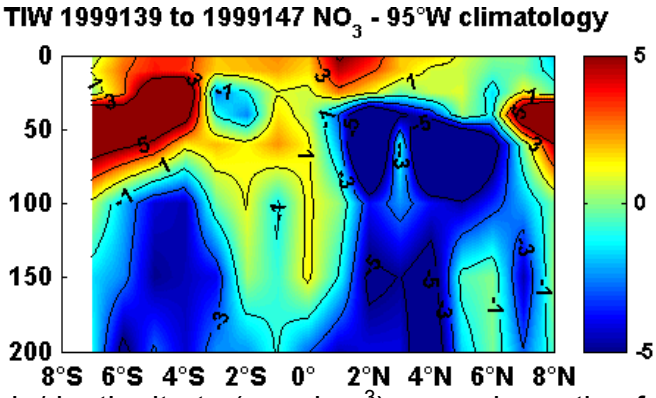

Figure 11: Latitude/depth nitrate (mmol m^{-3}) anomaly section for the May 1999 95°W TAO cruise which crossed a TIW in the northern hemisphere.

3.2.2 110°W TIW cruises

Two TAO cruises crossed TIWs on the 110°W mooring line. The first cruise was in October 1998 and crossed a TIW in the southern hemisphere. The second cruise was in November 1999 and crossed a TIW in the northern hemisphere. In general, upwelling along the equator did not appear to be substantially different between the two cruise periods.

The anomaly sections again illustrate large portions of the water column below 50 m where nutrient concentrations were substantially lower than climatological values both north and south of the equator (fig. 12; App. C, pg. 107, figs. 66 and 67). Regions of nutrient enhancement do appear on the equator within the upper 50-100 m, as well as south of the equator in the upper 50 m during the October 1998 cruise. No substantial increase in chlorophyll is apparent for either cruise.

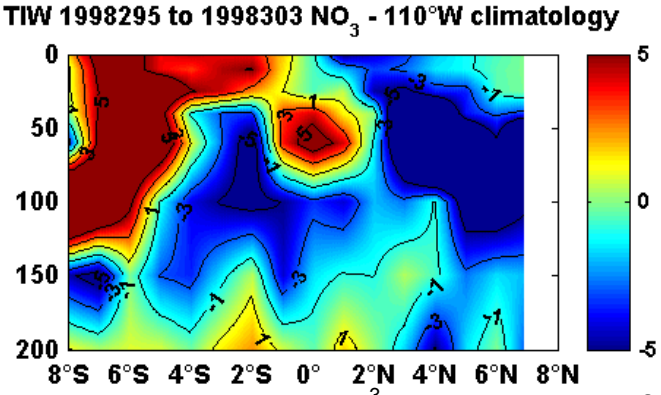

Figure 12: Latitude/depth nitrate (mmol m^{-3}) anomaly section for the October 1998 110°W TAO cruise which crossed a TIW in the northern hemisphere.

3.2.3 125°W TIW cruises

Five TAO cruises crossed TIWs on the 125°W mooring line. The first cruise was in September 1998 and crossed a TIW in the southern hemisphere. The second cruise was in February 1999 and crossed a TIW in the northern

hemisphere. The third and fourth cruises were in September 1999 and February 2000, respectively, and both crossed TIWs in the northern hemisphere. The September 1999 cruise also crossed a southern TIW. These two cruises were the focus of a comparative analysis incorporating ancillary data to understand how TIW intensity and seasonality in the thermocline topography impact the distributions of nutrients and chlorophyll. The last cruise crossed a southern hemisphere TIW in January of 2001.

In all five anomaly sections regions of enhanced nutrients were present within the upper 50 m on and south of the equator (fig. 13; App. C, pgs. 113-115, figs. 78-82). North of the equator only the January/February cruise data demonstrated enhanced nutrients while boreal fall cruises showed concentrations near or below climatological values within the upper 50 m, with the exception of a small region centered at 6°N in September 1999. Below 50 m the differences were even more striking, with January/February cruise data depicting nitrate concentrations more than 5 mmol m^{-3} above climatological values while the opposite occurred for boreal fall cruises.

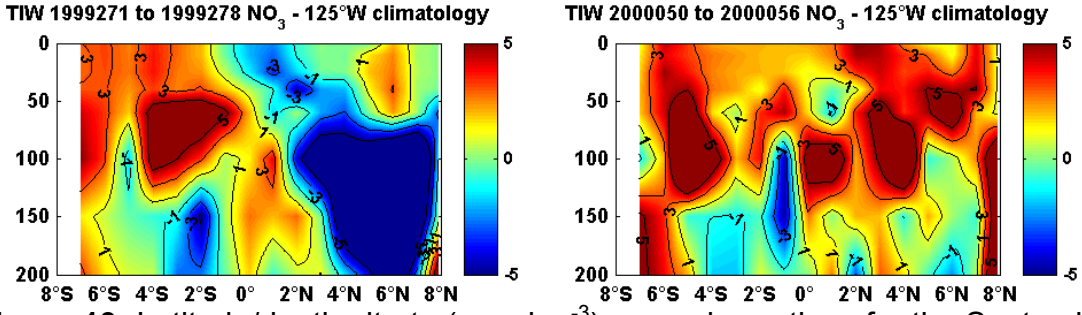

Figure 13: Latitude/depth nitrate (mmol m^{-3}) anomaly sections for the September 1999 (left panel) and February 2000 (right panel) TAO cruises along the 125°W line.

Only the September 1998 and February 2000 data illustrated substantial regions where chlorophyll concentrations were elevated above climatological values, though in different regions in the water column (fig. 14). In September 1998 the increase in chlorophyll concentration is confined to the equator while in February 2000 the region of increased chlorophyll extended from 2°N to 8°N. These large differences in nutrient and chlorophyll distributions between cruises that crossed TIWs was the impetus for incorporating ancillary satellite and mooring observations and these results are discussed in section 3.3 for this TAO line.

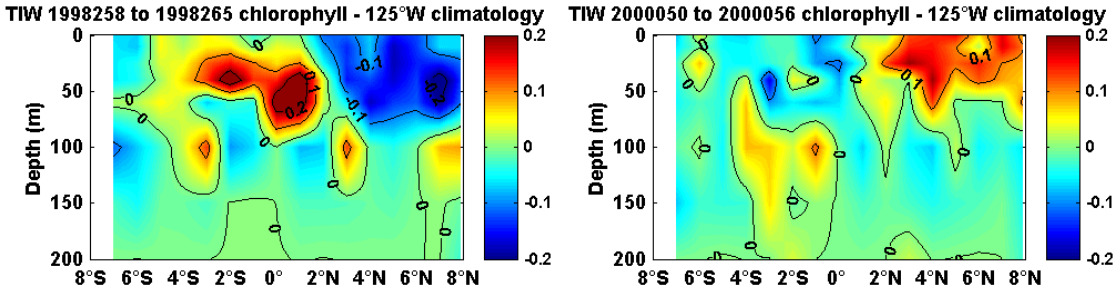

Figure 14: Latitude/depth chlorophyll (mg m^{-3}) anomaly sections for the September 1998 (left panel) and February 2000 (right panel) TAO cruises along the 125°W line. Chlorophyll increases above climatological values occurred for both these cruises but in different regions of the water column.

3.2.4 140°W TIW cruises

Six TAO cruises crossed TIWs on the 140°W mooring line. The September 1998 and January 1999 TAO cruises represent two of the most intense TIWs crossed by TAO cruises in this record; both TIWs were in the northern hemisphere although the September 1998 cruise also crossed a TIW in the southern hemisphere. The third and fourth cruises in September 1999 and February 2000 crossed TIWs in both hemispheres. The fifth cruise crossed a

northern hemisphere TIW in January 2001. The last cruise crossed a northern hemisphere TIW in August of 2002.

Similar to the 125°W mooring line, substantial variance was present in the nutrient anomaly sections. The September 1998 and 1999 cruises both demonstrated regions of enhanced nutrient concentrations south of the equator in the upper 50 m (fig. 15). North of the equator only the September 1999 cruise data showed evidence of substantial nutrient enhancement, with some of the highest levels of enhanced nutrients observed for any boreal fall cruise. In comparison the February 2000 cruise data illustrated the greatest coverage of enhanced nutrients observed from any cruise identified crossing a TIW (fig. 15; App. C, pg. 123, fig. 98).

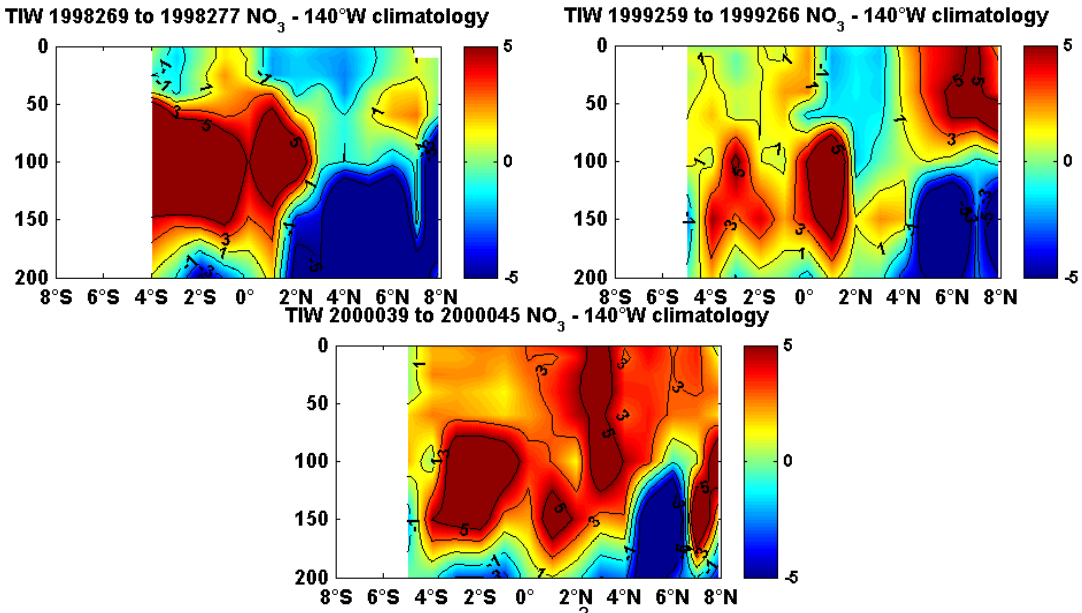

Figure 15: Latitude/depth nitrate (mmol m^{-3}) anomaly sections for the September 1998 (upper left panel), September 1999 (upper right panel) and February 2000 (lower panel) TAO cruises along the 140°W line.

For the first 3 cruises, chlorophyll concentrations were more than 0.1 mg m^{-3} above climatological values for regions near the equator (App. C, pgs. 121-

122, figs. 95-97). Data collected during the February 2000 and January 2001 cruises did not demonstrate chlorophyll concentrations above climatological values, though the coverage of chlorophyll concentrations above 0.2 mg m^{-3} extended further off the equator to the north and south (fig. 16).

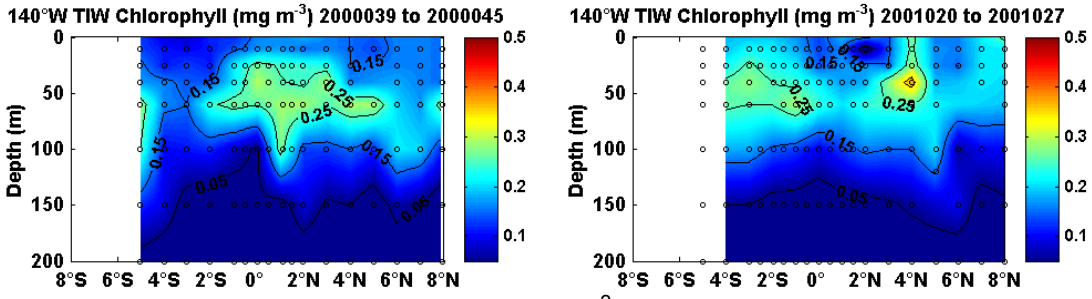

Figure 16: Latitude/depth chlorophyll (mg m^{-3}) sections for the February 2000 (left panel) and January 2001 (right panel) TAO cruises along the 140°W line.

3.2.5 155°W TIW cruises

Two TAO cruises crossed TIWs on the 155°W mooring line. Both cruises were in October and crossed TIWs in both hemispheres, the first in 1998 and the last in 1999. For both cruises nutrients were elevated above climatological values within the upper 50 m of the water column directly on and south of the equator, while only the October 1999 cruise demonstrated enhanced nutrients north of 2°N in the upper water column (fig. 17).

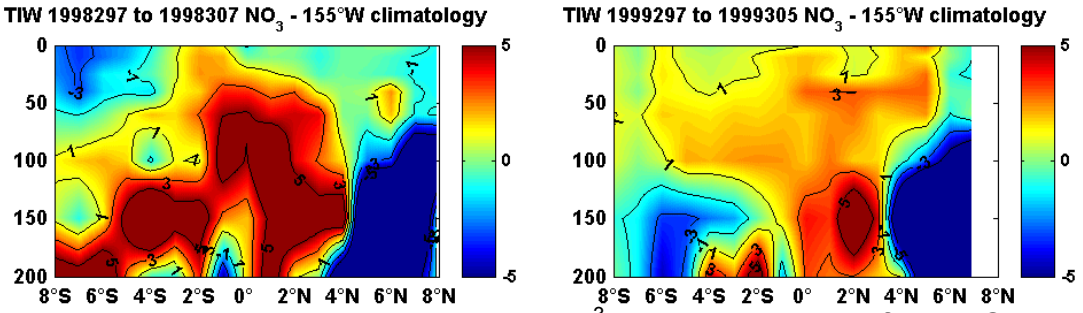

Figure 17: Latitude/depth nitrate (mmol m^{-3}) anomaly sections for the October 1998 (left panel) and October 1999 (right panel) TAO cruises along the 155°W line.

For both cruises, chlorophyll concentrations were ~ 0.1 mg m^{-3} above climatological values from 2°S to the equator, and the October 1998 cruise data depicted a tongue of elevated chlorophyll extending down into the water column near 2°N (fig. 18). Given the seasonal replication of these two cruises, a comparative analysis using ancillary data is presented in section 3.5 to develop an understanding of the differences in these two vortices.

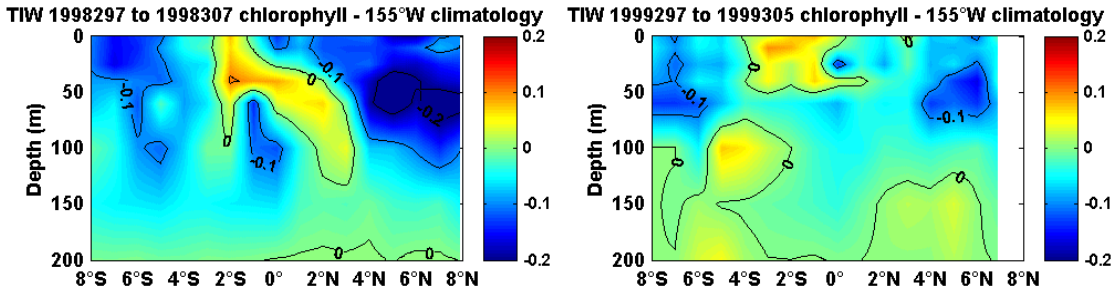

Figure 18: Latitude/depth chlorophyll (mg m^{-3}) anomaly sections for the October 1998 (left panel) and October 1999 (right panel) TAO cruises along the 155°W line.

3.2.6 170°W TIW cruises

Three cruises crossed TIWs on the 170°W mooring line, though the first cruise is divided into two segments due to the northern portion of the cruise line being surveyed ~25 days later. The first segment of this cruise crossed a TIW in the southern hemisphere in November 1998. The second segment crossed a TIW in the northern hemisphere in December. The last two cruises crossed northern TIWs in July 1999 and December 1999. Due to the incomplete nature of the sections, portions of this mooring line were only surveyed once which resulted in limited statistical power for comparing the differences in mean ML nutrient and chlorophyll concentrations between the TIW composite and the

climatology. This also resulted in uninformative anomaly sections, although some evidence of nutrient and chlorophyll enhancement was present.

3.2.7 180° TIW cruises

Three TAO cruises crossed TIWs on the dateline, two of which crossed vortices in both hemispheres. The first cruise occurred in November 1998 and crossed a small TIW south of the equator then a larger TIW in the northern hemisphere. The second cruise occurred in November of 1999, again crossing a small TIW in the southern hemisphere and a larger TIW in the north. The last cruise identified occurred in November of 2000 and crossed a TIW in the northern hemisphere.

No nutrient data were available for the November 2000 cruise. For the two cruises where nutrient sections were present, enhancements in the upper water column above climatological values appeared for nitrate and phosphate but silicic acid only appeared enhanced during the November 1999 cruise. Nutrients for both cruise sections were below climatological values between 4°N and 8°N in the lower water column (App. C, pgs. 136-137, figs. 125-127).

3.3 TIW cruise comparison

To develop an understanding of the differences in effects from TIWs of varying intensity, as well as how seasonality in the topography of the thermocline may alter these impacts, particular cruises were selected for further analysis based on either crossing TIWs during nearly the same month or crossing TIWs in the same hemisphere during different seasons. Satellite, mooring and ship-based

observations were juxtaposed with the chlorophyll and nutrient sections to develop this comparison. These cruise comparisons are described below for the selected 125°W, 140°W and 155°W TAO cruises.

3.3.1 125°W TIW cruise comparison

The September 1999 and February 2000 cruises were selected for comparison of boreal fall and winter TIWs along the 125°W TAO line (fig. 19). As mentioned previously, the September 1999 cruise crossed a strong TIW in the northern hemisphere during a period of active upwelling, as indicated by the enhanced spatial coverage of cooler SSTs. Average current velocities from 20 to 50 m showed the distinct rotation of the TIW vortex north of the equator; with currents toward the southwest just north of the equator, turning toward the northeast to the northwest and west at the northern periphery of the line. The southern portion of the cruise also crossed a TIW SST front, although the two were not symmetric about the equator. Little rotation, indicative of a vortex, is evident in the horizontal currents south of the equator.

The February 2000 cruise crossed a weak TIW in the northern hemisphere. The temperature gradient of the front appeared much sharper during the September 1999 cruise while the February 2000 cruise depicted a more diffuse frontal structure. It is clear from the microwave SST image that the dynamics north of the section appear completely different between the two time periods. Rotation in the horizontal currents was less apparent for this later cruise as the current speeds were substantially less than those in September. Horizontal current velocities south of the equator increased in magnitude but

remained oriented toward the southeast until the periphery of the line where current direction became erratic.

Chlorophyll composites from the cruise periods illustrate the significant differences in the dynamics occurring in the equatorial Pacific between boreal fall and winter (fig. 20). During the September cruise, the region of high chlorophyll was constrained to near 0° and distorted by TIWs both north and south of the equator for the entire composite image west of the Galapagos Islands (0°, 90°W). Contours of SST exemplify the same characteristics as the SST composite images, but emphasize their intricate relationship with the large-scale chlorophyll distributions. The vortex described by the rotation of horizontal velocities from the September cruise seemed to be confined by the 26°C isotherm. A region of slightly elevated chlorophyll, relative to the warmer adjacent waters to the north, was apparent in the region occupied by the vortex. The 26°C isotherm south of the equator appeared west of the cruise section with elevated chlorophyll following the isotherm south. Patchy regions of elevated chlorophyll also appeared south of the 25°C isotherm, again west of the cruise section. Near the Marquesas Islands (8°S, 140°W), high chlorophyll can be seen slightly west of the islands that is distinct from the regions of elevated chlorophyll in the vicinities of the 26°C and 25°C isotherms.

The SeaWiFS chlorophyll composite for the February 2000 TAO cruise showed an increase in phytoplankton biomass for the entire region from just south of the equator to approximately 12°N and from the coast of Central and South America west. Highest chlorophyll no longer appeared directly on the

equator (except near the Galapagos Islands; 0°, 90°W) as in September, but appeared north of the equator in a seemingly contiguous extension of elevated chlorophyll extending westward. An animation of SeaWiFS chlorophyll from January 2000 to April 2000 showed a general greening in the region from the 0° to 10°N, 90°W to 140°W. The increase in chlorophyll concentrations in this region is also apparent in maps of monthly SeaWiFS climatological chlorophyll (fig. 40).

The difference between the two chlorophyll composites illustrates the seasonal redistribution of chlorophyll concentrations in the equatorial Pacific. Highest chlorophyll concentrations in boreal fall occur directly on the equator, while conversely highest chlorophyll concentrations in boreal winter occur in the region north of the equator described above.

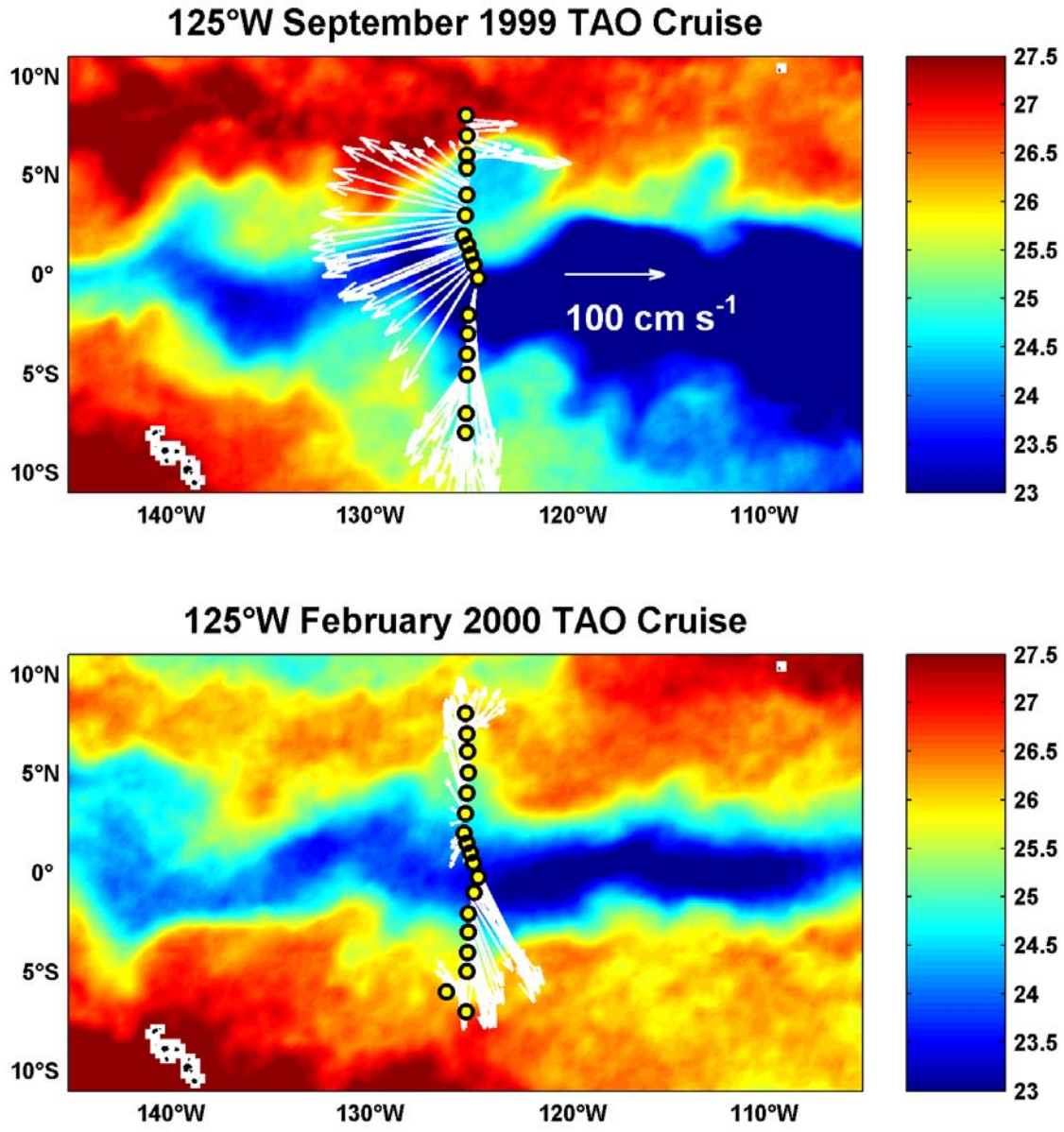

Figure 19: Mean SST (°C) for two cruises along the 125°W TAO line, one in September 1999 (9/28/99-10/5/99) and the other in February 2000 (2/19/00-2/25/00). During the earlier cruise TIW SST fronts were crossed in both hemispheres. The 2000 cruise crossed a TIW SST front in the northern hemisphere only. White arrows indicate the horizontal current velocity averaged from 20 to 50 meters from the ship-board ADCP. Zonal velocity components have been scaled down by a factor of 2 in order to emphasize the meridional component.

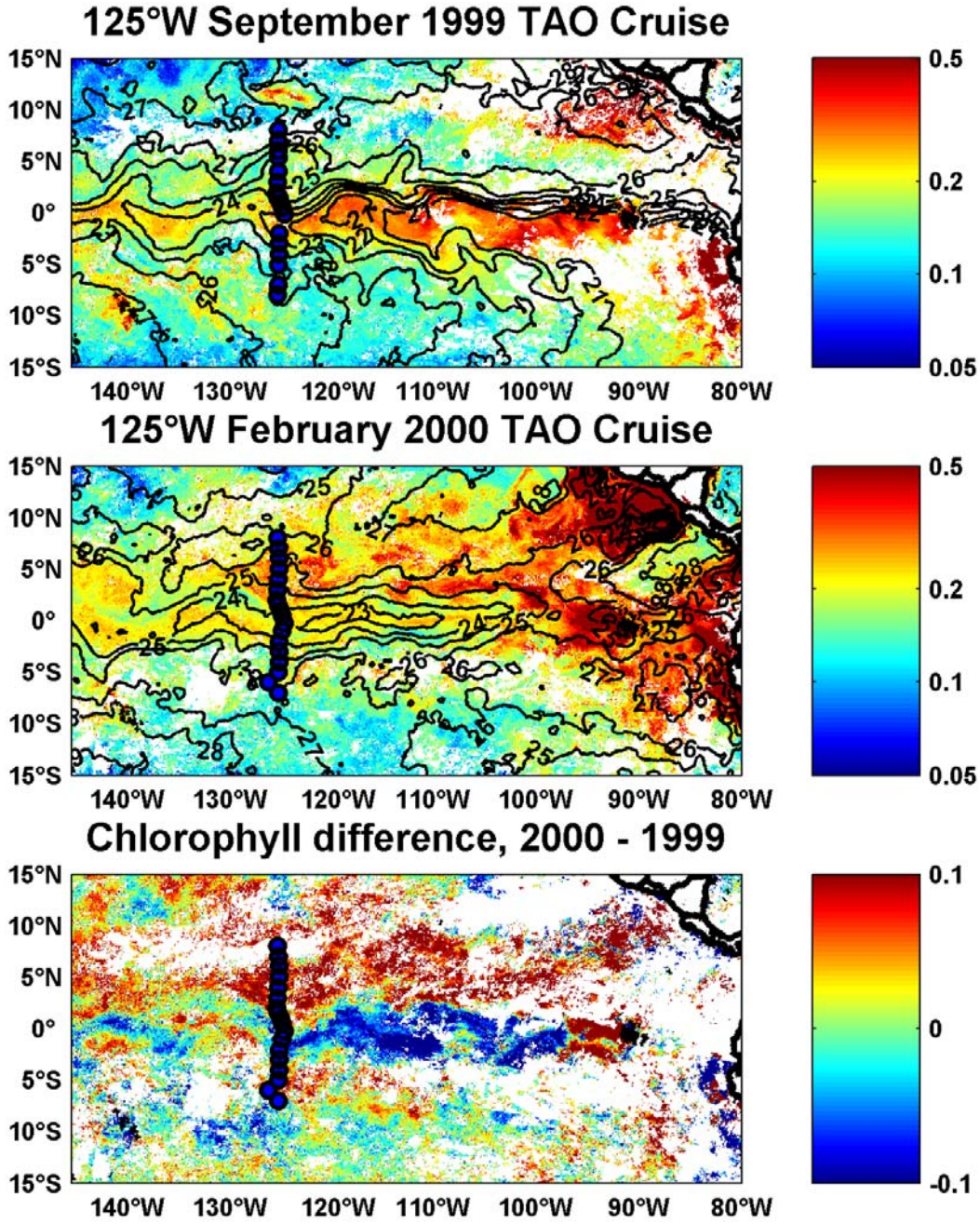

Figure 20: SeaWiFS chlorophyll (mg m^{-3}) averaged over the September 1999 (9/28/99-10/5/99) and February 2000 (2/19/00-2/25/00) cruise periods. Contours are SST averaged over the same periods. The blue circles represent station positions from those cruises. The lower panel shows the difference in chlorophyll between the two periods, with the cruise stations from the latter cruise shown for reference. Note that the two average plots are on a log scale but the difference plot is on a linear scale.

3.3.2 140°W TIW cruise comparison

The cruises selected for comparison along the 140°W TAO line were those occurring in January 1999, September 1999, February 2000 and January 2001 (figs. 21 and 23). The January cruises selected provided the opportunity to examine the impact of TIW intensity during boreal winter, while the September and February cruises allow for an inter-seasonal comparison. Note that the two cruises selected for comparison along the 140°W line occur during the same period as the two cruises listed above for the 125°W line. Both the September 1999 cruise and the February 2000 cruise sampled adjacent TIW vortices. An animation of SST showed that the 140°W cruise line sampled a TIW while heading south along the line, then while cruising north along the 125°W line crossed another TIW approximately a week later. These two cruise periods provide the opportunity to examine differences and similarities between TAO lines for TIWs sampled near continuously.

The January 1999 cruise crossed one of the strongest TIWs in this record, with well defined SST cusps extending to approximately 7°N. The September 1999 cruise also crossed a strong TIW in the northern hemisphere and a weak TIW SST frontal extension in the southern hemisphere. The February 2000 cruise crossed a TIW in the northern hemisphere which also appeared fairly strong as the northward extension of the SST front for both cruises reached approximately 6°N. SSTs along the cruise line were cooler near the equator in February 2000 compared to September 1999, though upwelling appeared quite evident east of the line in September. The January 2001 cruise crossed a

substantially weaker TIW in the northern hemisphere, as well as a weak TIW SST frontal extension in the southern hemisphere.

Both cruises in January 1999 and September 1999 crossed slightly east of the peak in the SST extensions. Warm water crosses the sections, with warmer SSTs in September. Southward horizontal velocities are only evident near the equator in January 1999. In September 1999 the southward horizontal velocities are substantially larger than velocities observed on any cruise selected for this comparative analysis. South of ~7°N the velocities decreased in magnitude and rotated clockwise. Substantial northward velocities were observed slightly south of the equator. Continuing in the southward direction, the velocities appeared to rotate counter-clockwise. Horizontal current velocities during the February 2000 cruise were minimal on the equator and increased toward the poleward directions in both hemispheres. Rotation in the current vectors is only evident in the northern hemisphere. In January 2001 southward horizontal velocities only appear near the equator, and north of the equator they rotate clockwise.

Composites of SeaWiFS chlorophyll again show substantial differences between boreal fall and winter cruise periods (figs. 22 and 24). The coverage of surface chlorophyll greater than 0.2 mg m^{-3} is substantially higher in the region north of the equator during the February 2000 cruise compared to any other selected 140°W cruise. As was the case for the September 1999 125°W cruise, highest chlorophyll values are confined to near the equator during the September 1999 140°W cruise. Also, the chlorophyll and SST fronts are both distorted by TIWs in January and September of 1999 while only moderately so in February

2000 and January 2001. The vortex, defined by the SST composite and rotating current vectors, during the September 1999 cruise is clearly delineated in the chlorophyll composite as a tongue of relatively high chlorophyll extending off the equator while a tongue of relatively lower chlorophyll extends equatorward from the north. The low chlorophyll tongue is also evident for TIWs occurring east of the cruise line during September. The chlorophyll composite for the February 2000 cruise shows no such tongue of relatively lower chlorophyll extending toward the equator. Higher chlorophyll values are evident within the TIW SST extension during this cruise. This pattern appears consistent with TIWs present both west and east of the cruise line during February 2000.

Both January cruises appear to have lower concentrations of chlorophyll in the region north of the equator compared to the February 2000 cruise period. Higher chlorophyll concentrations are confined to the equator during January 1999 compared to January 2001 (fig. 24). The difference between the chlorophyll composites for the two January cruise periods shows slightly higher chlorophyll within the January 2001 TIW north of the equator. Also a region of higher chlorophyll concentrations can be seen extending south along the cruise transect that is associated with the SST frontal extension of a southern TIW.

High chlorophyll concentrations are present south of the equator during both the January and September 1999 cruise periods but not during the February 2000 or January 2001 cruise periods, with the exception of near the Marquesas Islands. High chlorophyll appears extremely pronounced between the 25°C and 26°C isotherms east of the Marquesas Islands during the September 1999 cruise

period. This feature is related to the pattern discussed south of the equator for the 125°W September cruise as these lines are surveyed in sequence, with the 140°W line preceding the 125°W line. This implies that the same feature was observed in both composites and that during the 140°W September cruise period it was a sharp well defined region of high chlorophyll between two closely spaced isotherms. Approximately a week later, while the 125°W line was surveyed, the feature had degraded somewhat as the isotherms spread apart. It appears that the spreading of these isotherms is the result of the 25°C isotherm translating eastward, as the 26°C isotherm appears in the vicinity of 130°W during both cruise periods.

The January 1999 cruise period SeaWiFS composite also demonstrated elevated chlorophyll concentrations south of the equator, although a great deal west of the cruise section. Again, this region of enhanced chlorophyll appears associated with the 25°C and 26°C isotherms. In this case high chlorophyll can be seen as far as 10°S near 110°W. No such feature is present during the January 2001 cruise period.

The differences between the September 1999 and February 2000 chlorophyll composites again illustrate the redistribution of chlorophyll concentrations along the equator between boreal fall and winter. During boreal fall highest chlorophyll values are situated near the equator while in winter elevated chlorophyll occurs further north. The differences between the January 1999 and January 2001 chlorophyll composites illustrate that higher chlorophyll

concentrations were present along the equator during the January 2001 cruise period.

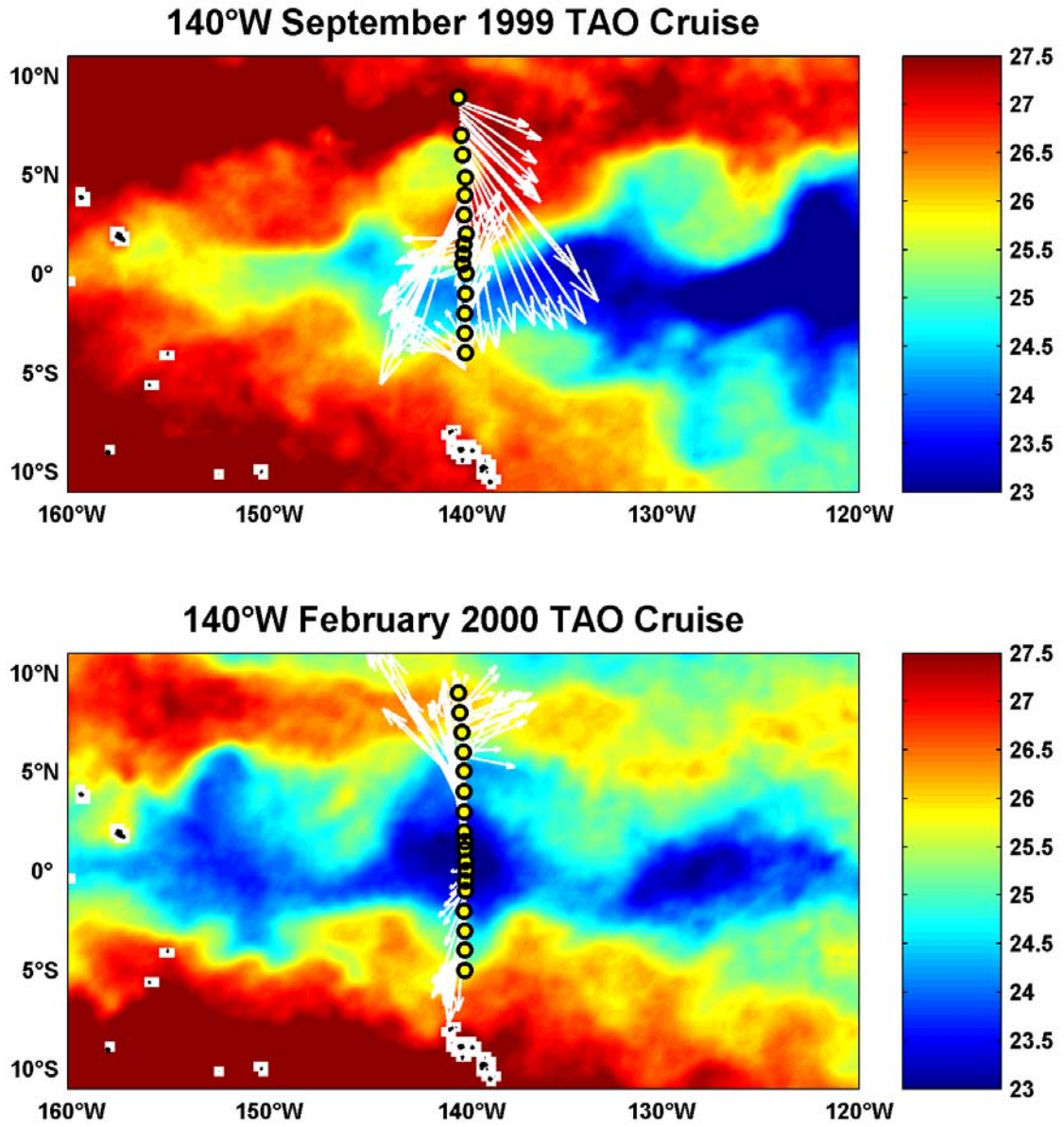

Figure 21: Mean SST (°C) for two cruises along the 140°W TAO line, one in September 1999 (9/14/99-9/22/99) and the other in February 2000 (2/7/00-2/14/00). In both cruises TIWs were crossed in both hemispheres. White arrows indicate the horizontal current velocity averaged from 20 to 50 meters. Zonal velocity components have been scaled down by a factor of 2 in order to emphasize the meridional component.

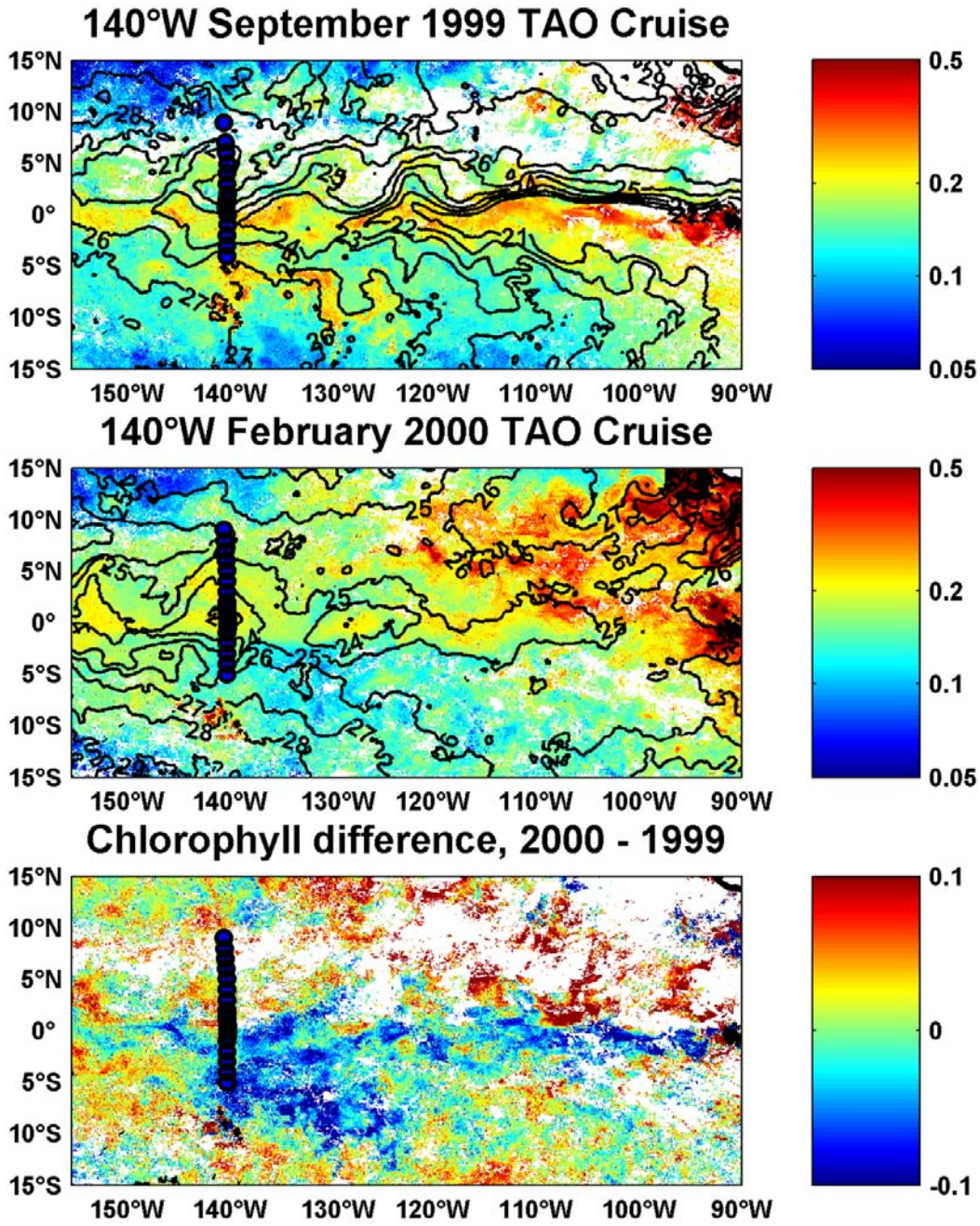

Figure 22: SeaWiFS chlorophyll (mg m^{-3}) averaged over the September 1999 (9/14/99-9/22/99) and February 2000 (2/7/00-2/14/00) cruise periods. Contours are SST averaged over the same periods. The blue circles represent station positions from those cruises. The lower panel shows the difference in chlorophyll between the two periods, with the cruise stations from the latter cruise shown for reference. Note that the two average plots are on a log scale but the difference plot is on a linear scale.

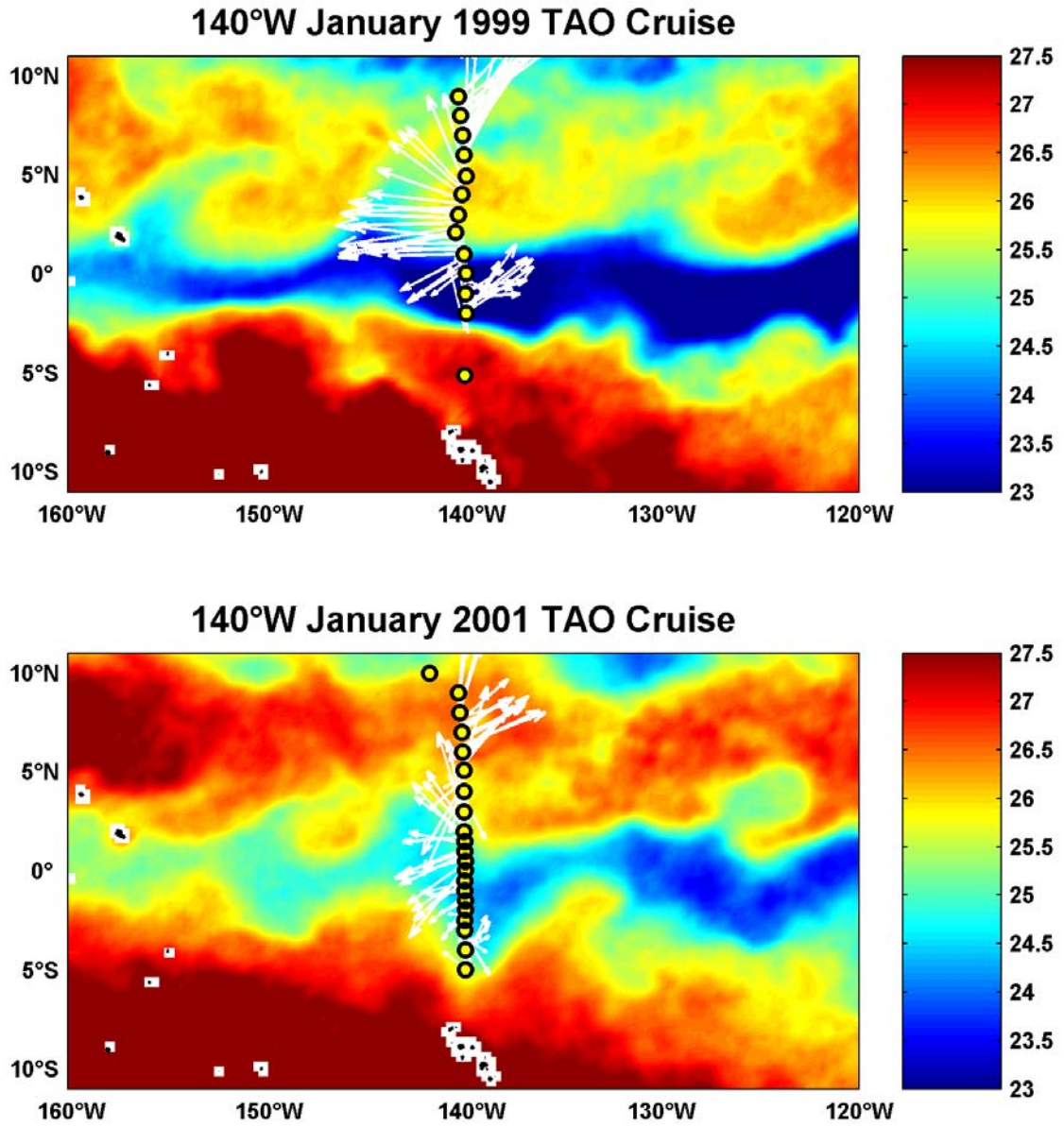

Figure 23: Mean SST (°C) for two cruises along the 140°W TAO line, one in January 1999 (1/30/99-2/6/99) and the other in January 2001 (1/20/01-1/27/01). During the January 2001 cruise TIWs were crossed in both hemispheres, while only a northern TIW was crossed during January 1999. White arrows indicate the horizontal current velocity averaged from 20 to 50 meters. Zonal velocity components have been scaled down by a factor of 2 in order to emphasize the meridional component.

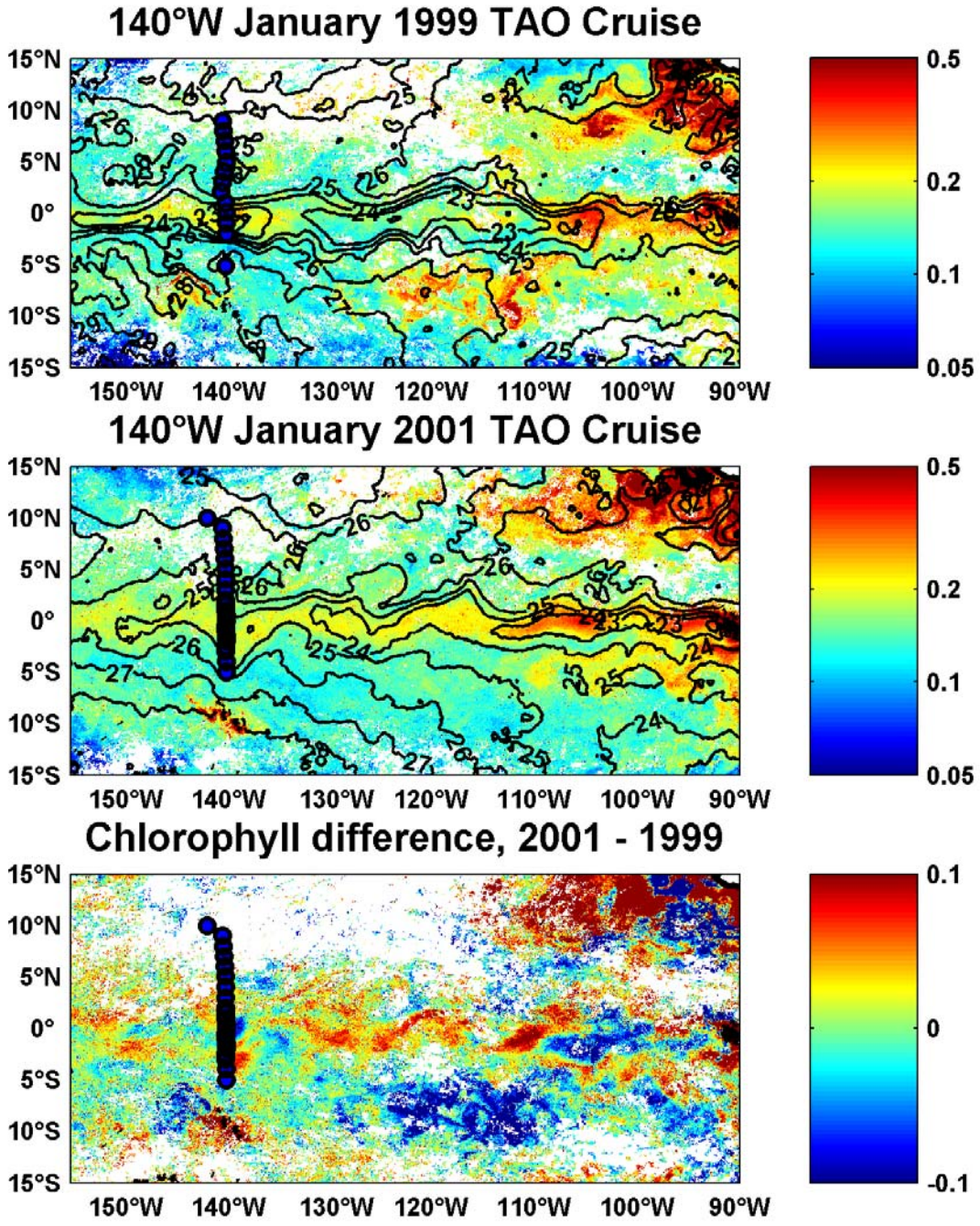

Figure 24: SeaWiFS chlorophyll (mg m^{-3}) averaged over the January 1999 (1/30/99-2/6/99) and January 2001 (1/20/01-1/27/01) cruise periods. Contours are SST averaged over the same periods. The blue circles represent station positions from those cruises. The lower panel shows the difference in chlorophyll between the two periods, with the cruise stations from the latter cruise shown for reference. Note that the two average plots are on a log scale but the difference plot is on a linear scale.

3.3.3 155°W TIW cruise comparison

The cruise comparisons for the 155°W line provide the opportunity to examine the effect of TIW intensity on vortices which occurred during boreal fall (fig. 25). The first cruise in 1998 appeared to take place during a period of more active upwelling compared to the 1999 cruise. Both cruises crossed strong TIWs in the northern hemisphere and weak TIW SST fronts in the southern hemisphere. Rotation in the current vectors was evident during both cruises, with the 1998 cruise containing greater current speeds. A small degree of rotation was evident south of the equator during 1998, while during 1999 flow south of the equator is predominately toward the WNW. No southward velocities were evident north of the equator for either cruise.

Chlorophyll composites for both time periods appear very similar, with highest values constrained near the equator (fig. 26). In both 1998 and 1999 the chlorophyll and SST fronts are both significantly distorted by TIWs. During 1998 the cold tongue extended west of the dateline while in 1999 the cold tongue appeared to terminate near 170°W. High chlorophyll values appeared west of the cruise line in 1998, while in 1999 highest chlorophyll values along the equatorial band were east of the cruise line.

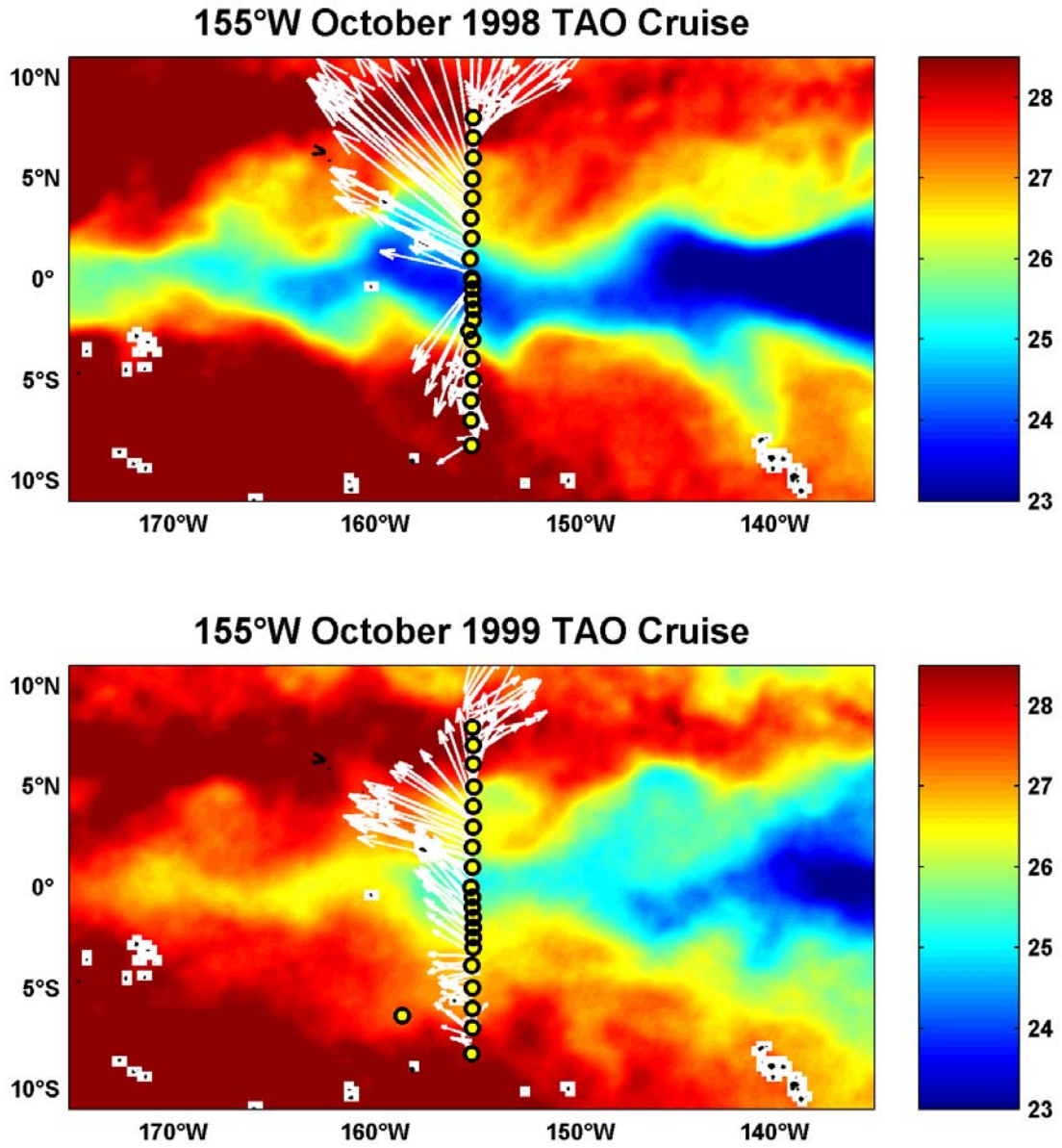

Figure 25: Mean SST (°C) for two cruises along the 155°W TAO line, one in October 1998 (10/24/98-11/3/98) and the other in October 1999 (10/24/99-11/1/99). In both cruises TIWs were crossed in both hemispheres. White arrows indicate the horizontal current velocity averaged from 20 to 50 meters. Zonal velocity components have been scaled down by a factor of 2 in order to emphasize the meridional component.

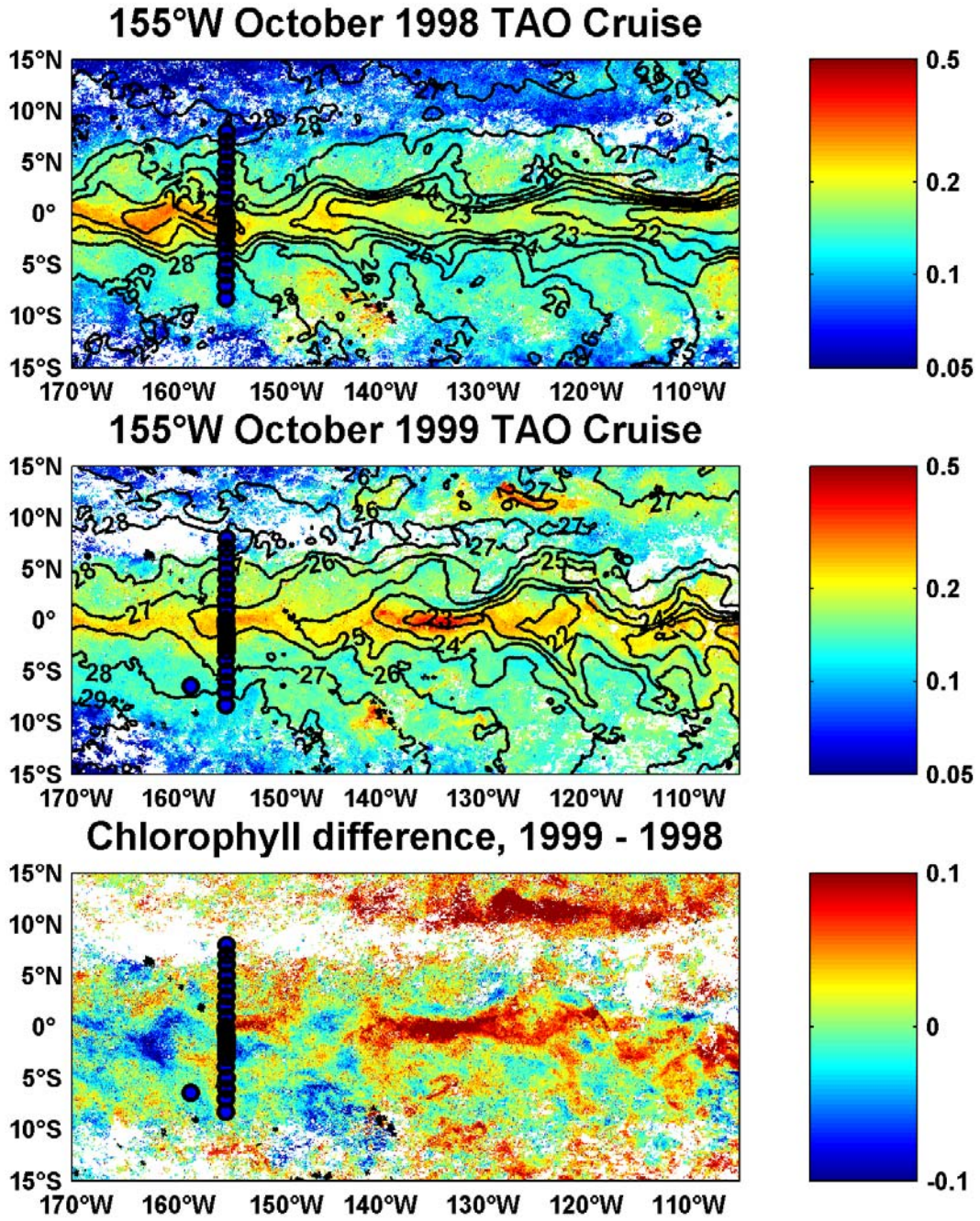

Figure 26: SeaWiFS chlorophyll (mg m^{-3}) averaged over the October 1998 (10/24/98-11/3/98) and October 1999 (10/24/99-11/1/99) cruise periods. Contours are SST averaged over the same periods. The blue circles represent station positions from those cruises. The lower panel shows the difference in chlorophyll between the two periods, with the cruise stations from the latter cruise shown for reference. Note that the two average plots are on a log scale but the difference plot is on a linear scale.

3.4 TAO mooring 20°C isotherm depth variability

Five-day averaged 20°C isotherm depth data, from the TAO moorings along the 125°W, 140°W and 155°W lines for the period from July 1998 to April 2001, demonstrate substantial seasonal variability off the equator (fig. 27), particularly at the 5°N and 5°S moorings. The seasonal variation at these moorings appears to decrease toward the west along the equator. Philander (1990) suggested that variability in the 20°C isotherm depth is out of phase at 10°N and 3°N due to the seasonality of the trade winds. This trend does not appear in this record as seasonal variation appears phase locked at 5°N and 8°N.

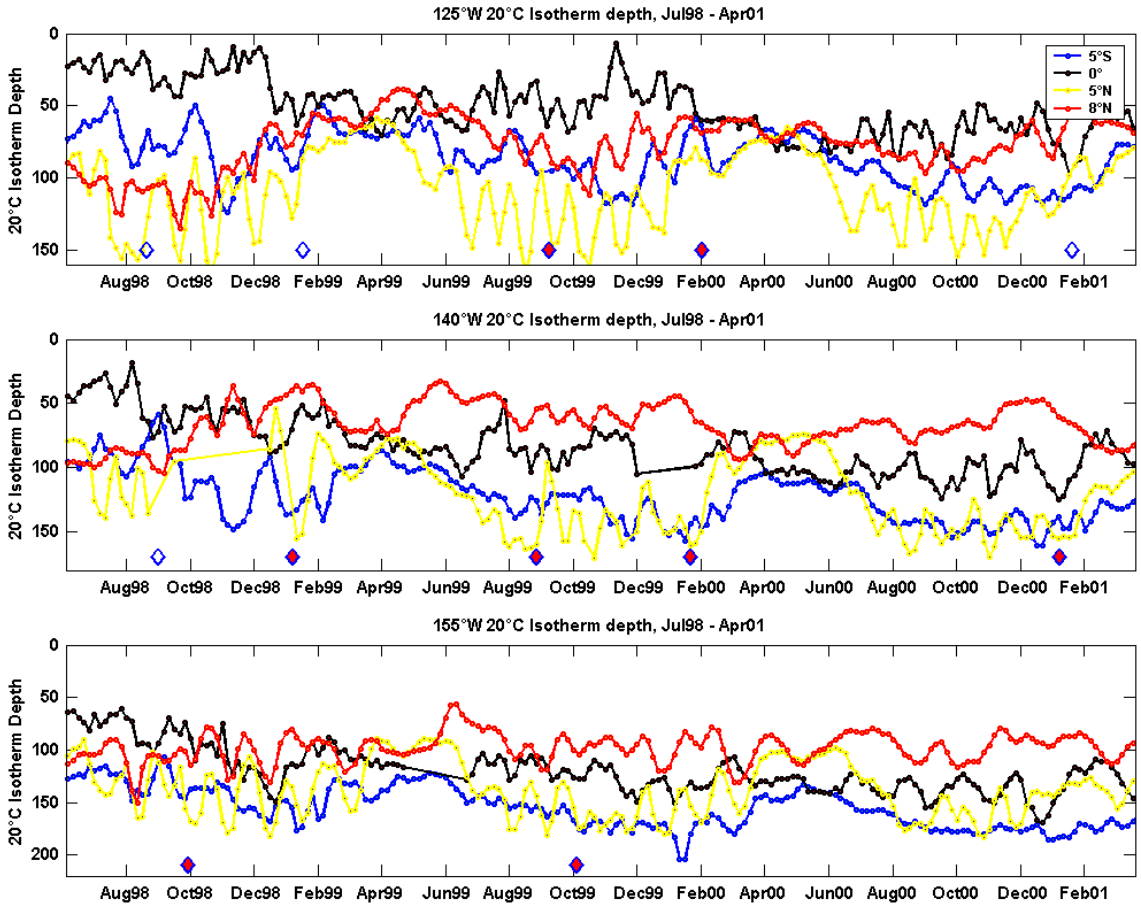

Figure 27: 20°C isotherm depth for the 5°S, 0°, 5°N and 8°N (9°N for the 140°W line) TAO moorings along the 125°W, 140°W and 155°W lines. TIW cruise periods selected for the comparative analysis are identified as red filled blue diamonds. Other cruises that crossed TIWs during this period but not included in the comparative analysis are represented as empty blue diamonds.

Substantial variability in the 20°C isotherm depth with a ~30 day periodicity can be seen at all the mooring locations along all three TAO lines from approximately June to February of the following year. No TIW activity indicated by variability at this periodicity appears present from March to May during either 1999 or 2000.

3.5 TIW composite/climatology comparison

Latitudinal and longitudinal comparisons between TIW composite and climatological mean ML nutrient and chlorophyll concentrations are presented in figures 28-35. Some latitude bins show statistically significant differences in concentrations from climatological values (represented as red stars), with trends evident in the distributions of both average ML nutrient and chlorophyll concentrations.

In general, both climatological and TIW composite mean ML nutrient concentrations are higher south of the equator for all lines east of 140°W. The enhancement in TIW composite mean ML nutrient concentrations for the eastern and central mooring lines (east of 155°W) shifts to near and north of the equator on the western lines (west of and including 140°W). North of the equator, TIW composite ML nutrient concentrations appear above climatological values in regions where the cold upwelled water was recirculated in the TIW vortex. An example of this can be seen in the anomaly section presented in left panel of figure 13 and the CTD station/SST map in figure 19. The TIW crossed during this September 1999 cruise contained a region of colder nutrient rich water near 6°N that was being recirculating in the TIW vortex. These recirculating portions of TIW vortices were observed on central and western Pacific cruises.

TIW composite mean ML chlorophyll concentrations are always near or below climatological values. TIW composite ML chlorophyll concentrations appear lower than the climatological values for the entire latitude range on the 95°W and 140°W mooring lines, with statistical differences on the 110°W to

140°W lines. For the 155°W line, TIW composite ML chlorophyll values are near climatological values on the equator and lower than the climatology at the periphery of the line. For the 170°W and 180° TAO lines TIW composite mean ML chlorophyll concentrations are below climatological values on the equator.

Significant statistical differences appear in the longitudinal trends of mean ML nutrient and chlorophyll concentrations between the TIW composite and the climatology. Mean ML nutrients are significantly elevated on all TAO mooring lines, though differences exist between nutrients for each line. East of 140°W, only silicic acid and nitrate appear significantly higher than climatological values while west of this line phosphate appears significantly higher for the TIW composites. All three nutrients appear significantly elevated on the 180° line. Mean ML chlorophyll is less than climatological values for all the eastern and central TAO mooring lines.

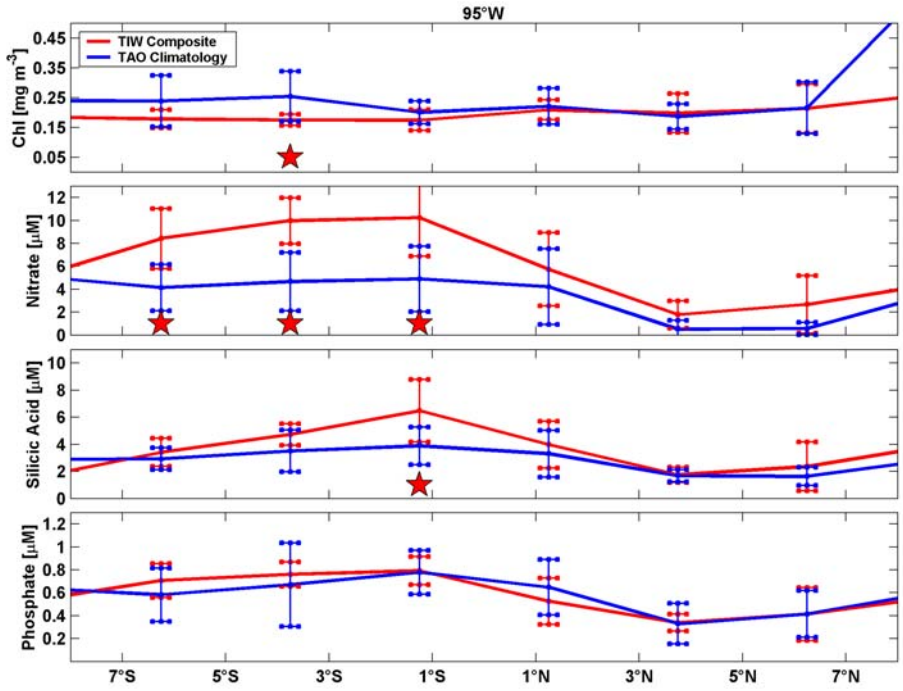

Figure 28: Mean ML chlorophyll, nitrate, silicic acid and phosphate for the 95°W mooring line climatology (blue) and TIW composite (red). Error bars are the standard deviation from the mean for every latitude bin. Red stars are latitudes for which significant differences were found using two-tailed *t* tests ($p < 0.05$).

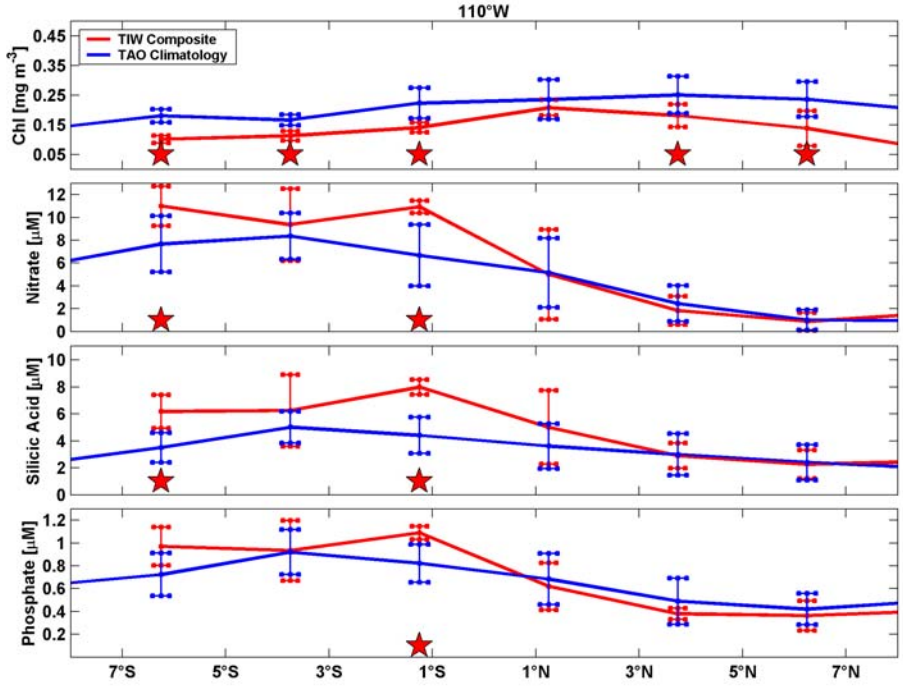

Figure 29: Mean ML chlorophyll, nitrate, silicic acid and phosphate for the 110°W mooring line climatology (blue) and TIW composite (red). Error bars are the standard deviation from the mean for every latitude bin. Red stars are latitudes for which significant differences were found using two-tailed *t* tests ($p < 0.05$).

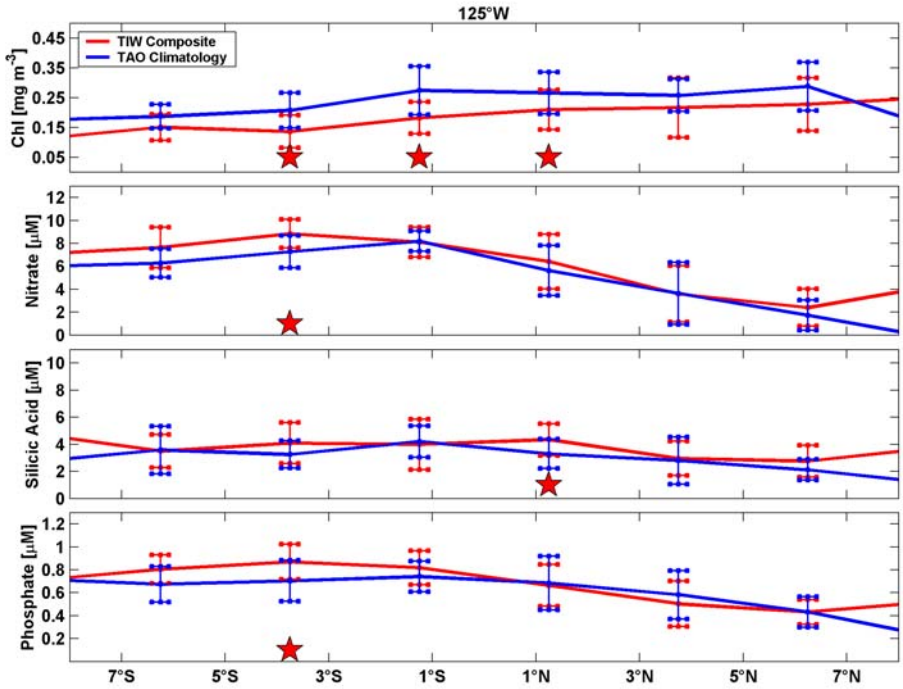

Figure 30: Mean ML chlorophyll, nitrate, silicic acid and phosphate for the 125°W mooring line climatology (blue) and TIW composite (red). Error bars are the standard deviation from the mean for every latitude bin. Red stars are latitudes for which significant differences were found using two-tailed *t* tests ($p < 0.05$).

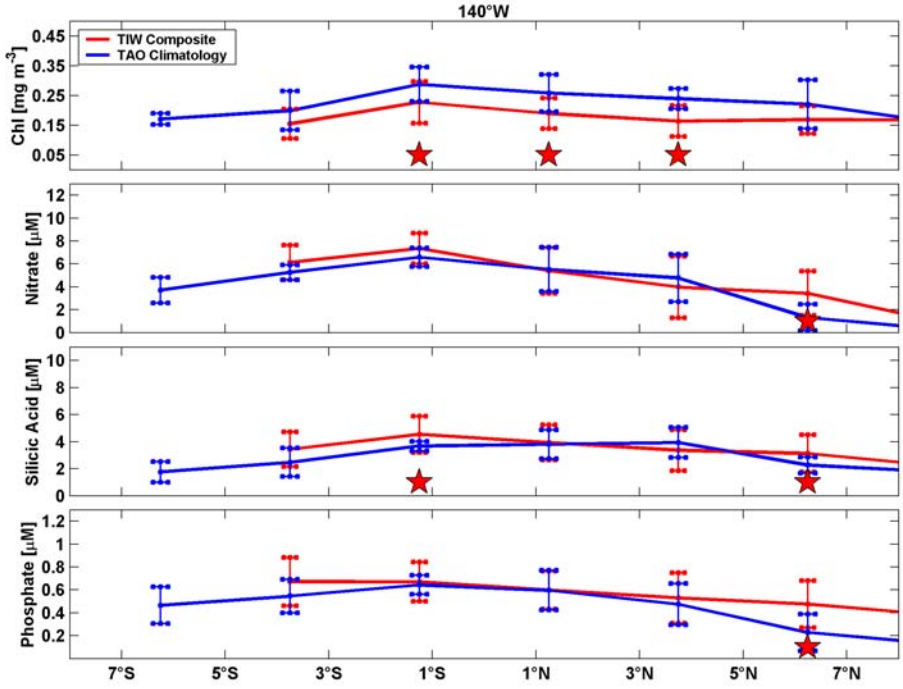

Figure 31: Mean ML chlorophyll, nitrate, silicic acid and phosphate for the 140°W mooring line climatology (blue) and TIW composite (red). Error bars are the standard deviation from the mean for every latitude bin. Red stars are latitudes for which significant differences were found using two-tailed *t* tests ($p < 0.05$).

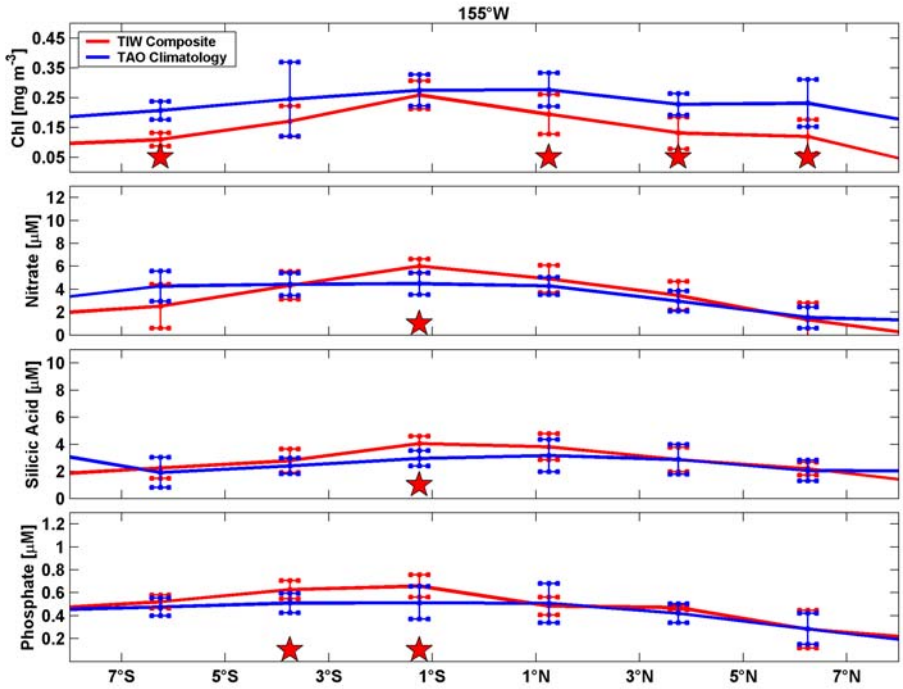

Figure 32: Mean ML chlorophyll, nitrate, silicic acid and phosphate for the 155°W mooring line climatology (blue) and TIW composite (red). Error bars are the standard deviation from the mean for every latitude bin. Red stars are latitudes for which significant differences were found using two-tailed *t* tests ($p < 0.05$).

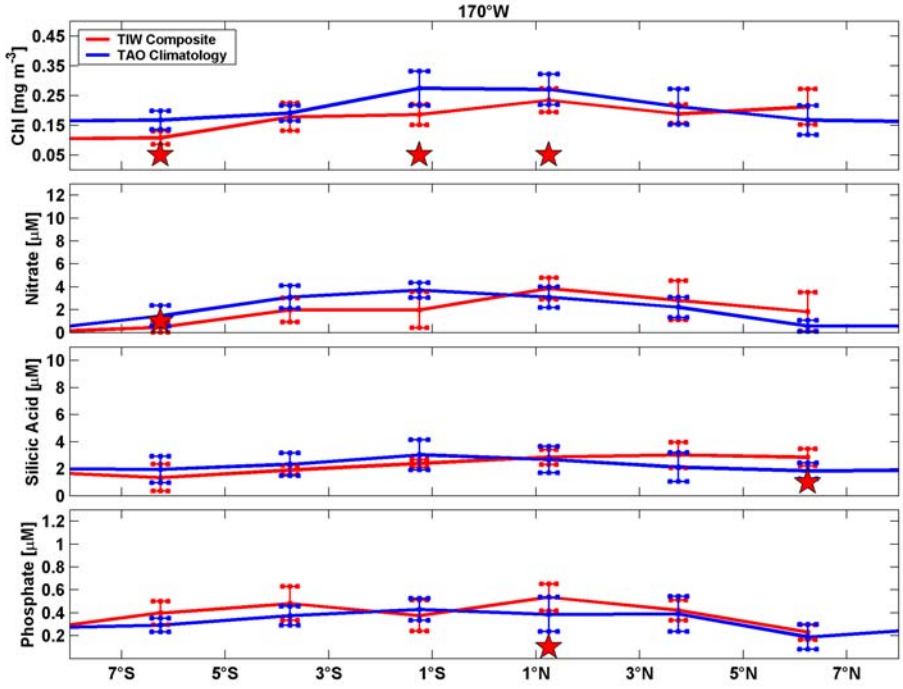

Figure 33: Mean ML chlorophyll, nitrate, silicic acid and phosphate for the 170°W mooring line climatology (blue) and TIW composite (red). Error bars are the standard deviation from the mean for every latitude bin. Red stars are latitudes for which significant differences were found using two-tailed *t* tests ($p < 0.05$).

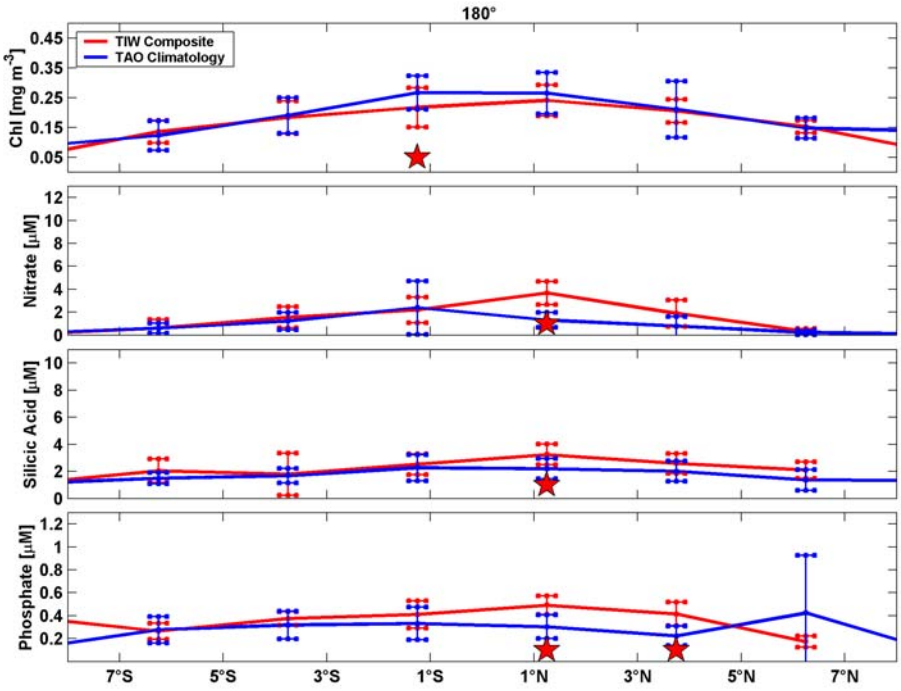

Figure 34: Mean ML chlorophyll, nitrate, silicic acid and phosphate for the 180° mooring line climatology (blue) and TIW composite (red). Error bars are the standard deviation from the mean for every latitude bin. Red stars are latitudes for which significant differences were found using two-tailed *t* tests ($p < 0.05$).

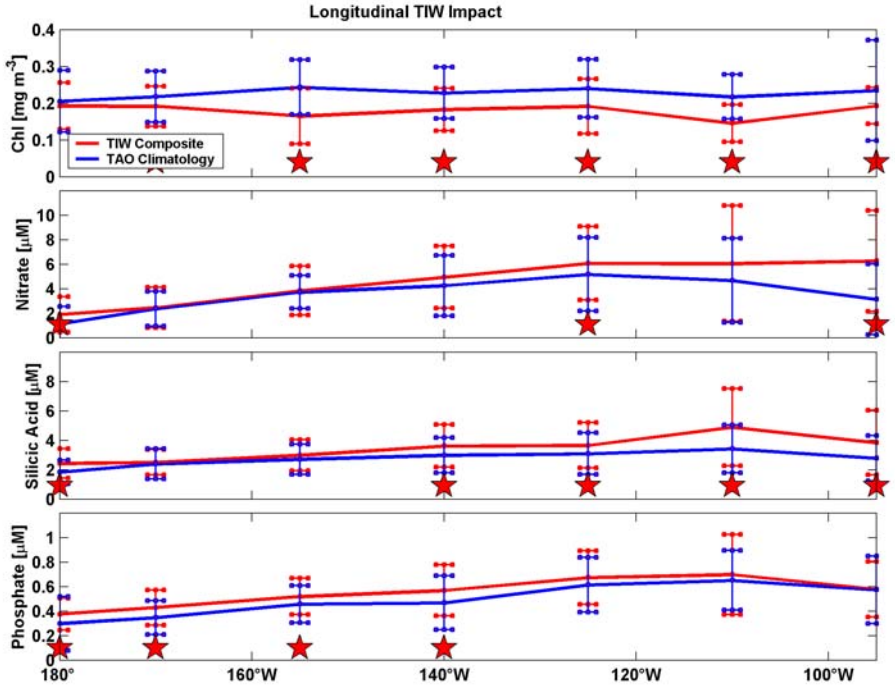

Figure 35: Longitudinal trend in TAO climatology and TIW composite mean ML nutrients and chlorophyll from 8°S to 8°N along the TAO lines from 95°W to the dateline. Error bars are the standard deviation from the mean. Red stars are longitudes for which significant differences were found using two-tailed *t* tests ($p < 0.05$).

4 Discussion

Of the 24 cruises that crossed TIWs, a large number occurred during boreal fall, from September to November. Several cruises were also observed crossing TIWs during boreal winter, from December to February, and one exceptional example occurred in May when the westward flowing zonal current velocities are typically reduced (Philander, 1990). This seasonal variability in TIW observations allows discussion of not only the effect of TIW intensity on nutrient and chlorophyll distributions but also the possible modification of TIW effects due to seasonal changes in the thermocline depth. It should be noted that the majority of TIWs observed that permit the following discussion were in the northern hemisphere. Southern hemisphere TIWs appear very different than northern TIWs, and it was not possible to discern differences in intensity among southern hemisphere TIWs in this analysis.

This thesis has focused on two broad categories of TIW impacts; individual TIW effects and their mean effect on nutrient and chlorophyll distributions. The effects from individual TIWs can be broken down into three categories: (1) The impacts from strong versus weak vortices, (2) Differences caused by the seasonality in the zonal currents and the depth of the thermocline, and (3) Interannual modulation of TIW impacts. The mean TIW effects are quantified by the differences in mean ML nutrients and chlorophyll between the TAO climatology and TIW composites. The results from the individual TIW and mean ML comparisons will be used to briefly discuss the role of TIWs in shaping the monthly distributions of SeaWiFS derived climatological chlorophyll.

4.1 Individual TIW impacts

4.1.1 TIW intensity

Strong and weak TIWs occurring during boreal fall were observed in the northern hemisphere along 155°W. During 1998 the TIW was intense with high horizontal current velocities and strong evidence of rotation indicative of the vortex. The 1999 TIW was substantially weaker with slower horizontal current velocities. During October 1998 the cold tongue was more developed indicating enhanced upwelling relative to the cruise period in October 1999. The cruise sections (figs. 36 and 37) and the SeaWiFS chlorophyll composites for the cruise periods (fig. 26) illustrate the extensive differences in impact between these two vortices. During both cruise periods the thermocline trough near 5°N was well developed (~150 m) while the thermocline near the equator in 1998 was slightly (~30 m) shallower.

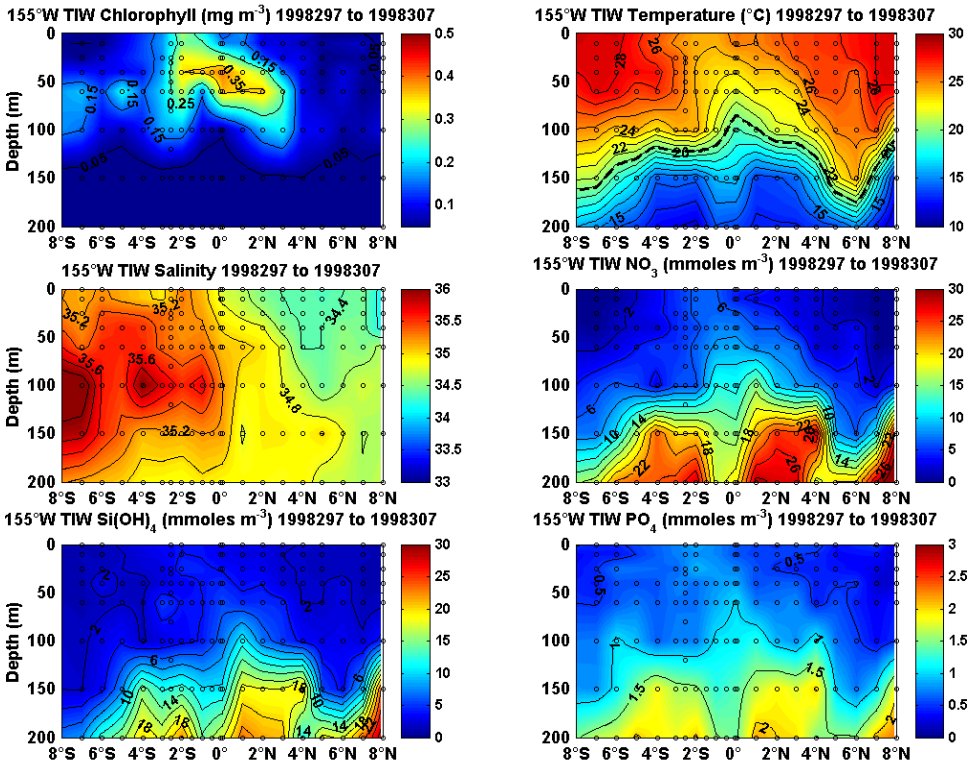

Figure 36: Latitude/depth sections of chlorophyll (mg m^{-3}), temperature (°C), salinity, nitrate (mmol m^{-3}), silicic acid (mmol m^{-3}) and phosphate (mmol m^{-3}) for the 1998 155°W TAO cruise which crossed a strong TIW during boreal fall.

The impact of the vortices is considerably different between years, particularly above the thermocline north of the equator. In 1998 there was an intrusion from the north of warm, lower salinity water within the upper 100 m which is indicative of the tropical water mass present north of the equatorial front (Chavez and Brusca, 1991). These water mass characteristics have also been used as an indicator of the NECC (Wyrtki and Kilonsky, 1984). This water mass was low in nutrients and chlorophyll, and so the resultant nutrient concentrations in the upper 100 m north of the equator were very low, with silicic acid concentrations less than 2 mmol m^{-3} and chlorophyll concentrations of ~0.1 mg m^{-3}. Only within 2° of the equator were chlorophyll concentrations above 0.25 mg m^{-3} observed, with the highest surface values just south of the equator. This was

likely the result of the shallow thermocline on the equator which enhanced nutrient concentrations within the upper 100 m above climatological values (App. C, pg. 126, fig. 105). North of the equator the 0.15 mg m^{-3} chlorophyll isopleth appeared to protrude down into the water column as the low salinity water mass moved toward the equator in the recirculating flow of the TIW vortex. The SeaWiFS chlorophyll composite (fig. 26) showed a low chlorophyll tongue directed toward the equator east of the extension of higher chlorophyll associated with the TIW SST frontal extension. The TIW vortices in this composite image appear to constrict the high chlorophyll concentrations near the equator.

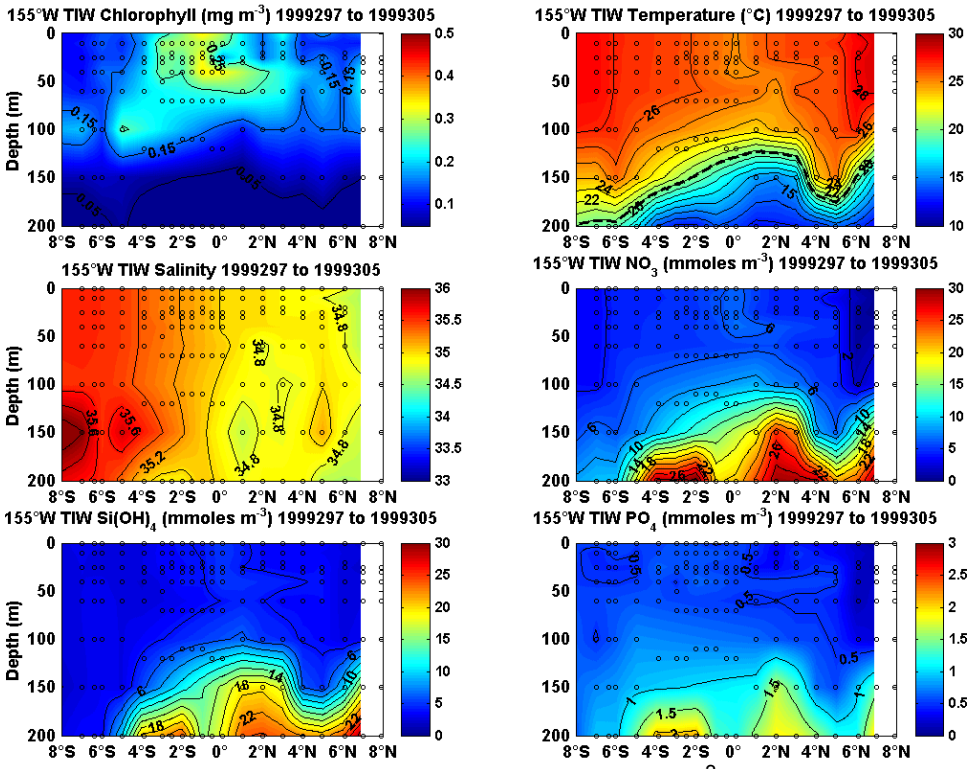

Figure 37: Latitude/depth sections of chlorophyll (mg m^{-3}), temperature (°C), salinity, nitrate (mmol m^{-3}), silicic acid (mmol m^{-3}) and phosphate (mmol m^{-3}) for the 1999 155°W TAO cruise which crossed a weak TIW during boreal fall.

In October 1999 the restriction of high chlorophyll concentrations to near the equator is less evident as no tongue of lower chlorophyll is apparent in the

composite image and the difference between the composites show higher chlorophyll concentrations within the 1999 TIW (fig. 26). It should be noted that with the shallower thermocline, the October 1998 cruise section showed higher chlorophyll concentrations directly on the equator. The intrusion of the fresher tropical water from north of the equator appeared near 6°N during October 1999, compared to nearly reaching the equator in October of 1998. Nutrient concentrations are generally higher across the northern portion of the section, with silicic acid concentrations never falling below 2 mmol m^{-3}. Also the coverage of chlorophyll concentrations greater than 0.15 mg m^{-3} is substantially enhanced compared to the chlorophyll distribution in October 1998.

The consecutive TIWs sampled on 125°W and 140°W cruises in September 1999 and in February 2000 do not appear to be substantially different from each other in terms of intensity, although the 1999 cruises did appear to cross different portions of the TIW. As mentioned in the previous chapter the 140°W September 1999 cruise seemed to cross slightly east of the SST frontal extension as the horizontal current velocities showed a predominance of southward flow (fig. 21). Regardless, the impacts in the water column appear very similar for the two boreal fall cruises. Both TIWs were strong and nutrient concentrations are lower than climatological values between the equator and ~4°N in the upper 100 m, although data from both cruises demonstrated a slight enhancement north of 4°N from the entrainment of upwelled water in the recirculating portion of the vortex (fig. 38; see also figs.19 and 21). Cruise sections from both cruises demonstrate low chlorophyll concentrations in the

northern portions of the line with higher values only appearing from the equator to 2°S. Between the two cruise sections the highest chlorophyll concentrations were observed on the 140°W line just south of the equator, with values in excess of 0.35 mg m^{-3}.

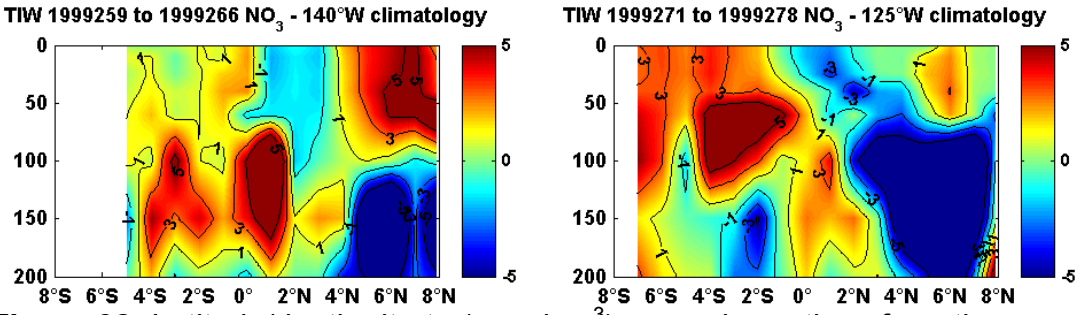

Figure 38: Latitude/depth nitrate (mmol m^{-3}) anomaly sections from the consecutive September 1999 cruises on the 140°W (left panel) and 125°W (right panel) TAO lines.

Two 140°W cruises in January of 1999 and 2001 demonstrated the varying impact of strong versus weak TIWs occurring during boreal winter. It should be noted that the TIW SST frontal extension for the 1999 140°W cruise appeared quite large, but the horizontal current velocities are substantially slower than those from boreal fall cruises. Nonetheless, the 1999 140°W cruise crossed a strong TIW as indicated by both the SST field and the ADCP horizontal current velocities (fig. 23). Upwelling appeared to be considerably greater during this period. Nutrient concentrations were enhanced during 1999 both north and south of the equator because of entrainment of upwelled water in the vortex. A region of impoverishment was visible where warm fresh tropical water from the north intersected the transect. Where this water mass crosses the cruise section a deep trough (~150 m) is present in the thermocline which does not appear during the 125°W cruise that occurred approximately a week later (App. C, pgs. 111 and

119, figs. 74 and 90). Conversely, the January 2001 cruise section showed a greater spatial extent of nutrient enhancement which was continuous from the northern to southern portions of the line within the upper 100 m (fig. 39). Chlorophyll concentrations reached a greater magnitude during the January 1999 cruise, but only south of the equator and confined to a very tight latitudinal range (1.5°S to 0°). North of the equator concentrations were very low (<0.15 mg m^{-3}). Chlorophyll concentrations during the January 2001 cruise were higher in the region north of the equator.

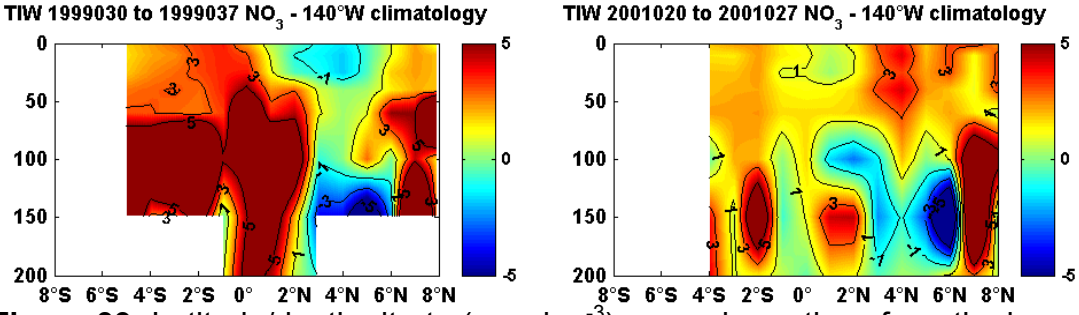

Figure 39: Latitude/depth nitrate (mmol m^{-3}) anomaly sections from the boreal winter cruises of the 140°W TAO line in 1999 (left panel) and 2001 (right panel).

These comparisons provide evidence that strong TIWs result in enhanced recirculating (equatorward) flow, as is indicated by the differences in the horizontal currents for both the October 155°W cruises and the January 140°W cruises (figs. 23 and 25). The recirculating flow advects warmer, fresher, nutrient- and chlorophyll-poor tropical water toward the equator, resulting in decreases in nutrient concentrations within the upper 100 m. Chlorophyll on some sections can be seen to protrude down into the water column which can be viewed as evidence of subduction occurring as the less dense water mass over-rides the denser water mass on the equator (fig. 36). Therefore, the strong TIWs observed in the northern hemisphere drive reductions in nutrients and chlorophyll north of

the equator; whereas weak TIWs retain higher nutrient concentrations thus permitting higher chlorophyll concentrations across the cruise sections.

These reductions in nutrient concentrations below climatological values were only observed for cruises which crossed TIWs in the northern hemisphere. In the southern hemisphere, the recirculating flow was weaker. The equatorward current velocities observed within southern TIWs during September 1999 and January 2001 along the 140°W line were considerably smaller than equatorward velocities observed in the northern hemisphere (figs. 21 and 23). This observation may be biased by insufficient observations of southern TIWs, in particular strong TIWs. This suggests that the dynamics are different between southern and northern hemisphere TIWs, as has been observed previously (Chelton *et al*., 2000; 2001). It should be noted that cruise sections crossing TIWs in the northern hemisphere were easily identified whereas southern hemisphere TIW crossings were more difficult to discern. The differences in the TIWs between the two hemispheres may be the result of the differences in the southern and northern surface countercurrents. TIWs north of the equator have a very regular appearance whereas southern TIWs do not (Legeckis *et al*., 2004), likely due to weaker shear associated with the weak SECC.

The differences in northern and southern TIWs may imply considerable differences in carbon cycling driven by TIWs in the two hemispheres. Archer *et al.* (1997) discussed the possibility of a ‘leak’ in the biological pump in the northern hemisphere associated with a TIW wave front, whereby upwelled nutrients are subducted at the convergent boundary of the wave front before they

can be assimilated by phytoplankton. South of the equator there is little evidence of convergence, so possibly no 'leak' in the biological pump, since flow in the SECC is low and variable (Eldin, 1983; Kessler and Taft, 1987). This has important consequences for the region south of the equator as there is a considerable difference in the iron input between the two hemispheres. Aeolian iron input south of the equator is considerably lower than in the north (Jickells *et al*., 2005), thus the only iron source to the south is from southward lateral advection of upwelled EUC waters which are relatively high in dissolved and particulate iron concentrations (Coale *et al*., 1996). This difference in iron sources between the two hemispheres has been used to explain the asymmetry in equatorial nitrate concentrations in the surface water (Pennington *et al*., 2006) as iron limitation negatively affects nitrate uptake in phytoplankton (Timmermans *et al*., 1994). The present view is that export production in the southern hemisphere is lower than in the north (Murray *et al*., 1996), but the transport of nutrients (and possibly iron from the EUC) southward by TIWs, as shown here, could drive episodic enhancements of southern hemisphere carbon export.

4.1.2 Seasonal differences of TIW impacts

There is a general greening in the area from about to equator to approximately 12°N and from the coast of Central America to west of 160°W that seems to persist from February to about May (fig. 40). The term greening, as opposed to bloom, is used because the chlorophyll increase is small (~0.1 mg m^{-3}), but occurs over a considerably large area so is potentially important in shaping the ecosystem structure in the eastern tropical Pacific. This apparent

seasonality in the region north of the equator has been observed in SeaWiFS imagery, as described here, but apparently not in ship-based observations (Pennington et al., 2006). This region is economically important as it sustains a significant multinational yellowfin tuna fishery. Spatial variability in catch per unit effort recorded by the Mexican fleet appears to lag behind the seasonality of the region, with high catches being recorded for the region from May through August (Ortega-Garcia *et al*., 2003).

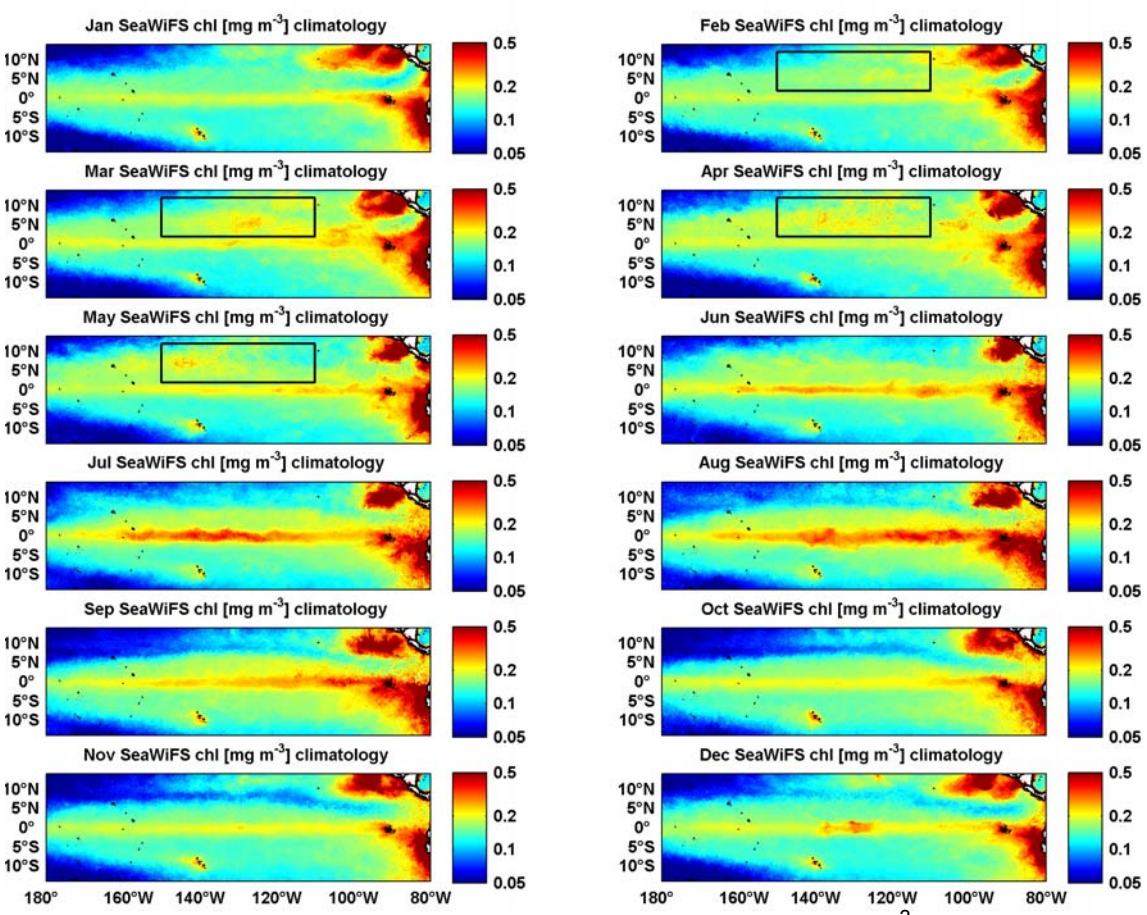

Figure 40: Climatological monthly SeaWiFS chlorophyll (mg m^{-3}) for the equatorial Pacific. The general region of greening mentioned in the text above is indicated by the black box north of the equator. Note chlorophyll concentrations are presented on a logarithmic scale.

The TIW cruises identified during the initiation of this greening, i.e. during February, show increases in chlorophyll on the northern portions of the cruise

lines. This is particularly evident on the February 2000 125°W cruise where the spatial extent of increased chlorophyll is greater than any increase on or south of the equator for any other cruise in this record (fig. 41). Chlorophyll concentrations during this cruise reached values in excess of 0.3 mg m^{-3} from 2°N to 8°N within the upper ~100 m. It is plausible that TIWs amplify this seasonal signal near the equator. TIWs in this time frame would act to advect this now higher chlorophyll water from the north toward the equator, perhaps increasing the chlorophyll concentrations as a whole from 8°N to 8°S and expanding the range of the tuna fishery.

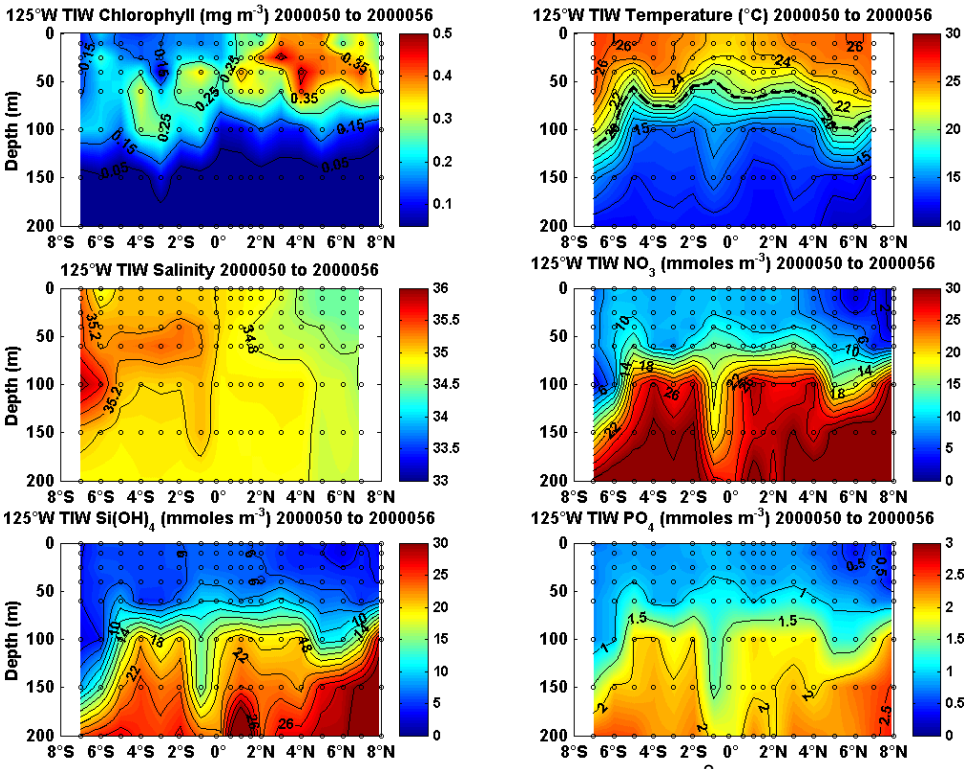

Figure 41: Latitude/depth sections of chlorophyll (mg m^{-3}), temperature (°C), salinity, nitrate (mmol m^{-3}), silicic acid (mmol m^{-3}) and phosphate (mmol m^{-3}) for the 2000 125°W TAO cruise which crossed a TIW during boreal winter.

The mechanism for this seasonality seems to be the large difference in thermocline topography between fall and winter. Another possibility may be the

advection of high chlorophyll concentrations westward from Tehuantepec eddies (seen in chlorophyll animations), but they do not appear to extend west of 120°W. The strong convergence that is generated when the SEC and NECC are flowing at their maximum during boreal fall forms the trough in the thermocline near ~5°N (Kessler and Taft, 1987; fig. 2). During boreal winter these currents relax and the thermocline trough shoals, providing a shallower more accessible nutrient source for the euphotic zone north of the equator. TIWs acting at this time are likely incorporating more nutrients into the surface ocean through enhanced upwelling and so magnifying this seasonality. The EUC is also flowing at its maximum during this period (Philander, 1990) which could be providing both the shear source for the TIWs as well as iron and silicic acid from the lower EUC waters (Dugdale *et al.* 2002). These nutrients could stimulate phytoplankton assemblage shifts toward more diatom dominated communities which would enhance export production north of the equator during boreal winter.

4.1.3 Interannual modulation of TIW impact

Although it has been shown that strong TIWs reduce nutrient and chlorophyll concentrations, enhanced upwelling is still occurring on the equator during both weak and strong TIWs (*e.g.* 155°W cruises, figs. 36 and 37). Changes in the source water nutrient concentrations of this upwelled water would alter the impact of TIWs on both nutrient and chlorophyll distributions. In examining the thermocline depth variability, it is clear that substantial seasonal variability is present off the equator (fig. 27). On the equator, thermocline depth variability seems driven mainly by interannual forcing. A gradual increase in the

thermocline depth since the 1998 La Nina event at the equator can be seen in figure 42. If the assumption is made that the source waters from the TIW-enhanced upwelling are coming from the EUC, which is the iron source for the region (Coale *et al.*, 1996), this interannual variability in the depth of the thermocline would imply interannual variability in the TIW nutrient enhancement. To summarize, significant differences exist between individual TIWs. Some of these differences are due to variability of the vortices themselves, while others are due to seasonal and interannual modification of the physical environment within which the vortices exist. This variability makes it difficult to generalize regarding TIW influences on nutrient and chlorophyll distributions.

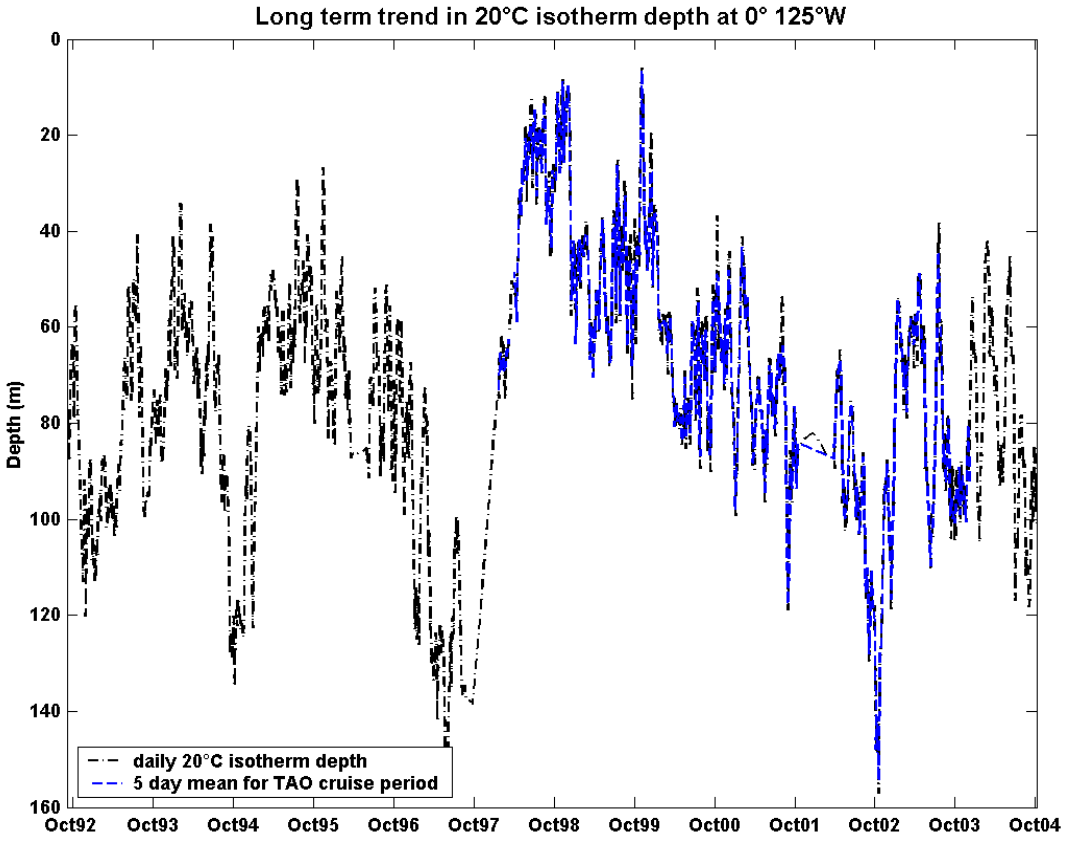

Figure 42: Long term trend in daily 20°C isotherm depth of the 0° 125°W TAO mooring, with the 5 day mean plotted in blue for the TAO cruise database period of observation used for this analysis.

4.2 Mean TIW impacts

Comparison of mean ML nutrient and chlorophyll concentrations from the TAO line climatology and the TIW composites illustrate the average effect of TIWs on the mixed layer in the equatorial Pacific. From this comparison there is no evidence of enhanced chlorophyll from TIWs within the mixed layer across all TAO lines, although nutrient concentrations do appear enhanced in the mixed layer south of the equator in the eastern Pacific and on and north of the equator in the central western Pacific.

This trend in nutrient enhancement can be explained by considering the differences between northern and southern TIWs. North of the equator, the majority of TIWs observed were during boreal fall. Strong vortices present at this time drive reductions in nutrient and chlorophyll concentrations due to enhanced equatorward transport of impoverished water from adjacent to the upwelling zone. South of the equator, strong southward advection of nutrient replete water was observed with little evidence of recirculating flow in TIW vortices. This increased nutrient concentrations in the mixed layer south of the equator in the eastern Pacific. The southern enhancement decreased from east to west across the basin due to stronger southward flow observed on the eastern TAO lines which was not seen on the central and western lines (figs. 19 and 25). In the west, southward advection of nutrients is less pronounced; so no change in nutrient concentrations from the climatological average is apparent there (*e.g.* fig. 34).

West of 125°W, enhanced nutrients appear on the equator, with some enhancement present in the mixed layer near 6°N due to the entrainment of upwelled water in the recirculating (southward) flow of a TIW vortex. This entrainment in the recirculating flow of a vortex brings into question exactly how much of a 'leak' may be present in northern TIWs as some of the nutrients may not be subducted unused.

The lines where this comparison is most robust (*i.e.* having the highest number of TIW observations) are the 125°W and 140°W TAO lines (figs. 30 and 31). Across both of these lines chlorophyll concentrations in the mixed layer were depressed as a result of the recirculating flow in TIW vortices advecting nutrient- and chlorophyll-poor water towards the equator from the north. In the southern hemisphere, chlorophyll was not observed to increase concomitant with nutrient increases. This may have been the result of the lag time between nutrient enhancement and increases in phytoplankton biomass, or missing chlorophyll increases in unsampled portions of the southern TIWs. Composite images from September 1999 for both the 140°W and 125°W cruise periods illustrate regions of increased chlorophyll which were not transected by the TAO cruises (figs. 20 and 22). To summarize the individual and mean TIW impacts, strong TIWs reduce nutrient and chlorophyll concentrations through enhanced horizontal advection while weak TIWs retain higher nutrient concentrations which allows a greater spatial extent of elevated chlorophyll. The average effect from TIWs is to reduce chlorophyll concentrations below climatological values within the mixed layer, but mixed layer nutrient enhancements are evident.

4.3 Monthly SeaWiFS chlorophyll climatology

Two interesting features that arose from this analysis are the general greening north of the equator in boreal winter and the difference in TIW nutrient enhancement between the northern and southern hemispheres. These results will be used to explain the monthly distribution of chlorophyll as depicted in SeaWiFS monthly climatologies.

Figure 43 shows the latitudinal and longitudinal variation of monthly climatological SeaWiFS chlorophyll. The area of greening is clearly shown north of the equator from February through May in the upper panel. During this period, TIWs may act to redistribute chlorophyll concentrations, advecting water from this region of greening toward the equator. In June the southeast trade winds intensify (Philander, 1990) causing the SEC and NECC to increase, and the trough near ~5°N to develop. This results in a strong delineation of chlorophyll concentrations between the northern and southern sides of the convergent boundary. During boreal fall TIWs are strong, which further sharpens this boundary north of the equator and restricts high chlorophyll concentrations to the region directly near the equator, as was seen in the composite image in figures 20 and 22. The maximum in chlorophyll concentrations occurs within these months directly on the equator, and is a result of both enhanced wind-driven upwelling and the focusing of chlorophyll concentrations near the equator by strong TIWs.

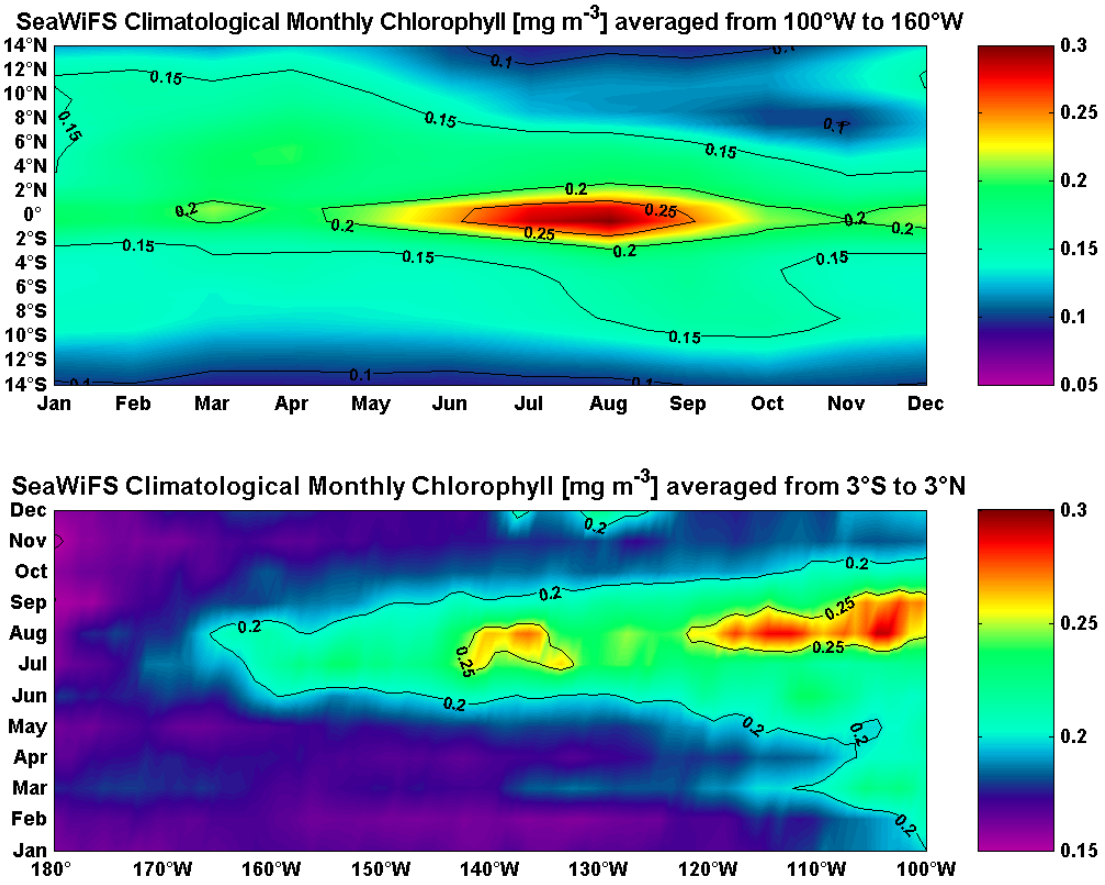

Figure 43: Latitudinal (top panel) and longitudinal (lower panel) trend in monthly climatological SeaWiFS chlorophyll (mg m-3).

Another component of the September peak in chlorophyll appears to be some form of (Kelvin) wave forcing as the peak first appears in the west Pacific in July and translates east to 100°W by September (lower panel of fig. 43). This is consistent with large blooms in the equatorial Pacific being forced by Kelvin wave activity which shoals the thermocline (Ryan *et* al., 2002). Further evidence for the role of Kelvin waves is that the annual cycle of upwelling favorable wind stress curl intensifies in the eastern Pacific in June, moving to the central/western Pacific in July/August (Amador *et al.*, 2006), opposite to Kelvin wave propagation. That is the chlorophyll pattern follows the Kelvin wave pattern, not the pattern in upwelling favorable wind stress curl. At the start of boreal winter

chlorophyll concentrations decrease on the equator and the latitudinal range of chlorophyll concentrations ~0.2 mg m^{-3} is further restricted to the equator as strong TIWs are persistent until approximately January. One final interesting point concerning the monthly latitudinal SeaWiFS chlorophyll climatology is the slight increase in chlorophyll concentrations south of the equator during the peak TIW season. This is evidence of enhanced chlorophyll concentrations derived from the enhanced southward advection of nutrients, as observed on the cruises crossing southern TIWs.

5 Conclusions

The goal of this thesis was to address three specific questions concerning the role of TIWs in shaping nutrient and chlorophyll distributions in the equatorial Pacific. The objectives were to identify how nutrient concentrations changed in response to TIWs, how phytoplankton biomass responded to these changes, and how the alteration of these fields changes as a function of latitude and longitude. To develop this understanding, a case study approach of individual TIWs as well as a first attempt to calculate their average effect on the mixed layer was established. From this retrospective analysis of TIW seasons some general conclusions about their affects on nutrient and chlorophyll distributions can be made.

Nutrient and chlorophyll concentrations change a great deal due to TIW-enhanced vertical and horizontal advection. Enhanced vertical advection is present during both strong and weak TIWs (*e.g.* 155°W TIW cruises), which increase nutrient concentrations directly on the equator. Increased chlorophyll was also present directly on the equator, but generally below the mixed layer. North of the equator, enhanced horizontal advection from strong TIWs transports warm, low salinity water toward the equator in the recirculating portion of the vortex. This water mass is low in nutrients and chlorophyll which reduces their concentrations north of the equator. During one cruise through a strong TIW, the 0.15 mg m^{-3} chlorophyll isopleth protruded down into the water column as the southward movement of the less dense water mass from the north forced the subduction of the denser chlorophyll rich waters on the equator. This recirculation

is less apparent during weak TIWs which retain higher concentrations of nutrients and increase the spatial extent of chlorophyll above 0.15 mg m^{-3}.

Southern hemisphere TIWs appear very different from northern TIWs as they do not display the degree of recirculating flow that is present in the north. Recirculating flow within southern TIWs was observed on the 140°W TAO line during January 1999, September 1999 and January 2001, but was consistently less pronounced than the recirculating flow within northern TIWs. Most of the horizontal advection observed south of the equator was directed south, especially in the eastern Pacific. This enhanced southward advection lead to increases in nutrient concentrations south of the equator, and abated toward the west. There were no observations from TAO cruises of increased chlorophyll concomitant with this southern hemisphere nutrient enhancement, though SeaWiFS chlorophyll composites show regions of elevated chlorophyll which appear to be associated with TIW fronts not sampled by TAO cruises.

This difference in transport within TIW vortices implies substantial differences in the carbon fluxes between TIWs in the northern and southern hemispheres. Strong convergence associated with northern hemisphere TIW fronts (Johnson, 1996) will result in the subduction of unassimilated nutrients (Archer *et al.*, 1997), while this is not the case in the southern hemisphere as convergence is less evident (Eldin, 1983; Kessler and Taft, 1987). Therefore, the apparent ‘leak’ in the biological pump from TIW fronts in the northern hemisphere (Archer *et al.*, 1997) may not exist in the southern hemisphere. Note that nutrient enhancements were observed in the central Pacific on the northern portions of

the TAO lines due to the entrainment of upwelled water in the recirculating portion of the vortex. This brings into question the magnitude of the ‘leak’ in the biological pump within northern TIWs. Regardless, episodic southward lateral injection of nutrients (and possibly iron from the EUC) from TIWs may be an important component of export production south of the equator.

In combination with the varying impact from differences in TIW intensity, as well as the north/south differences in TIW effects, the seasonal change in the depth of the thermocline north of the equator also modulates TIW impacts. The thermocline shoaling during boreal winter, combined with weak TIWs which retain elevated nutrient concentrations, drive nutrients well above climatological values from 8°N to 8°S. The largest increase in chlorophyll north of the equator, in terms of magnitude and spatial extent, was observed in February when a weak TIW was crossed on the 125°W TAO line during the seasonal minimum in the thermocline depth. From this observation the hypothesis can be made that a synergistic effect on nutrient and chlorophyll concentrations exists from the combined impact of weak TIWs and a shallow thermocline during boreal winter. This possibility should be further examined as the region sustains an economically important yellowfin tuna fishery, and horizontal advection by TIWs could affect the spatial extent of this fishery. The shallower nutrient source waters in combination with a stronger and shallower EUC could also facilitate phytoplankton assemblage shifts that may result in boreal winter maxima in export production north of the equator.

Lastly, these conclusions concerning the role of TIWs in shaping nutrient and chlorophyll distributions have been expanded to explain the monthly distribution of chlorophyll from SeaWiFS climatologies in the equatorial Pacific. TIWs play a significant role in confining high chlorophyll concentrations near the equator during their peak season, as was seen in the composite images. Also, the southern hemisphere increase in climatological chlorophyll during boreal fall provides some evidence of increased phytoplankton biomass associated with the southern transport of nutrients within TIWs. Finally, TIWs may be amplifying and/or extending the spatial extent of the seasonal signal north of the equator. TIWs are therefore fundamental in shaping equatorial Pacific climatological chlorophyll distributions.

6 Future work

A potential criticism of this analysis is that the coarse temporal and spatial resolution of ship observations may provide an incomplete representation of the phytoplankton response to TIWs. While this may be true, the compilation of multiple cruises and the case study approach have facilitated significant progress towards understanding the role of TIWs in shaping nutrient and chlorophyll distributions. One potential enhancement of this analysis would be to incorporate optical instrumentation for quantifying phytoplankton biomass and particle abundance on TAO moorings. This strategy would provide high temporal resolution measurements, but at a limited spatial resolution. From the conclusions of this thesis, we can discern the best deployment locations for resolving the impacts of both northern and southern hemisphere TIWs, as well as their role in the seasonal greening north of the equator. These locations are along the 125°W or 140°W TAO lines at the 5°N, 0° and 5°S moorings. Bio-optical instruments were deployed on the 0° 140°W mooring during boreal fall 2005, and comparisons between this deployment and future deployments will be one focal point of continuing work.

A second focus area should be the development of a better understanding of the mechanisms driving the observed impacts via model/data comparisons. A three-dimensional model capable of resolving TIWs has been developed at the University of Maine (Shi *et al*., 2006) and comparisons of the TIW observations presented in this thesis with model output will enable us to follow TIW impacts

from physics, to nutrient and biological effects, to the impact on carbon fluxes and air-sea CO_2 exchange.

Lastly, assemblage shifts within the phytoplankton have important consequences for equatorial carbon cycling. From this thesis we can frame several hypotheses concerning assemblage shifts, for instance: (1) Strong TIWs facilitate assemblage shifts in equatorial phytoplankton, (2) Assemblage shifts are more pronounced north of the equator during boreal winter because of the synergistic effect of TIWs and seasonal changes in the thermocline depth, and (3) Lateral nutrient additions from TIWs in the southern hemisphere facilitate episodic assemblage shifts which enhance southern export production.Evidence for these shifts can be provided through biogenic silica distributions, size-fractionated chlorophyll and accessory pigment analyses, and backscatter/beam *c* ratios. These data exist and we will use them to address future research questions.

7 References

Archer, D., J. Aiken, W. Balch, D. Barber, J. Dunne, P. Flament, W. Gardner, C. Garside, C. Goyet, E. Johnson, D. Kirchman, M. McPhaden, J. Newton, E. Peltzer, L. Welling, J. White and J. Yoder (1997), A meeting place of great ocean currents: shipboard observations of a convergent front at 2°N in the Pacific, *Deep-Sea Research II*, 44, 1827-1850.

Amador, J.A., E.J. Alfaro, O.G. Lizano and V.O. Magaña (2006), Atmospheric forcing of the eastern tropical Pacific: A review, *Progress in Oceanography*, 69, 101-142.

Barber, R.T. and F.P. Chavez (1991), Regulation of Primary Production Rate in the Equatorial Pacific, *Limnology and Oceanography*, 36(8), 1803-1815.

Barber, R.T., M.P. Sanderson, S.T. Lindley, F. Chai, J. Newton, C.C. Trees, D.G. Foley and F.P. Chavez (1996), Primary Productivity and its regulation in the equatorial Pacific during and following the 1991-1992 El Niño, *Deep-Sea Research II*, 43, 933-970.

Bjerknes, J. (1969) Atmospheric Teleconnections from the Equatorial Pacific, *Monthly Weather Review*, 97(3), 163-172.

Chavez, F.P. and R.C. Brusca (1991), The Galapagos Islands and Their Relation to Oceanographic Processes in the Tropical Pacific, In M.J. James (Ed.), *Galapagos Marine Invertebrates* (pp. 9-33), Plenum Press, New York.

Chavez, F.P. and J.R. Toggweiler (1995), Physical estimates of global new production: the upwelling contribution, In C.P. Summerhayes, K.C. Emeis, M.V. Angel, R.L. Smith and B. Zeitzschel (Eds.), *Upwelling in the Ocean: Modern Processes and Ancient Records* (pp. 313-320), Wiley, New York.

Chavez, F.P., P.G. Strutton, G.E. Friederich, R.A. Feely, G.C. Feldman, D.G. Foley and M.J. McPhaden (1999), Biological and Chemical Response of the Equatorial Pacific to the 1997-98 El Niño, *Science*, 286, 2126-2131.

Chelton, D.B., F.J. Wentz, C.L. Gentemann, R.A. de Szoeke and M.G. Schlax (2000), Satellite Microwave SST Observations of Transequatorial Tropical Instability Waves, *Geophysical Research Letters*, 27, 1239-1242.

Chelton, D.B., S.K. Esbensen, M.G. Schlax, N Thum, M.H. Freilich, F.J. Wentz, C.L. Gentemann, M.J. McPhaden and P.S. Schopf (2001), Observations of Coupling between Surface Wind Stress and Sea Surface Temperature in the Eastern Tropical Pacific, *Journal of Climate*, 14, 1479-1498.

Coale, K.H., S.E. Fitzwater, R.M. Gordon, K.S. Johnson and R.T. Barber (1996), Control of community growth and export production by upwelled iron in the equatorial Pacific Ocean, *Nature*, 379, 621-624.

Dam, H.G., X. Zhang, M. Butler and M.R. Roman (1995), Mesozooplankton grazing and metabolism at the equator in the central Pacific: Implications for carbon and nitrogen fluxes, *Deep-Sea Research II*, 42(2-3), 735-756.

Dugdale, R.C., F.P. Wilkerson and H.J. Minas (1995), The role of a silicate pump in driving new production, *Deep-Sea Research I*, 42(5), 697-719.

Dugdale, R.C., A.G. Wischmeyer, F.P. Wilkerson, R.T. Barber, F. Chai, M.-S. Jiang and T.-H. Peng (2002), Meridional asymmetry of source nutrients to the equatorial Pacific upwelling ecosystem and its potential impact on ocean-atmosphere CO_2 flux; a data and modeling approach, *Deep-Sea Research II*, 49, 2513-2531.

Dunne, J.P., J.W. Murray, M. Rodier, and D.A. Hansell (2003), Export flux in the western and central equatorial Pacific: zonal and temporal variability, *Deep-Sea Research I*, 47, 901-936, 2003.

Eldin, G. (1983), Eastward Flows of the South Equatorial Central Pacific, *Journal of Physical Oceanography*, 13, 1461-1467.

Eldin, G., and M. Rodier (2003), Ocean Physics and nutrient fields along 180° during an El Niño-Southern Oscillation cold phase, *Journal of Geophysical Research*, 108(C12), 8137, doi:10.1029/2000JC000746.

Feely, R.A., R. Wanninkhof, C.E. Cosca, P.P. Murphy, M.F. Lamb and M.D. Steckley (1995), CO_2 distributions in the equatorial Pacific during the 1991-1992 ENSO event, *Deep-Sea Research II*, 42(2-3), 365-386.

Feely, R.A., R. Wanninkhof, T. Takahashi and P. Tans (1999), The influence of El Niño on the equatorial Pacific contribution to atmospheric CO_2 accumulation, *Nature*, 398, 597-601.

Flament, P.J., S.C. Kennan, R.A. Knox, P.P. Niiler and R.L. Bernstein (1996), The three-dimensional structure of an upper ocean vortex in the tropical Pacific Ocean, *Nature*, 383, 610-613.

Foley, D.G., T.D. Dickey, M.J. McPhaden, R.R. Bidigare, M.R. Lewis, R.T. Barber, S.T. Lindley, C. Garside, D.V. Manov and J.D. McNeil (1997), Longwaves and primary productivity variations in the equatorial Pacific at 0°, 140°W, *Deep-Sea Research II*, 44, 1801-1826.

Gorgues, T., C. Menkes, O. Aumont, J. Vialard, Y. Dandonneau and L. Bopp (2005), Biogeochemical impact of tropical instability waves in the equatorial Pacific, *Geophysical Research Letters*, 32, L24615.

Halpern, D., R.A. Knox, D.S. Luther and S.G.H. Philander (1989), Estimates of Equatorial Upwelling Between 140° and 110°W During 1984, *Journal of Geophysical Research,* 94(C6), 8018-8020.

Holm-Hansen, O., C.J. Lorenzen, R.W. Holmes and J.D.H. Strickland (1965), Fluorometric Determination of Chlorophyll, *International Council for the Exploration of the Sea*, 30, 3-15.

Jickells, T.D., Z.S. An, K.K. Anderson, A.R. Baker, G. Bergametti, N. Brooks, J.J. Cao, P.W. Boyd, R.A. Duce, K.A. Hunter, H. Kawahata, N. Kubilay, J. laRoche, P.S. Liss, N. Mahowald, J.M. Prospero, A.J. Ridgwell, I. Tegen and R. Torres (2005), Global Iron Connections Between Desert Dust, Ocean Biogeochemistry, and Climate, *Science*, 308, 67-71.

Johnson, E.S. (1996), A convergent instability wave front in the central tropical Pacific, *Deep-Sea Research II*, 43, 753-778.

Johnson, G.C., and M.J. McPhaden (1999), Interior Pycnocline Flow from the Subtropical to the Equatorial Pacific Ocean, *Journal of Physical Oceanography,* 29, 3073- 3089.

Johnson, G.C., M.J. McPhaden, G.D. Rowe and K.E. McTaggart (2000), Upper equatorial Pacific Ocean current and salinity variability during the 1996-1998 El Niño-La Niña cycle, *Journal of Geophysical Research,* 105(C1), 1037-1053.

Johnson, G.C., M.J. McPhaden and E. Firing (2001), Equatorial Pacific Ocean Horizontal Velocity, Divergence, and Upwelling, *Journal of Physical Oceanography,* 31, 839-849.

Kennan, S.C., and P.J. Flament (2000), Observations of a Tropical Instability Vortex, *Journal of Physical Oceanography*, 30, 2277-2301.

Kessler, W.S., and B.A. Taft (1987), Dynamic Heights and Zonal Geostrophic Transports in the Central Tropical Pacific during 1979-84, *Journal of Physical Oceanography*, 17, 97-122.

Landry, M.R., J. Constantinou and J. Kirshtein (1995), Microzooplankton grazing in the central equatorial Pacific during February and August, 1992, *Deep-Sea Research II*, 42(2-3), 657-671.

Landry, M.R., R.T. Barber, R.R. Bidigare, F. Chai, K.H. Coale, H.G. Dam, M.R. Lewis, S.T. Lindley, J.J. McCarthy, M.R. Roman, D.K. Stoecker, P.G. Verity and J.R. White (1997), Iron and Grazing Constraints on Primary Production in the Central Equatorial Pacific: An EqPac Synthesis, *Limnology and Oceanography*, 42(3), 405-418.

Legeckis, R., C.W. Brown, F. Bonjean and E.S. Johnson (2004), The influence of tropical instability waves on phytoplankton blooms in the wake of the Marquesas Islands during 1998 and on the currents observed during the drift of the Kon-Tiki in 1947, *Geophysical Research Letters,* 31, L23307.

Levitus, S. (1982), Climatological Atlas of the World Ocean, NOAA/ERL GFDL Professional Paper 13, Princeton, N.J., 173 pp. (NTIS PB83-184093).

McGillicuddy Jr., D.J., A.R. Robinson, D.A. Siegel, H.W. Jannasch, R. Johnson, T.D. Dickey, J. McNeil, A.F. Michaels and A.H. Knap (1998), Influence of mesoscale eddies on new production in the Sargasso Sea, *Nature*, 394, 263-266.

McPhaden, M.J., A.J. Busalacchi, R. Cheney, J.R. Donguy, K.S. Gage, D. Halpern, M. Ji, P. Julian, G. Meyers, G.T. Mitchum, P.P Niiler, P. Picaut, R.W. Reynolds, N. Smith and K. Takeuchi (1998), The Tropical Ocean-Global Atmosphere observing system: A decade of progress, *Journal of Geophysical Research,* 103(C7), 14,169-14,240.

Menkes, C.E., S.C. Kennan, P. Flament, Y. Dandonneau, S. Masson, B. Biessy, E. Marchal, G. Eldin, J. Grelet, Y. Montel, A. Morlière, A.Lebourges-Dhaussy, C. Moulin, G. Champalbert and A. Herbland (2002), A whirling ecosystem in the equatorial Atlantic, *Geophysical Research Letters*, 29(11), 10.1029/2001GL014576.

Munk, W.H. (1950), On the wind-driven ocean circulation, *Journal of Meteorology*, 7(2), 79-93.

Murray, J.W., R.T. Barber, M.R. Roman, M.P. Bacon and R.A. Feely (1994), Physical and Biological Controls on Carbon Cycling in the Equatorial Pacific, *Science*, 266(5182), 58-65.

Murray, J.W., J. Young, J. Newton, J. Dunne, T. Chapin, B. Paul and J.J. McCarthy (1996), Export flux of particulate organic carbon from the central equatorial Pacific determined using a combined drifting trap-^{234}Th approach, *Deep-Sea Research II*, 43(4-6), 1095-1132.

Ortega-Garcia, S., D. Lluch-Belda and P.A. Fuentes (2003), Spatial, seasonal, and annual fluctuations in relative abundance of Yellowfin Tuna in the

eastern Pacific ocean during 1984-1990 based on fishery CPUE analysis, *Bulletin of Marine Science,* 72(3), 613-628.

Pennington, J.T., K.L. Mahoney, V.S. Kuwahara, D.D. Kolber, R. Calienes and F.P. Chavez (2006), Primary Production in the Eastern Tropical Pacific: A Review, *Progress in Oceanography*.

Philander, S.G., (1990), *El Niño, La Niña, and the Southern Oscillation*, Academic Press, San Diego, California.

Qiao, L., and R.H. Weisberg (1995), Tropical instability wave kinematics: Observations from the Tropical Instability Wave Experiment, *Journal of Geophysical Research*, 100, 8677-8693.

Reynolds, R.W., and T.M. Smith (1994), Improved Global Sea Surface Temperature Analyses Using Optimum Interpolation, *Journal of Climate*, 7, 929-948.

Ryan, J.P., P.S. Polito, P.G. Strutton and F.P., Chavez (2002), Unusual large-scale phytoplankton blooms in the equatorial Pacific, *Progress in Oceanography*, 55, 263-285.

Sakamoto, C., Friederich, G.E., and L.A. Codispoti (1990), MBARI procedures for automated nutrient analyses using a modified Alpkem series 300 rapid flow analyzer, MBARI Technical Report 90-2.

Shi L., F. Chai, R.C. Dugdale, Y. Chao and R.T. Barber (2006), Variability of Nutrients and Phytoplankton Dynamics in the Equatorial Pacific Ocean between 1990-2004: a Three-Dimensional Modeling Study, *Eos Transactions,* AGU, 87, Ocean Sciences Meeting, Supplied Abstract OS35F-06.

Strutton, P.G., J.P. Ryan and F.P. Chavez (2001), Enhanced chlorophyll associated with tropical instability waves in the equatorial Pacific. *Geophysical Research Letters*, 28, 2005-2008.

Strutton, P.G., and F.P. Chavez (2004), Scales of biological-physical coupling in the equatorial Pacific, In L. Seuront and P.G. Strutton (Eds.), *Handbook of Scaling Methods in Aquatic Ecology: Measurement, Analysis, Simulation* (pp. 51-64). CRC Press: Boca Raton.

Timmermans, K.R., W. Stolte and H.J.W. de Baar (1994), Iron-mediated effects on nitrate reductase in marine phytoplankton, *Marine Biology*, 121(2), 389-396.

Tomczak, M. and J.S. Godfrey (2003), *Regional Oceanography: An Introduction 2nd Edition*, Daya Publishing House, Delhi.

Weisberg, R.H. and L. Qiao (2000), Equatorial Upwelling in the Central Pacific Estimated from Moored Velocity Profilers, *Journal of Physical Oceanography*, 30, 105- 124.

Wolter, K., and M.S. Timlin. (1998), Measuring the strength of ENSO events: How does 1997/98 rank?, *Weather*, 53, 315-324.

Wyrtki, K. (1981), An estimate of equatorial upwelling in the Pacific, *Journal of Physical Oceanography*, 11, 1205-1214.

Wyrtki, K., and B. Kilonsky (1984), Mean Water and Current Structure during the Hawaii-to-Tahiti Shuttle Experiment, *Journal of Physical Oceanography,* 14, 242-254.

Yoder, J.A., S.G. Ackleson, R.T. Barber, P. Flament and W.M. Balch (1994), A line in the sea, *Nature*, 371, 689-692.

APPENDICES

8 APPENDIX A

TAO line climatological chlorophyll, temperature, salinity and nutrient distributions. Contour intervals are 0.1 mg m^{-3} for chlorophyll, 1 °C for temperature, 0.2 for salinity, 2 mmol m^{-3} for nitrate and silicic acid, and 0.5 mmol m^{-3} for phosphate. The 20°C isotherm representing the mid-thermocline (Kessler and Taft, 1987) is highlighted as a dashed black contour line in the temperature section. The 140°W cruise sections do not extend to 8°S due to the presence of the Marquesas Islands. Longitude/depth sections were also constructed from the CTD stations used for calculating the climatological chlorophyll, temperature, salinity and nutrients for the TAO lines. Data used in constructing longitude/depth sections are from CTD stations conducted within +/- 0.5 ° of the equator.

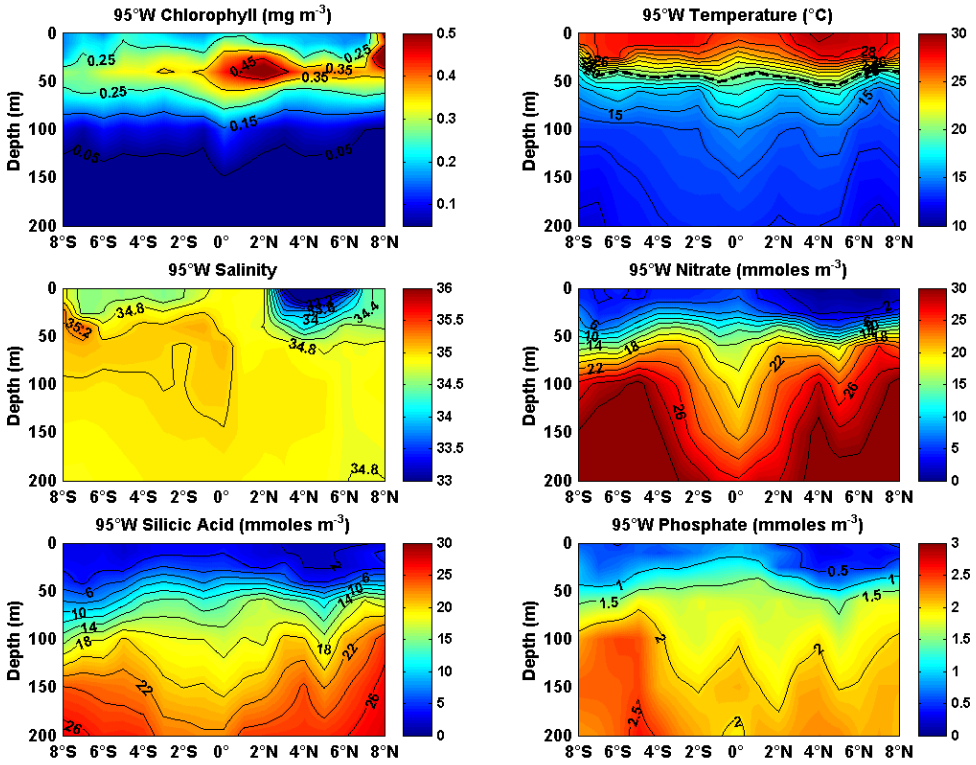

Figure 44: Latitude/depth section of the climatological mean chlorophyll, temperature, salinity and nutrients for the 95°W TAO mooring line.

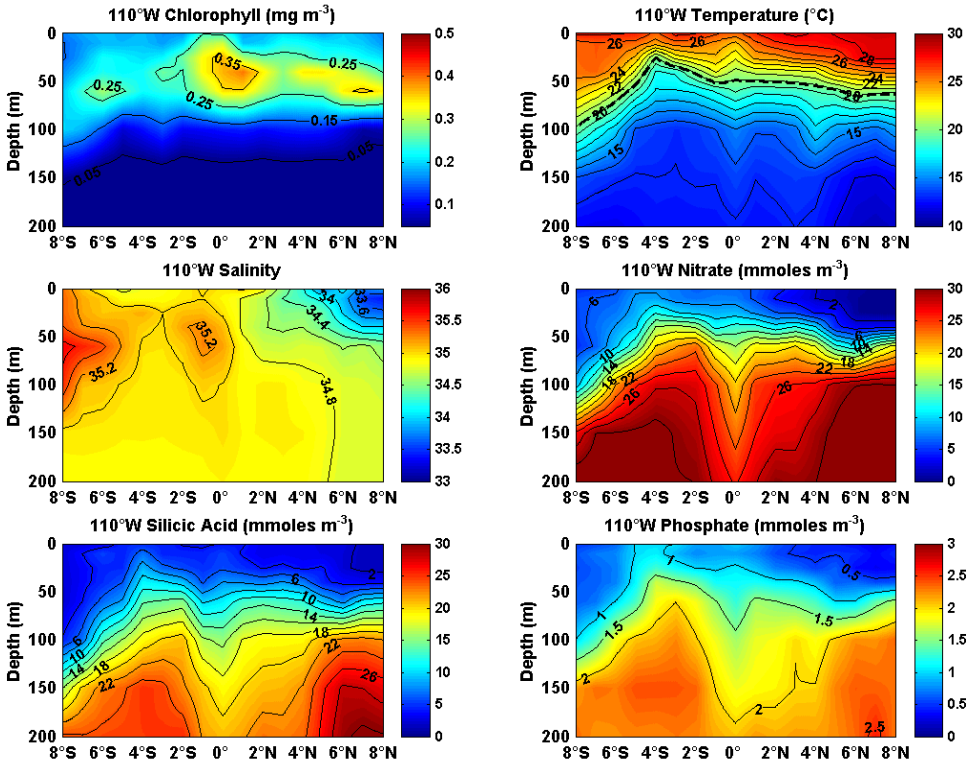

Figure 45: Latitude/depth section of the climatological mean chlorophyll, temperature, salinity and nutrients for the 110°W TAO mooring line.

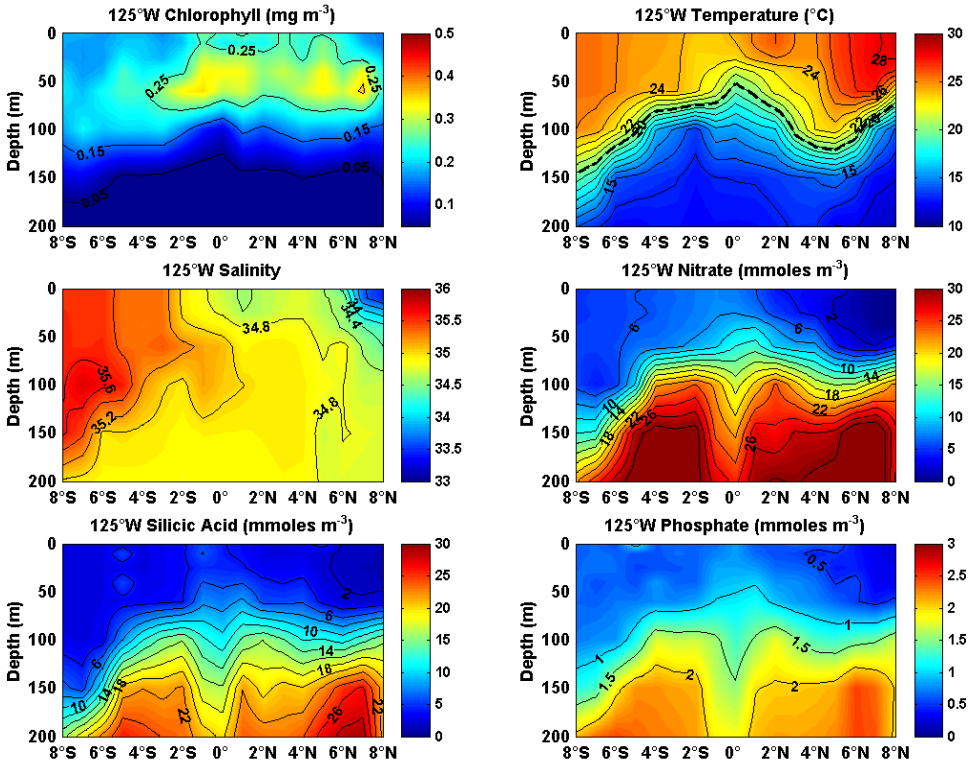

Figure 46: Latitude/depth section of the climatological mean chlorophyll, temperature, salinity and nutrients for the 125°W TAO mooring line.

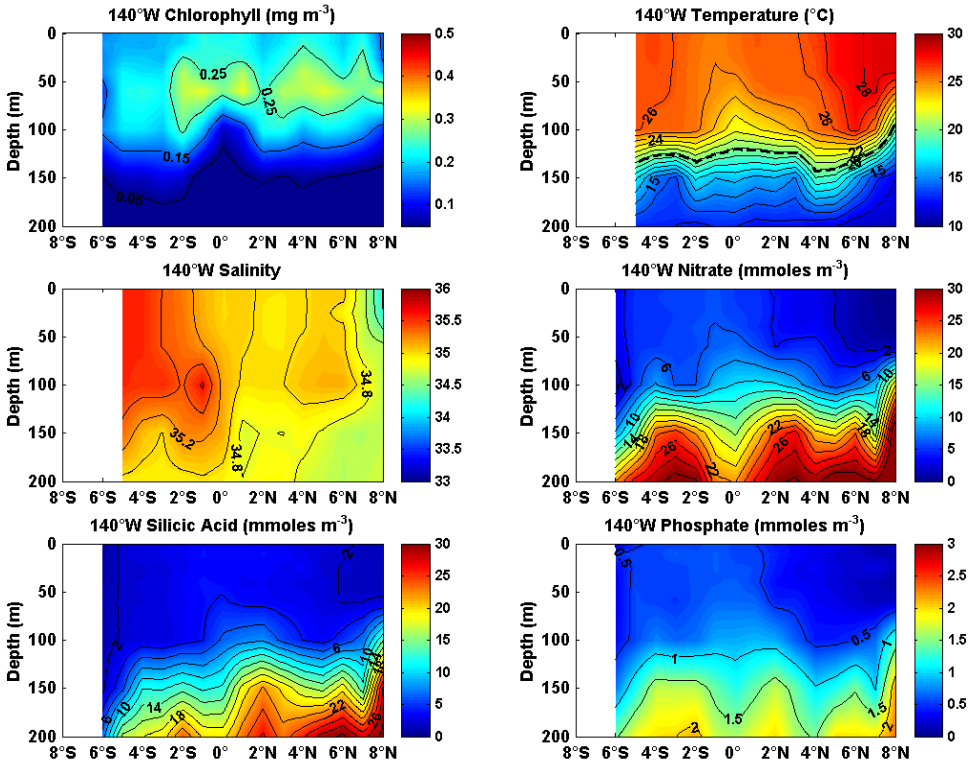

Figure 47: Latitude/depth section of the climatological mean chlorophyll, temperature, salinity and nutrients for the 140°W TAO mooring line.

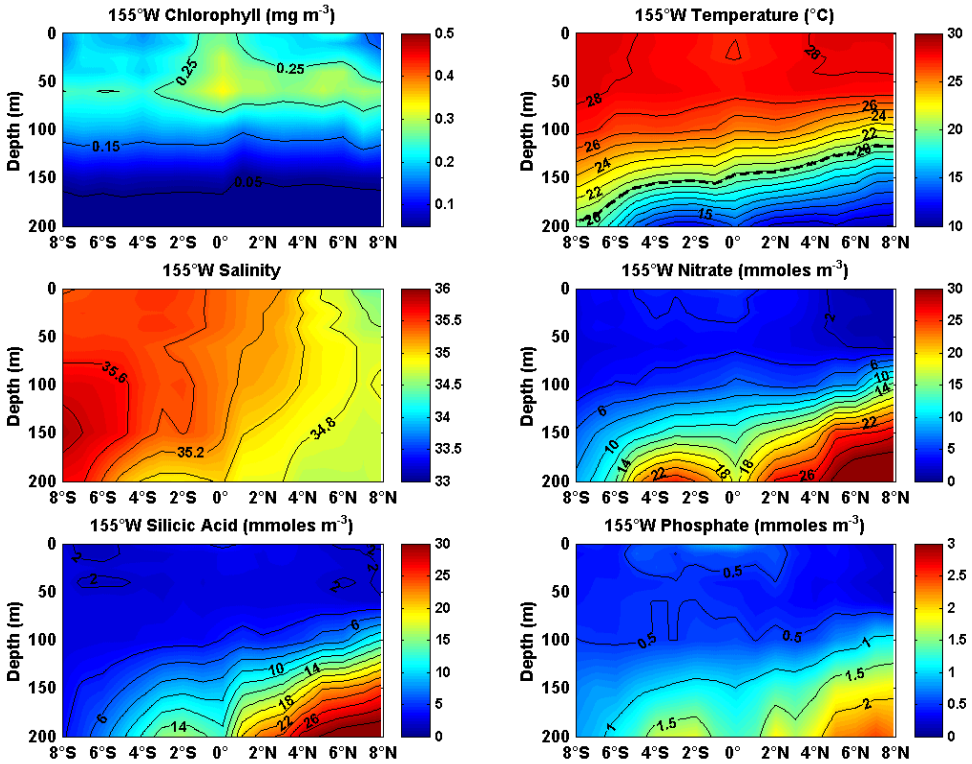

Figure 48: Latitude/depth section of the climatological mean chlorophyll, temperature, salinity and nutrients for the 155°W TAO mooring line.

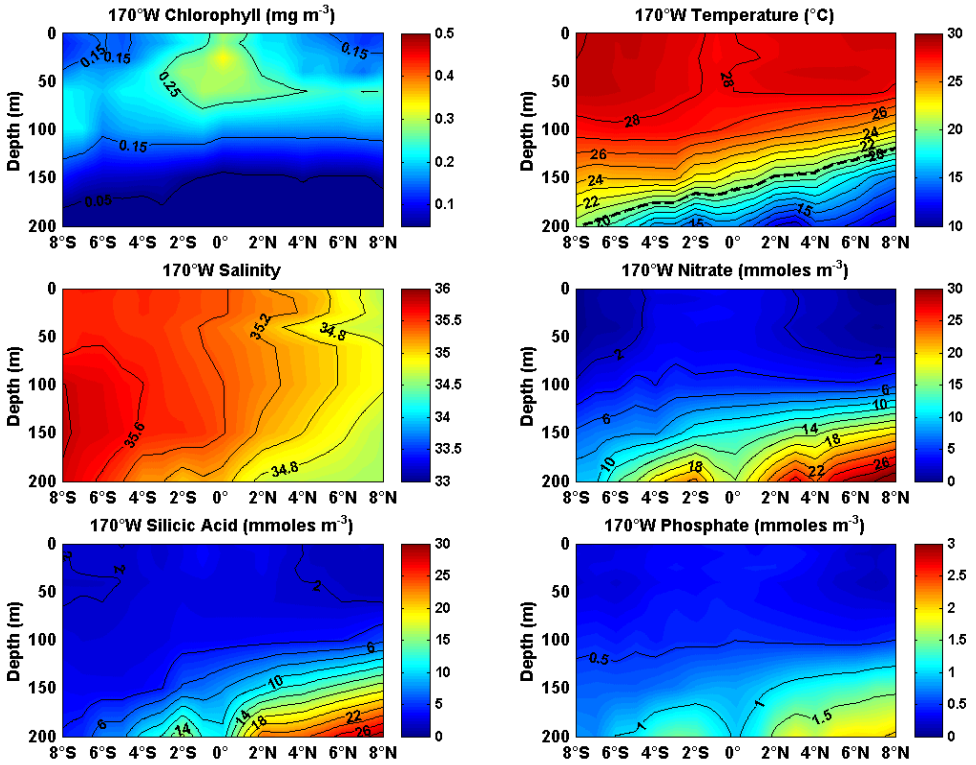

Figure 49: Latitude/depth section of the climatological mean chlorophyll, temperature, salinity and nutrients for the 170°W TAO mooring line.

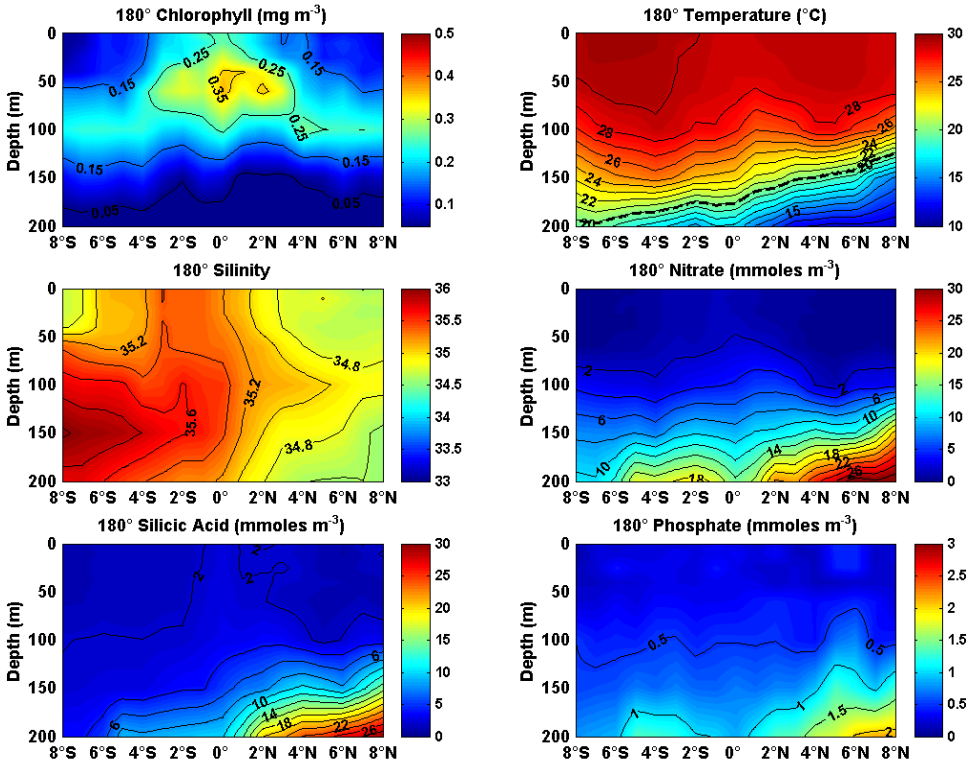

Figure 50: Latitude/depth section of the climatological mean chlorophyll, temperature, salinity and nutrients for the 180° TAO mooring line.

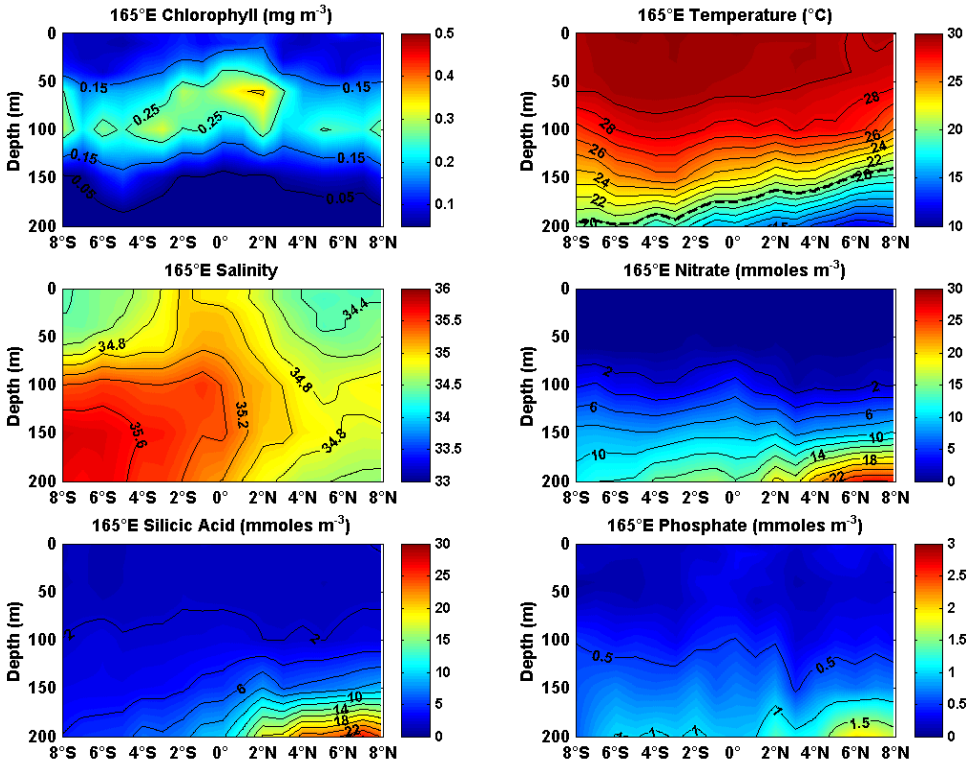

Figure 51: Latitude/depth section of the climatological mean chlorophyll, temperature, salinity and nutrients for the 165°E TAO mooring line.

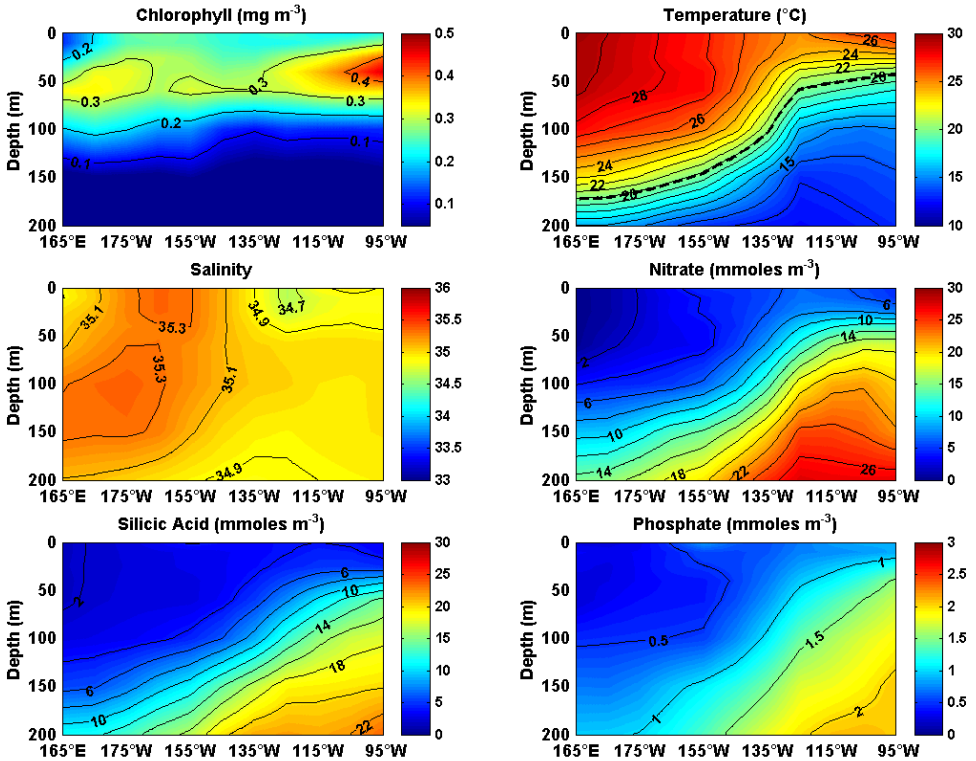

Figure 52: Longitude/depth section of the climatological mean chlorophyll, temperature, salinity and nutrients for data collected within +/- 0.5° of the equator.

9 APPENDIX B

Levitus94 nitrate and TAO nitrate climatology comparison.

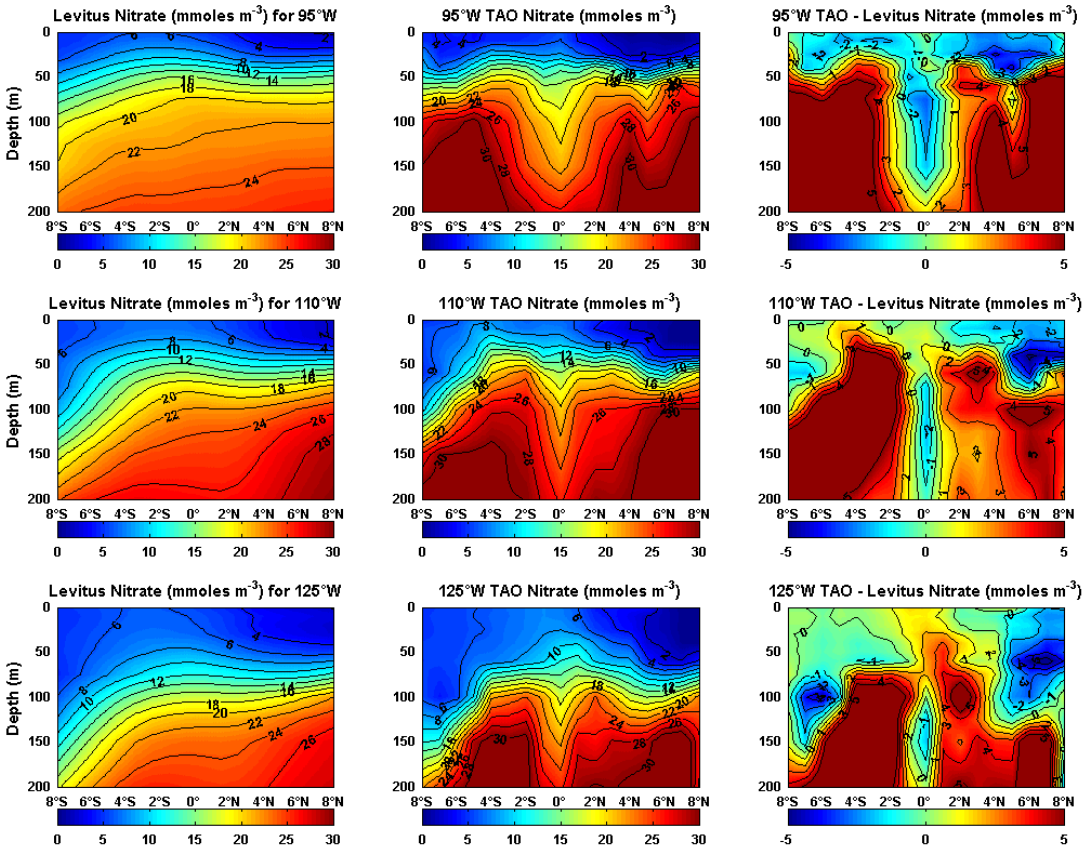

Figure 53: Levitus94 annual nitrate (left panels) comparison with TAO climatological nitrate (center panels) for the 95°W, 110°W and 125°W mooring lines. Contour interval is 2 mmol m^{-3}. The differences between the two climatologies are shown in the right panels.

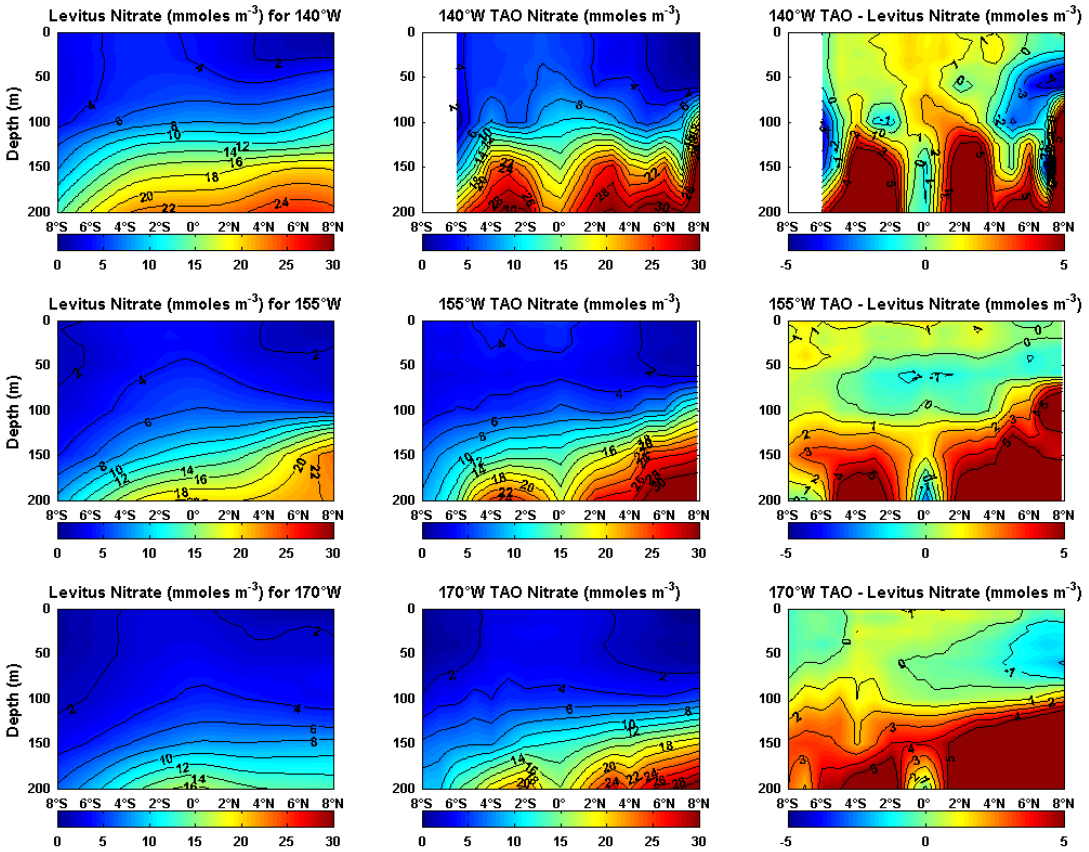

Figure 54: Levitus94 annual nitrate (left panels) comparison with TAO climatological nitrate (center panels) for the 140°W, 155°W and 170°W mooring lines. The contour interval is 2 mmol m^{-3}. Differences between the two climatologies are shown in the right panels.

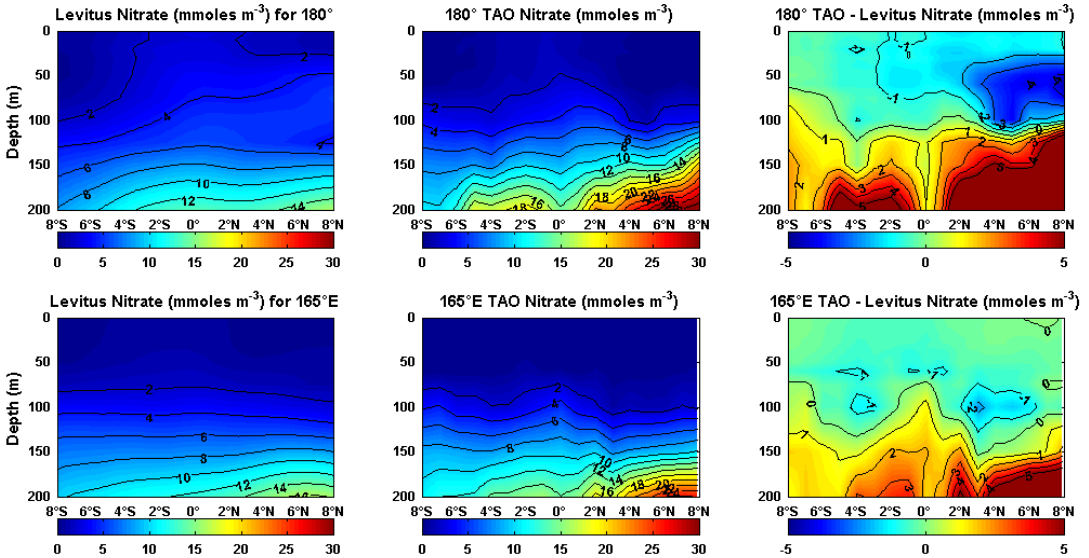

Figure 55: Levitus94 annual nitrate (left panels) comparison with TAO climatological nitrate (center panels) for the 180° and 165°E mooring lines. Contour interval is 2 mmol m^{-3}. The differences between the two climatologies are shown in the right panels.

10 APPENDIX C

CTD station/SST plots, latitude/depth sections and anomalies from the TAO climatology for cruises that crossed TIWs on the 95°W, 110°W, 140°W, 155°W, 170°W and 180° lines. Contour intervals same as Appendix A.

10.1 95°W TAO line

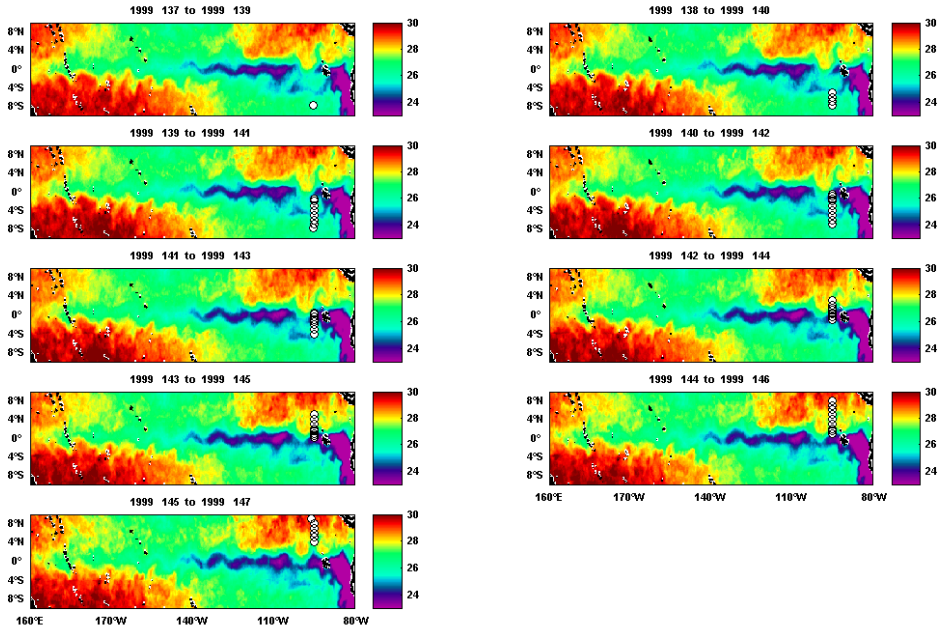

Figure 56: 95°W TAO cruise that crossed a TIW in the northern hemisphere in May of 1999.

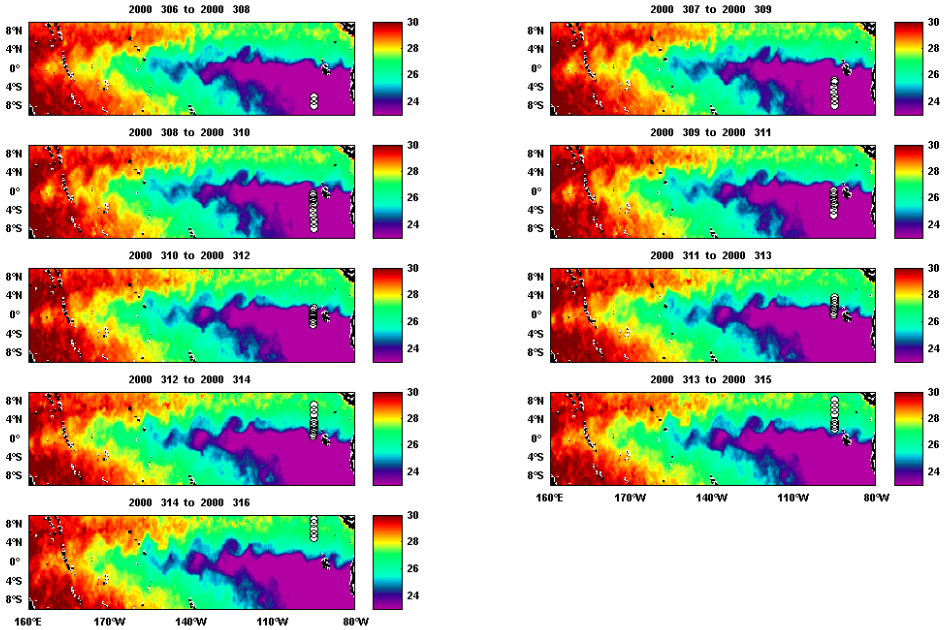

Figure 57: 95°W TAO cruise that crossed a TIW in the northern hemisphere in November of 2000.

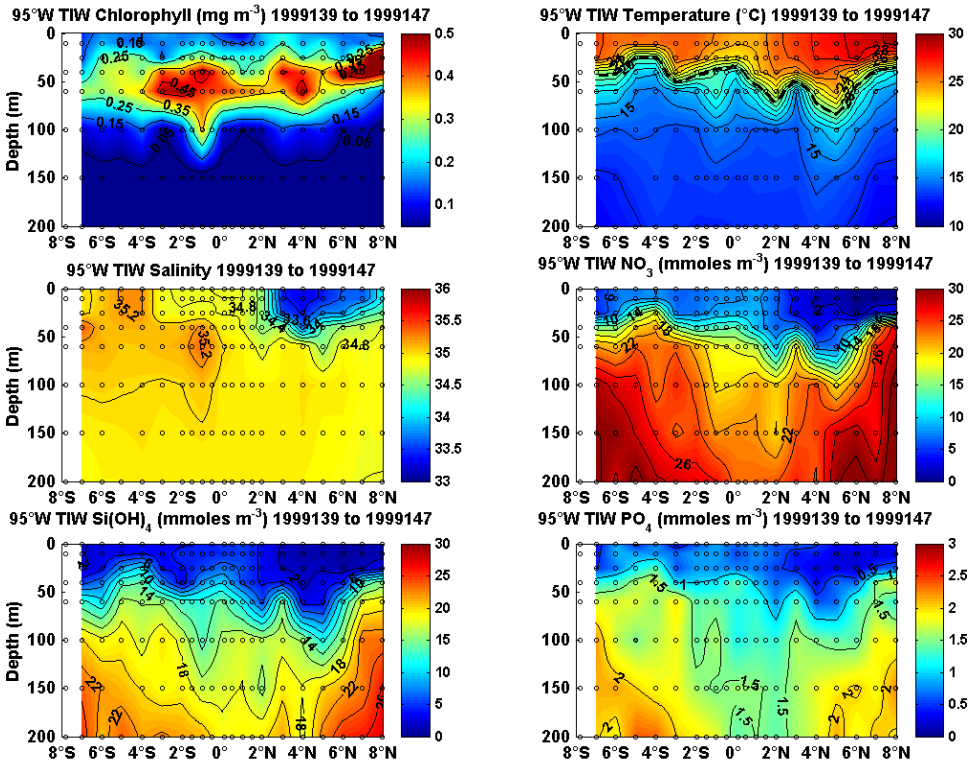

Figure 58: 95°W TAO latitude/depth section for the May 1999 cruise identified crossing a TIW in the northern hemisphere.

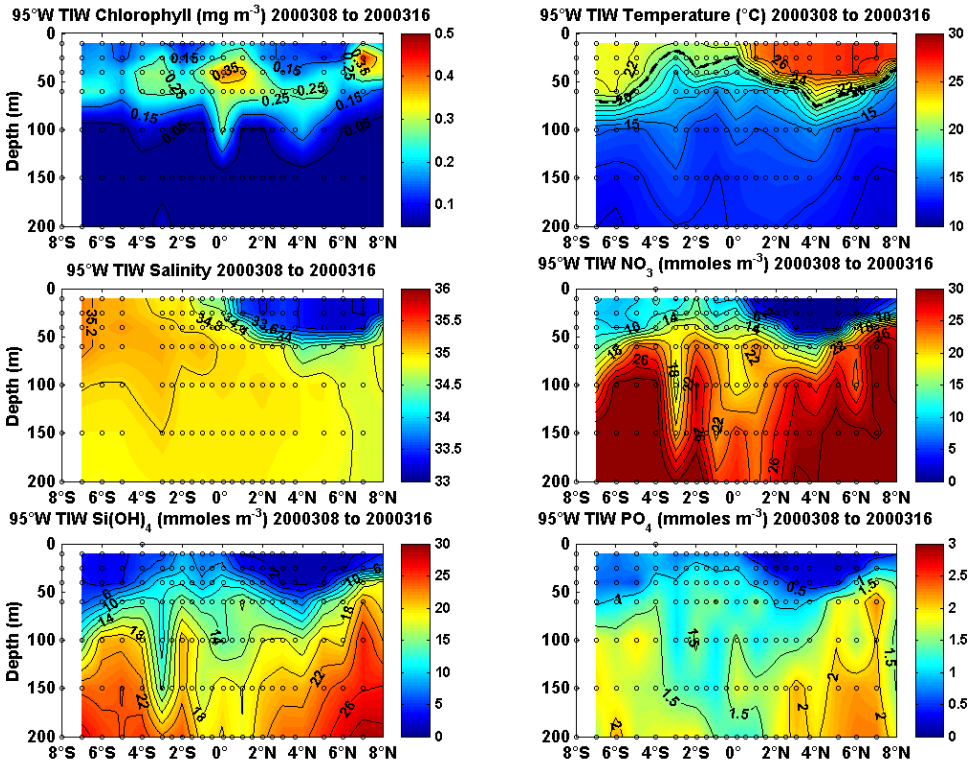

Figure 59: 95°W TAO latitude/depth section for the November 2000 cruise identified crossing a TIW in the northern hemisphere.

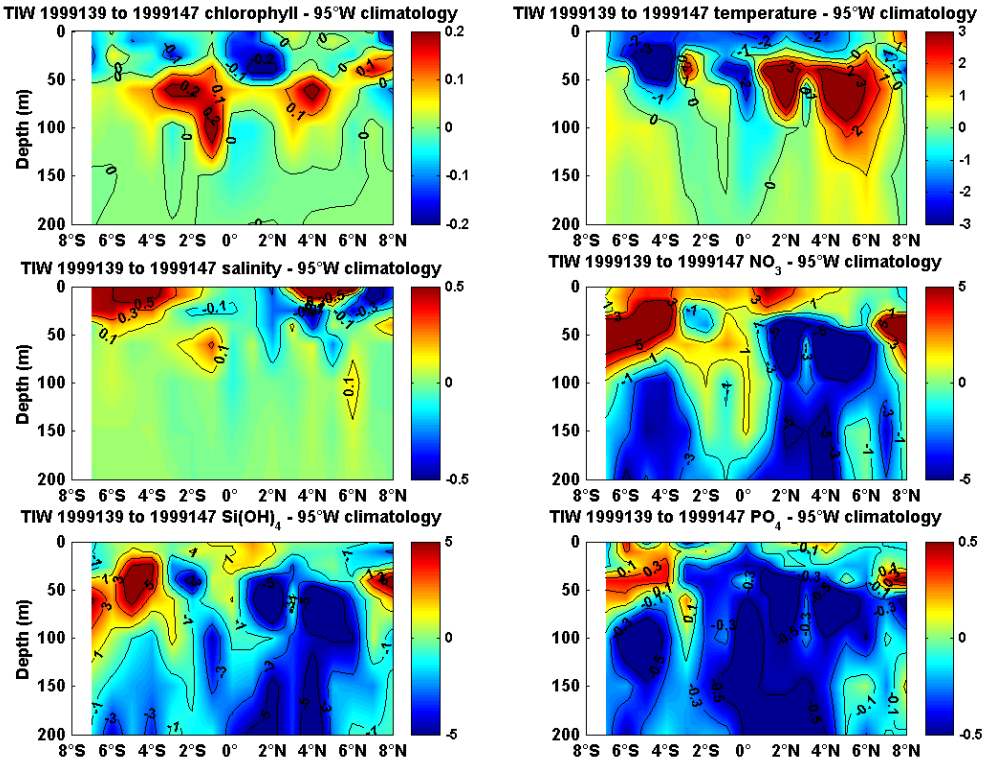

Figure 60: 95°W TAO latitude/depth anomaly section for the May 1999 cruise identified crossing a TIW in the northern hemisphere.

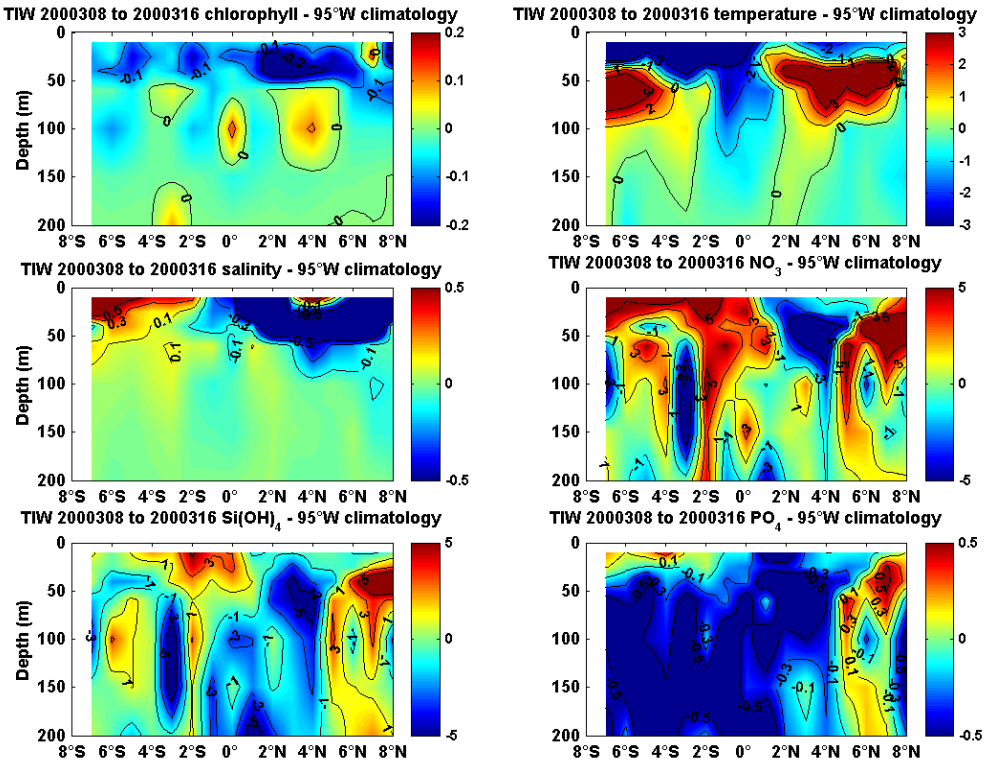

Figure 61: 95°W TAO latitude/depth anomaly section for the November 2000 cruise identified crossing a TIW in the northern hemisphere.

10.2 110°W TAO line

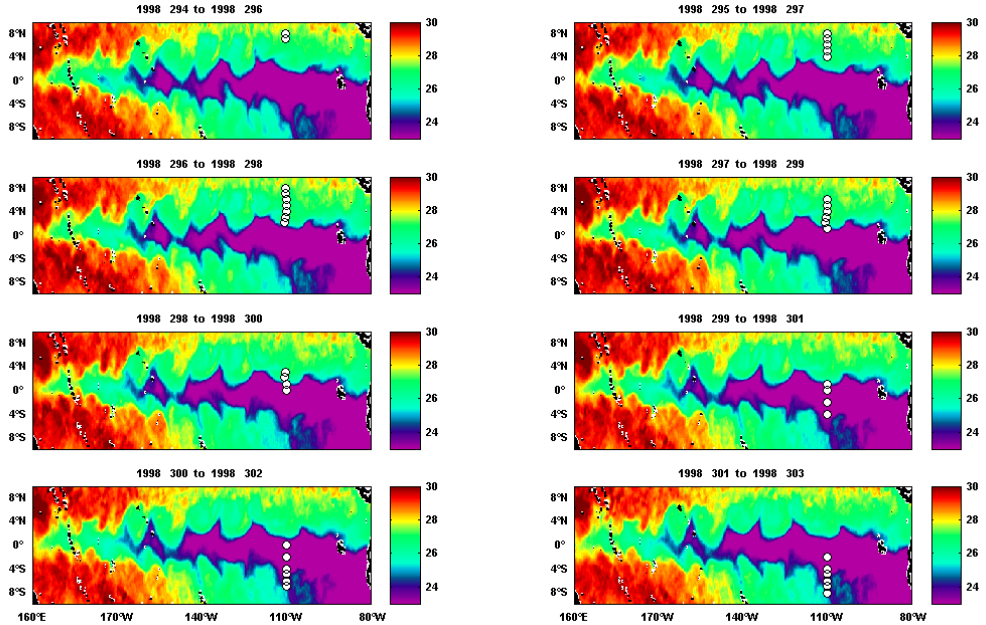

Figure 62: 110°W TAO cruise that crossed a TIW in the southern hemisphere in October of 1998.

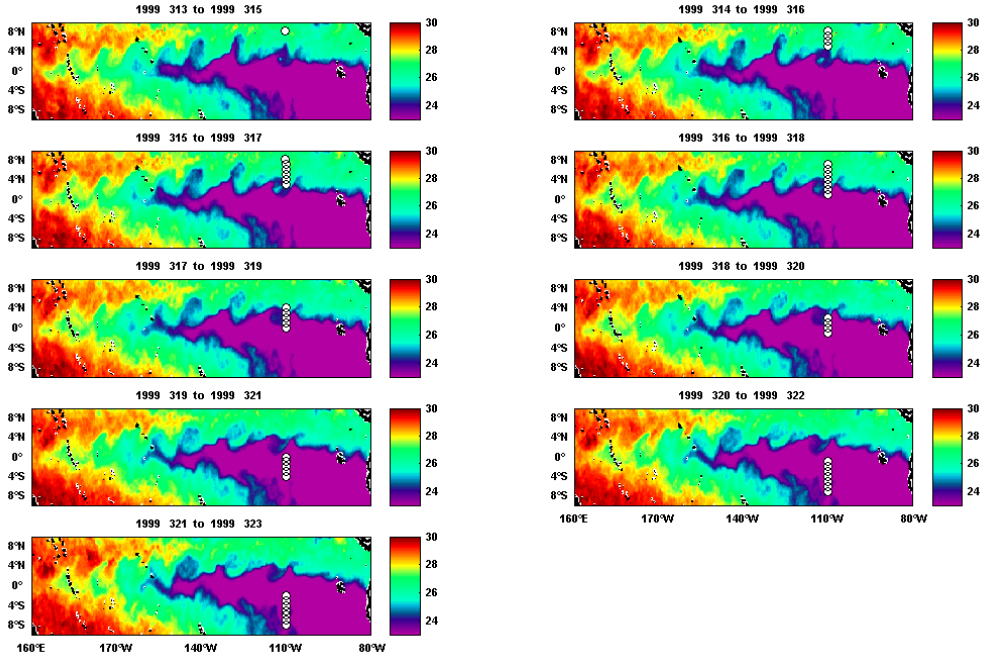

Figure 63: 110°W TAO cruise that crossed a TIW in the northern hemisphere in November of 1999.

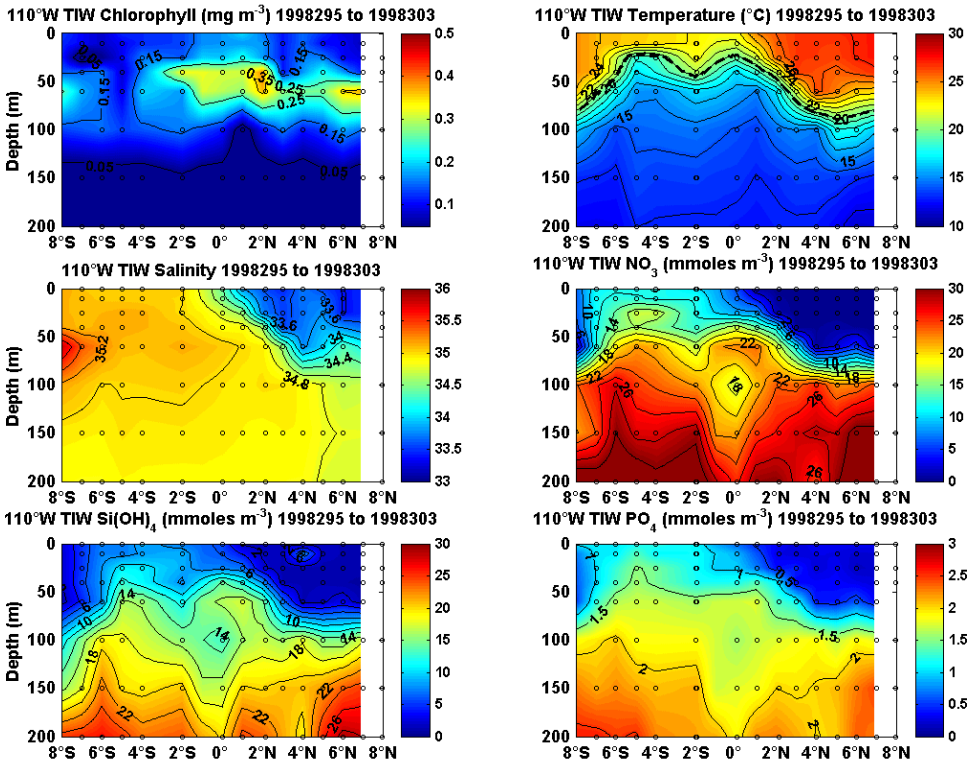

Figure 64: 110°W TAO latitude/depth section for the October 1998 cruise identified crossing a TIW in the southern hemisphere.

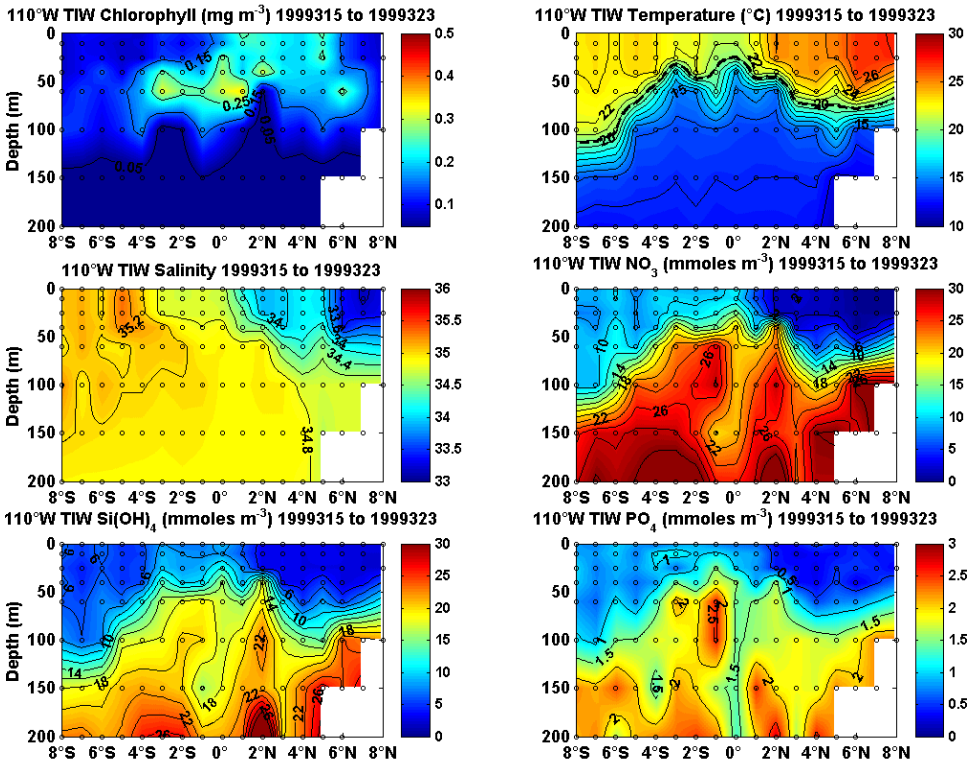

Figure 65: 110°W TAO latitude/depth section for the November 1999 cruise identified crossing a TIW in the northern hemisphere.

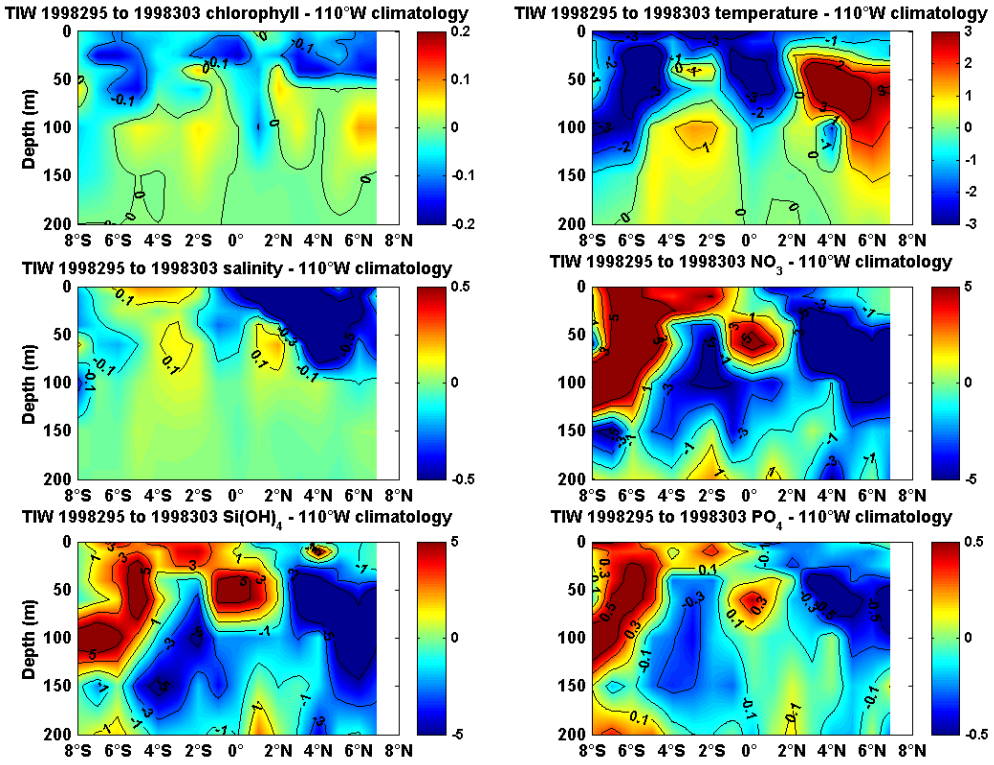

Figure 66: 110°W TAO latitude/depth anomaly section for the October 1998 cruise identified crossing a TIW in the southern hemisphere.

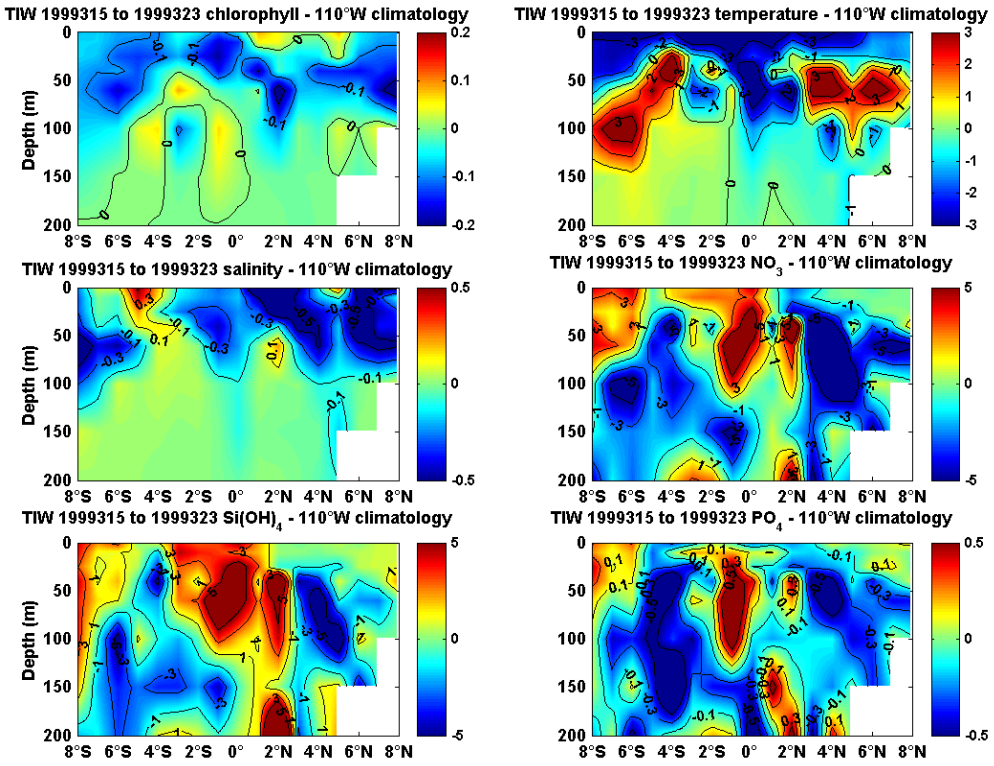

Figure 67: 110°W TAO latitude/depth anomaly section for the November 1999 cruise identified crossing a TIW in the southern hemisphere.

10.3 125°W TAO line

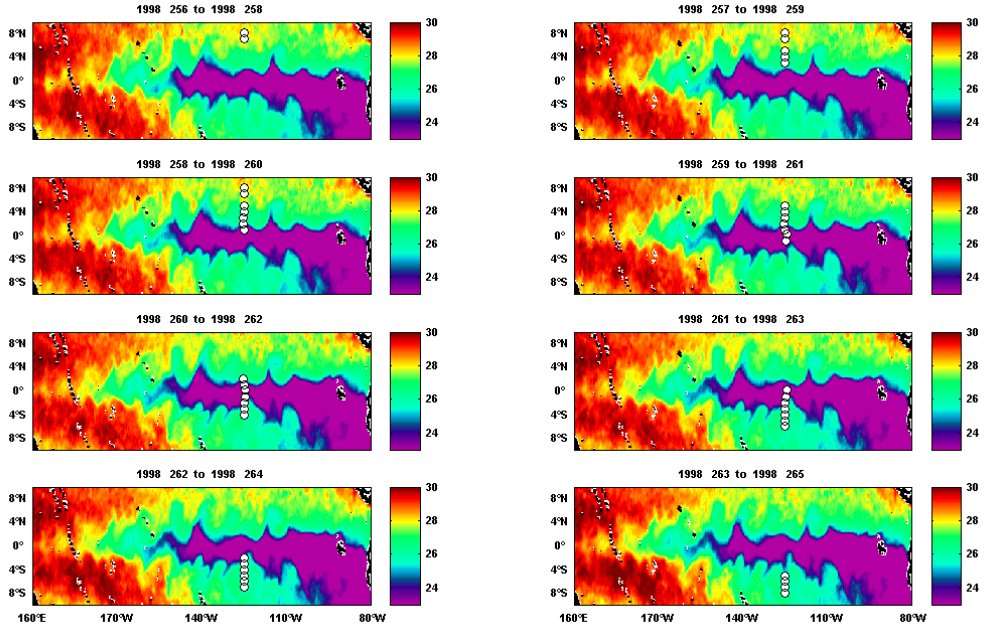

Figure 68: 125°W TAO cruise that crossed a TIW in the southern hemisphere in September of 1998.

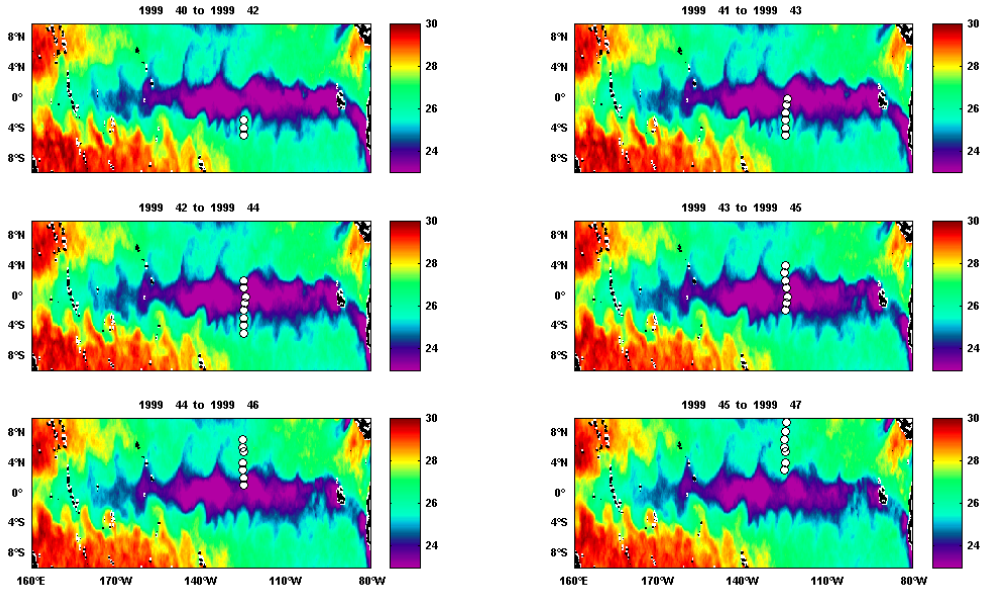

Figure 69: 125°W TAO cruise that crossed a TIW in the northern hemisphere in February of 1999.

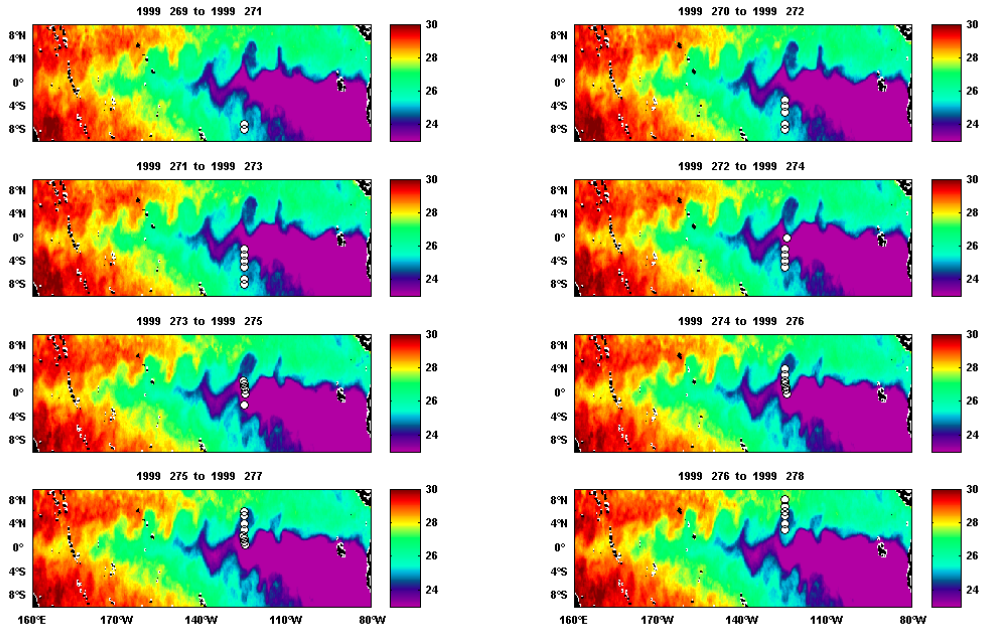

Figure 70: 125°W TAO cruise that crossed TIWs in both hemispheres in September of 1999.

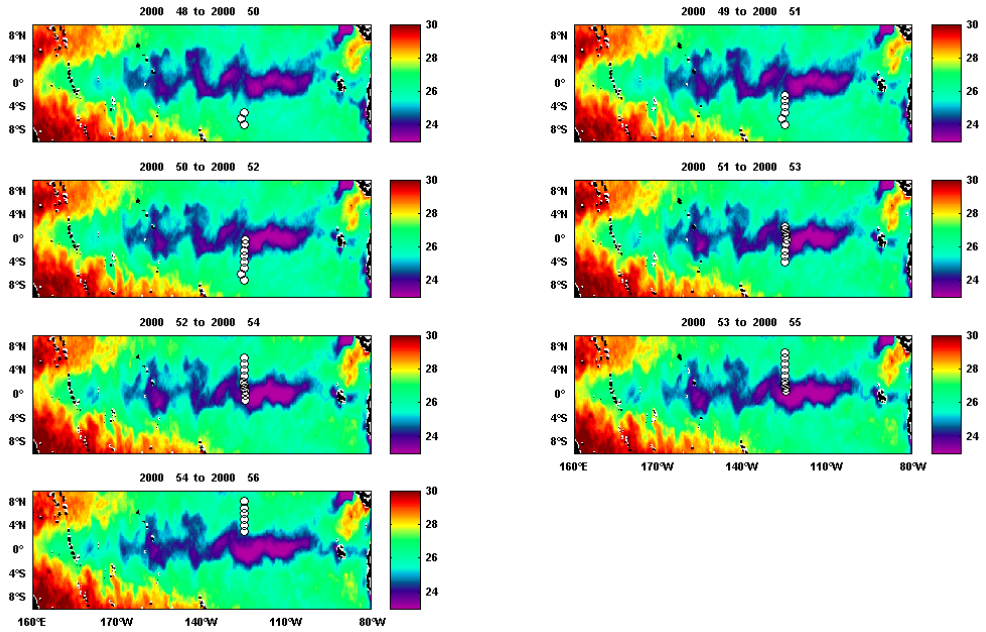

Figure 71: 125°W TAO cruise that crossed a TIW in the northern hemisphere in February of 2000.

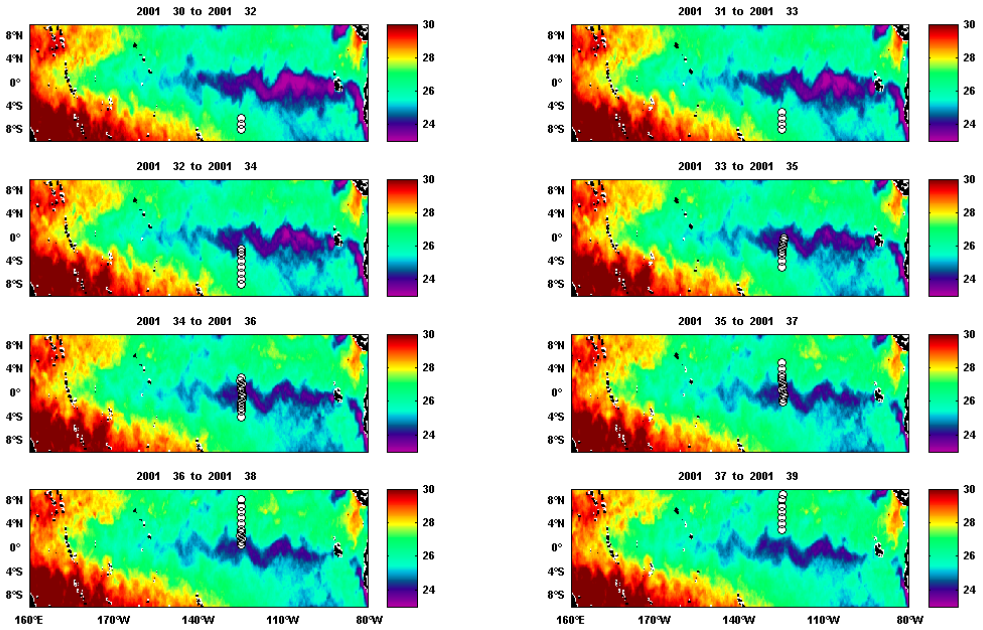

Figure 72: 125°W TAO cruise that crossed a TIW in the southern hemisphere in January of 2001.

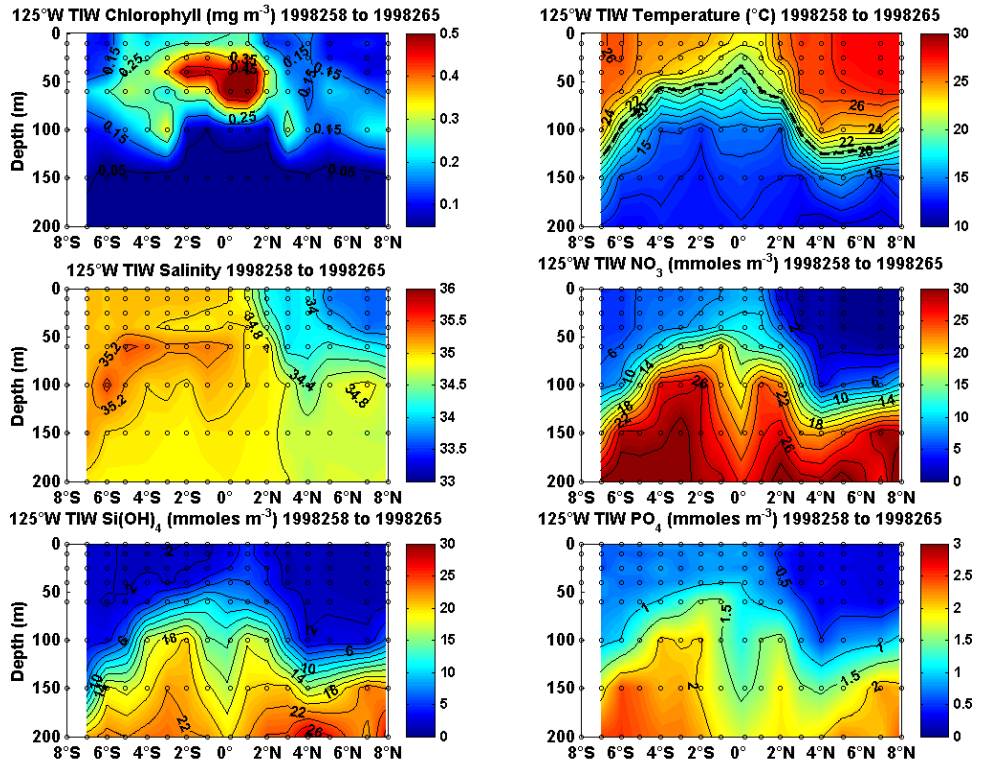

Figure 73: 125°W TAO cruise latitude/depth section for the September 1998 cruise identified crossing a TIW in the southern hemisphere.

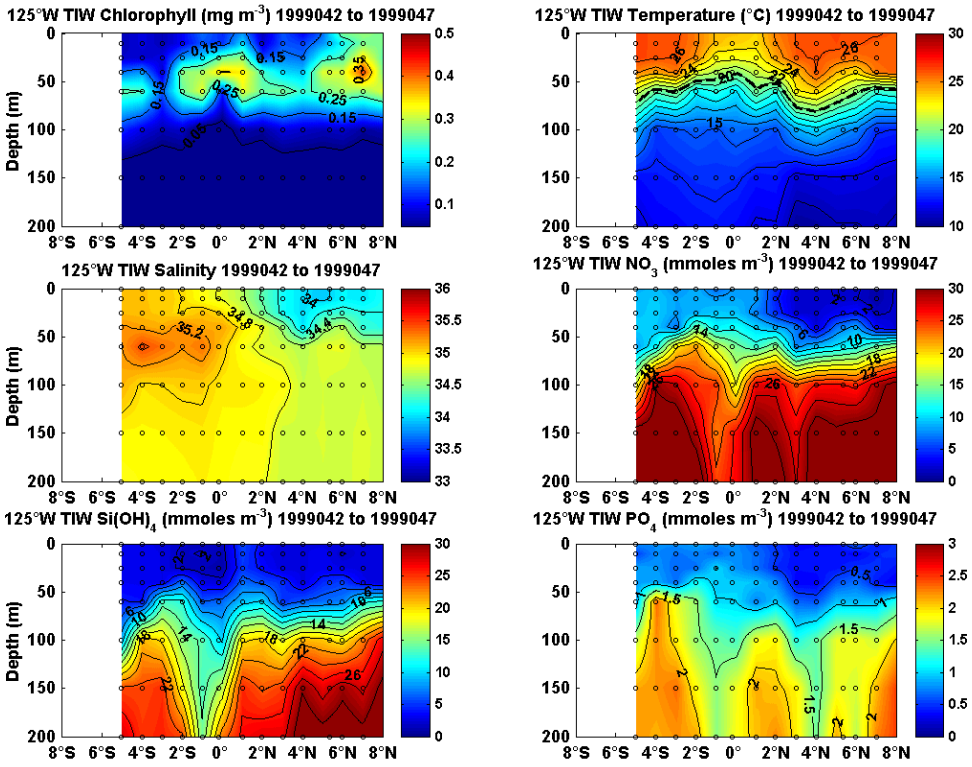

Figure 74: 125°W TAO cruise latitude/depth section for the February 1999 cruise identified crossing a TIW in the northern hemisphere.

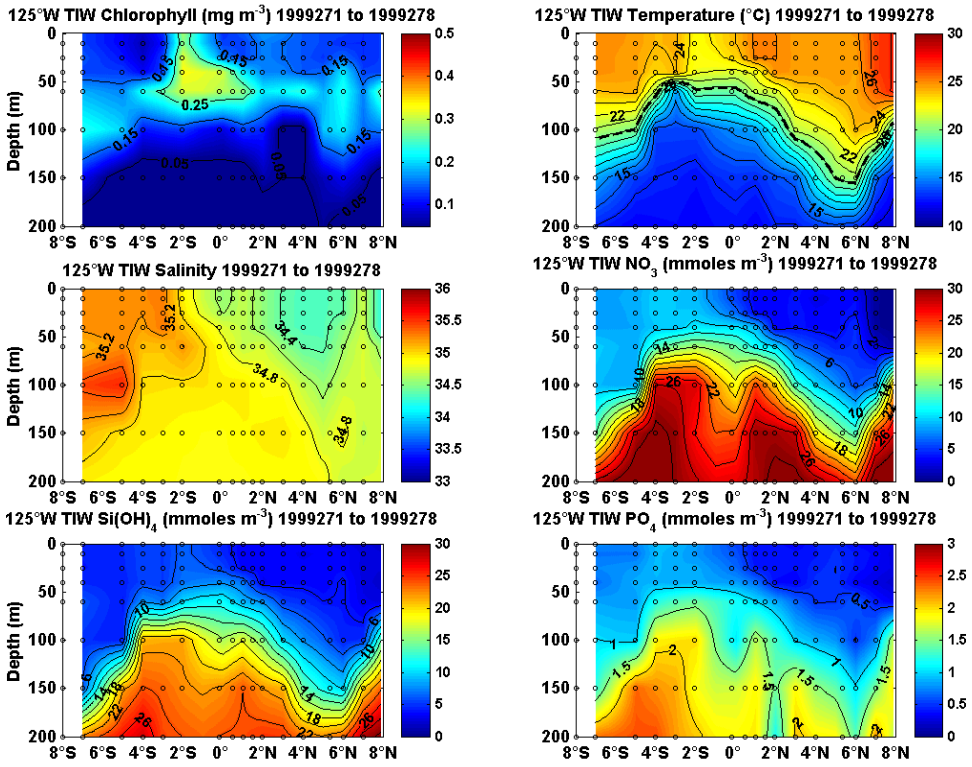

Figure 75: 125°W TAO cruise latitude/depth section for the September 1999 cruise identified crossing TIWs in both hemispheres.

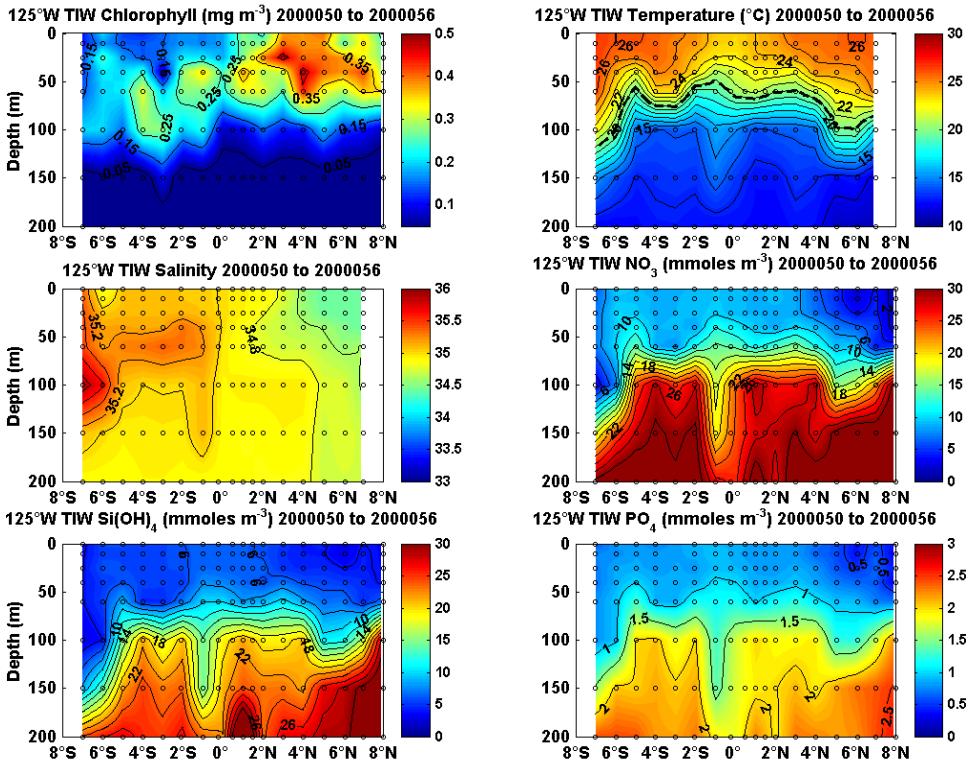

Figure 76: 125°W TAO cruise latitude/depth section for the February 2000 cruise identified crossing a TIW in the northern hemisphere.

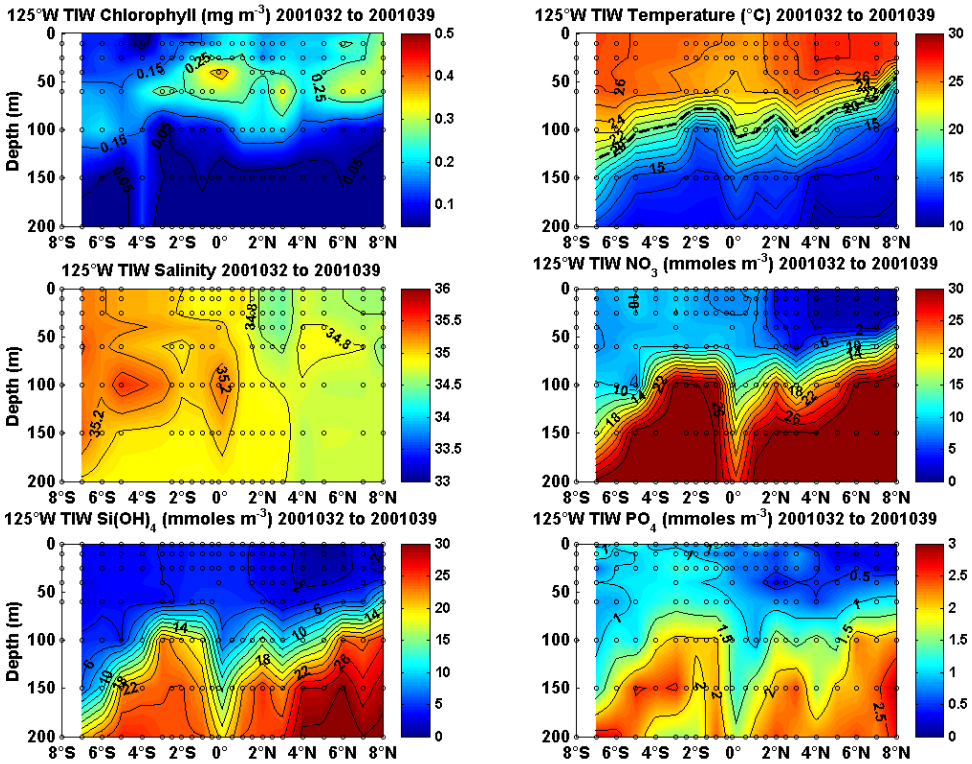

Figure 77: 125°W TAO cruise latitude/depth section for the January 2001 cruise identified crossing a TIW in the southern hemisphere.

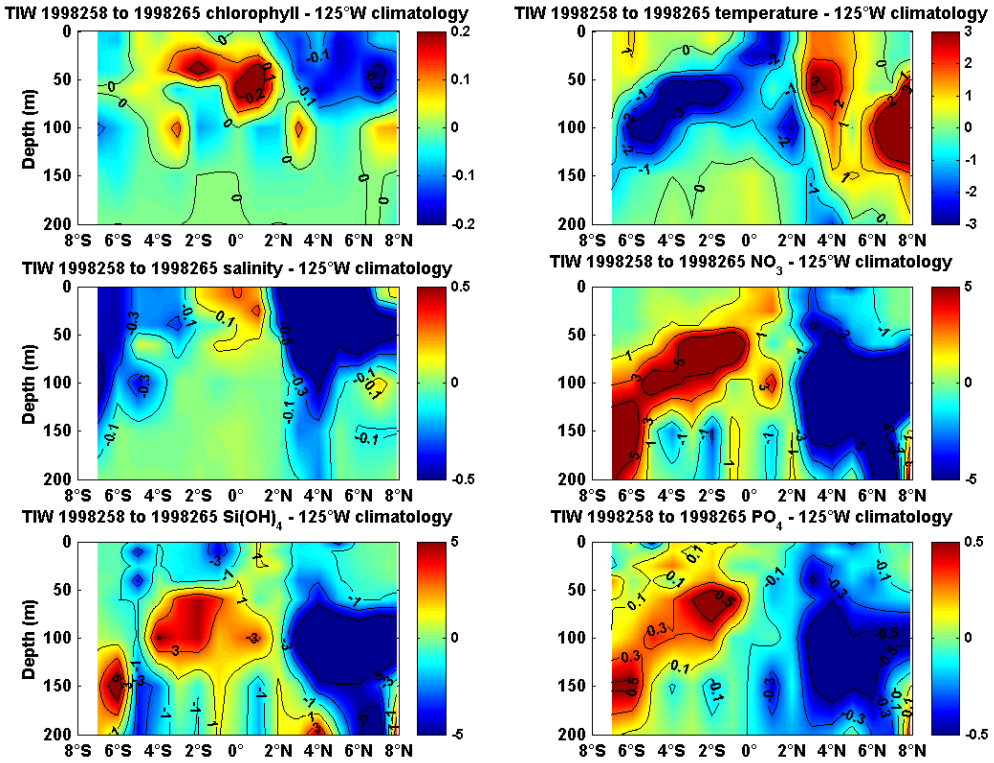

Figure 78: 125°W TAO cruise latitude/depth anomaly section for the September 1998 cruise identified crossing a TIW in the southern hemisphere.

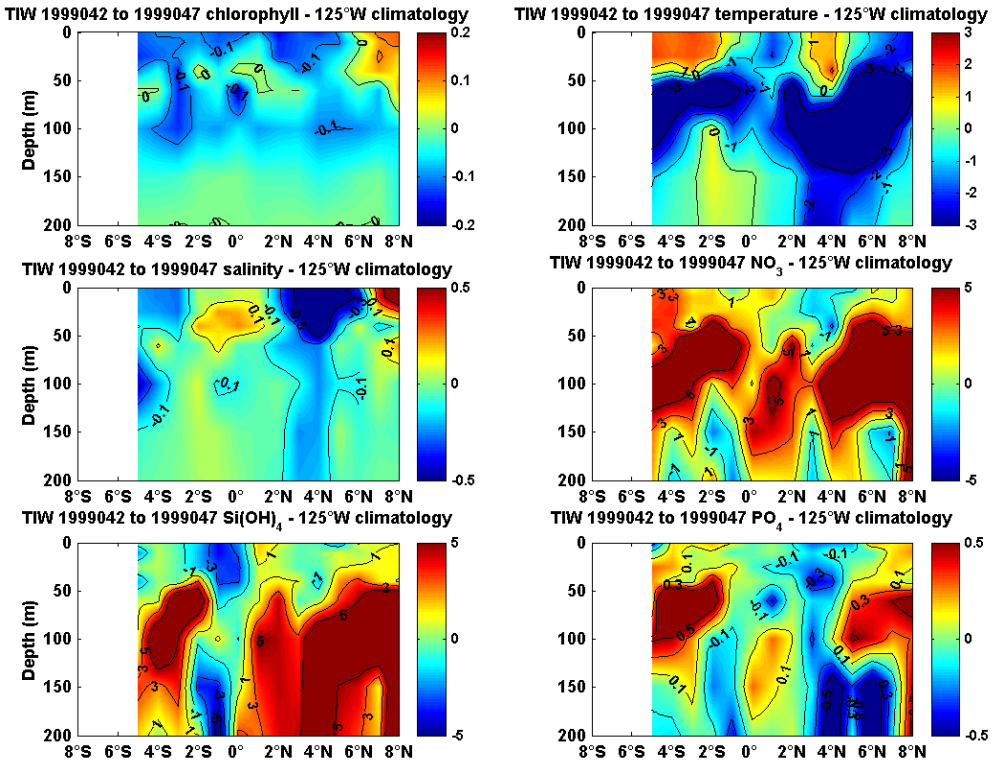

Figure 79: 125°W TAO cruise latitude/depth anomaly section for the February 1999 cruise identified crossing a TIW in the northern hemisphere.

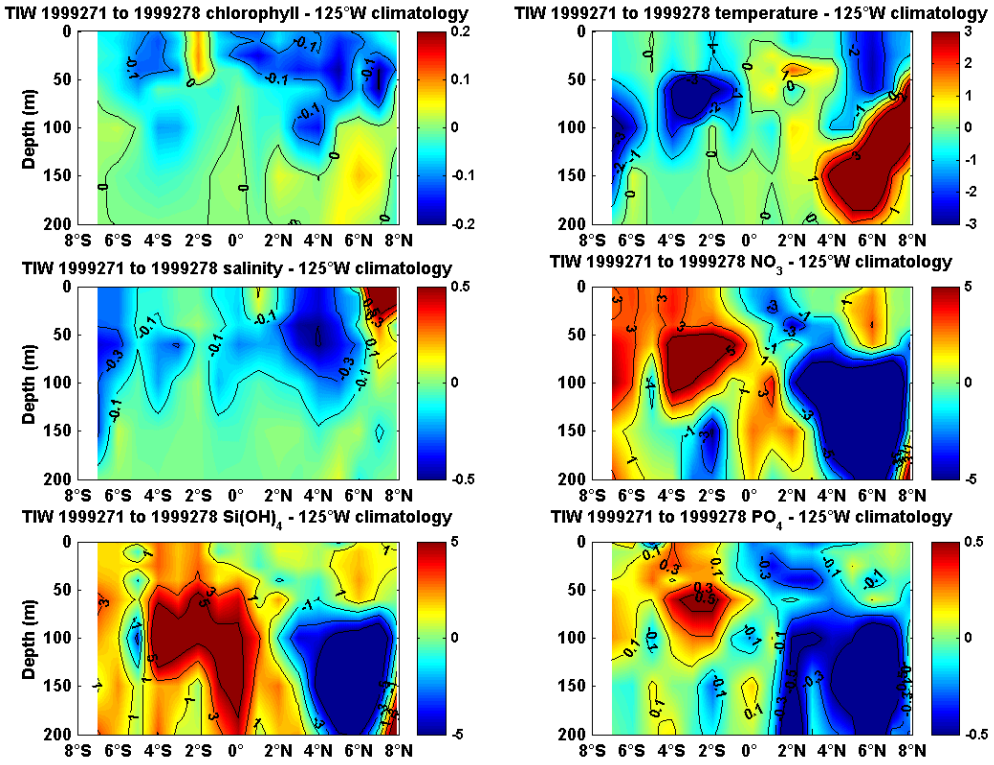

Figure 80: 125°W TAO cruise latitude/depth anomaly section for the September 1999 cruise identified crossing TIWs in both hemispheres.

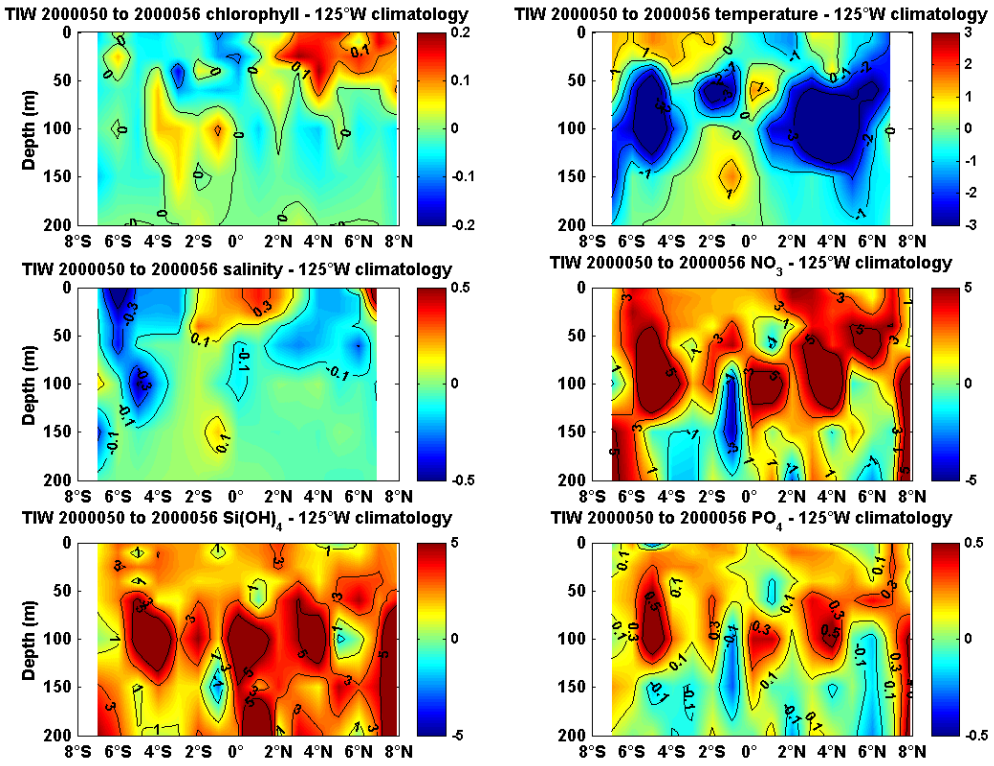

Figure 81: 125°W TAO cruise latitude/depth anomaly section for the February 2000 cruise identified crossing a TIW in the northern hemisphere.

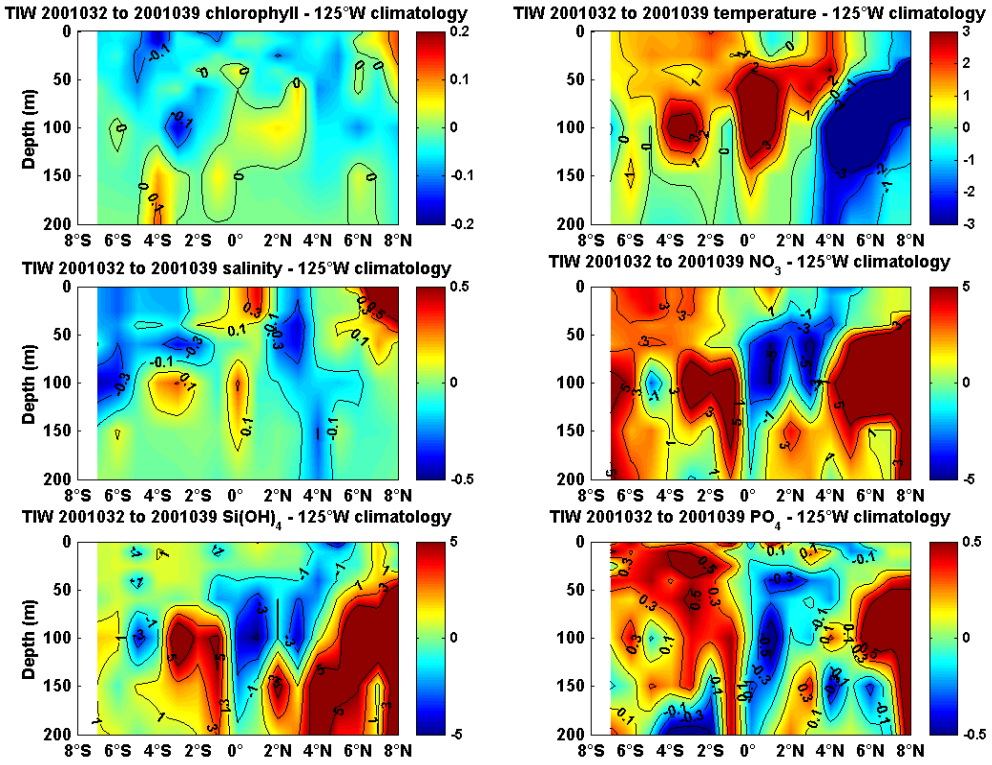

Figure 82: 125°W TAO cruise latitude/depth anomaly section for the January 2001 cruise identified crossing a TIW in the southern hemisphere.

10.4 140°W TAO line

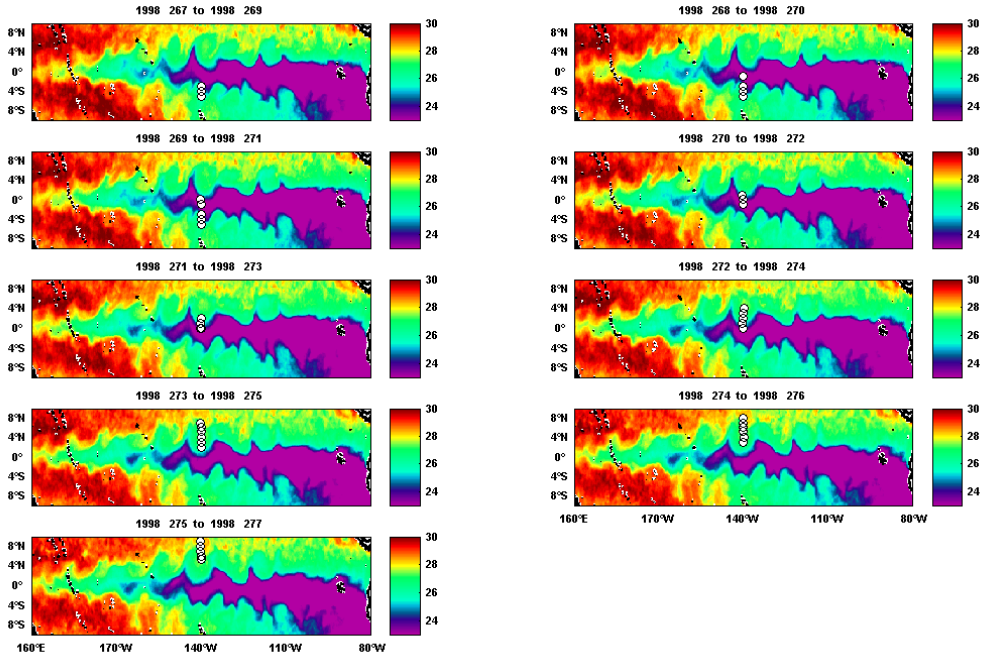

Figure 83: 140°W TAO cruise that crossed TIWs in both hemispheres in September of 1998.

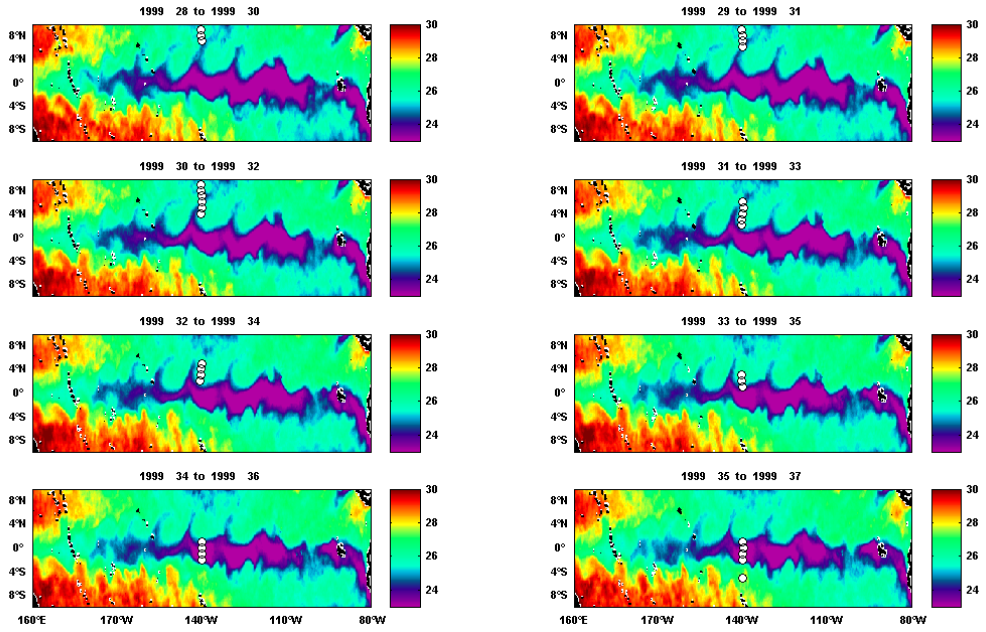

Figure 84: 140°W TAO cruise that crossed a TIW in the northern hemisphere in January of 1999.

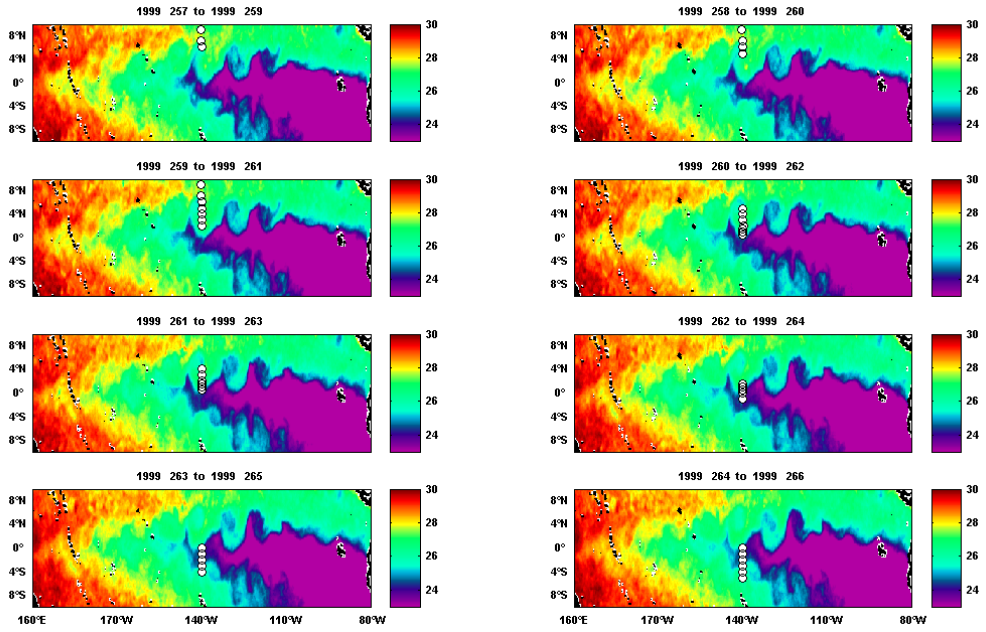

Figure 85: 140°W TAO cruise that crossed TIWs in both hemispheres in September of 1999.

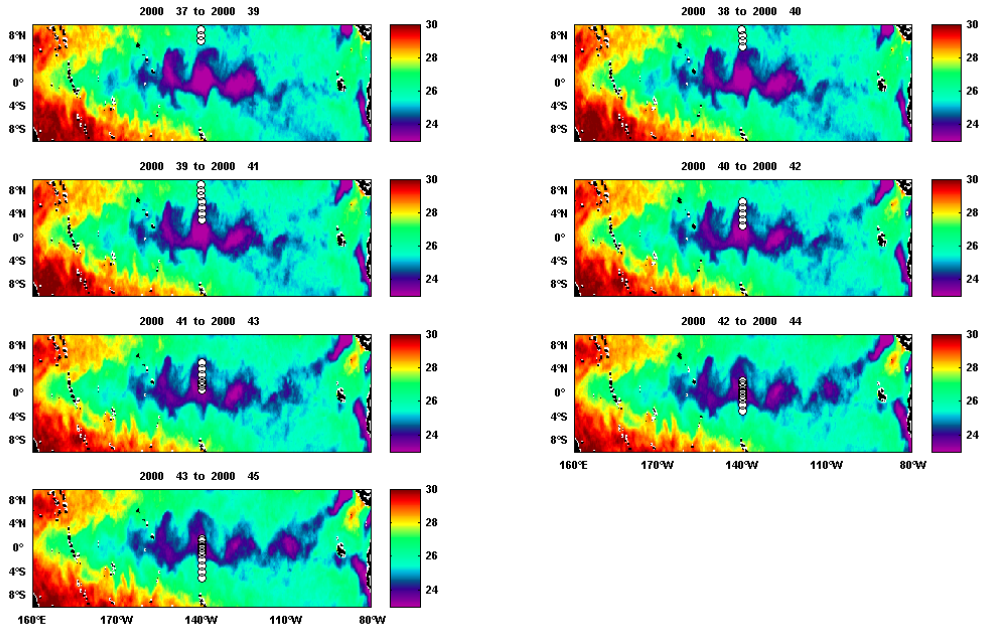

Figure 86: 140°W TAO cruise that crossed TIWs in both hemispheres in February of 2000.

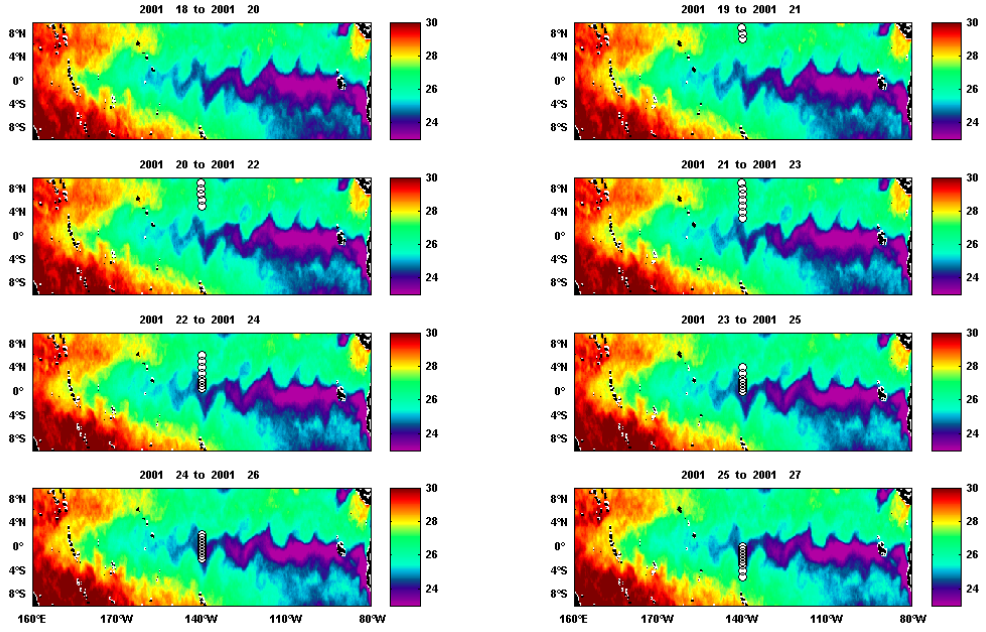

Figure 87: 140°W TAO cruise that crossed TIWs in both hemispheres in January of 2001.

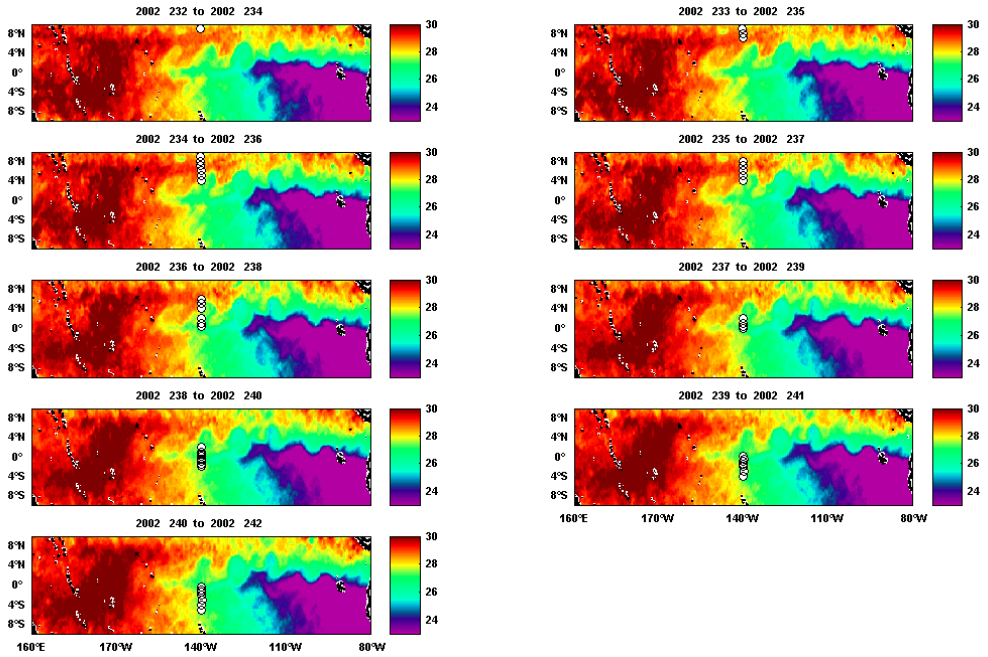

Figure 88: 140°W TAO cruise that crossed a TIW in the northern hemisphere in August of 2002.

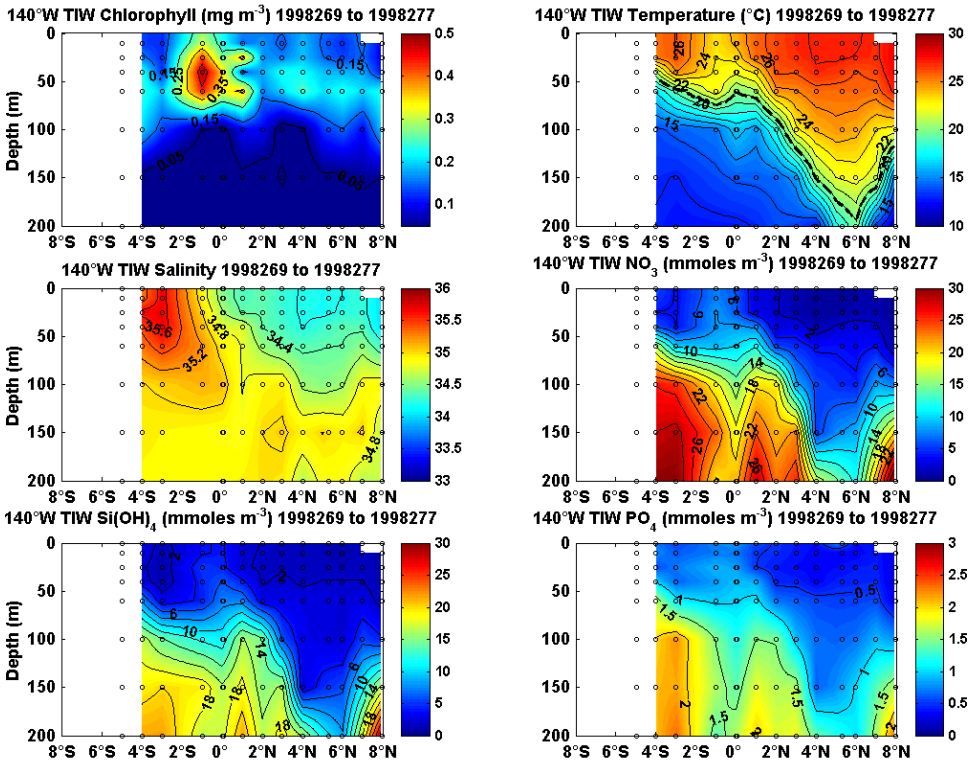

Figure 89: 140°W TAO cruise latitude/depth section for the September 1998 cruise identified crossing TIWs in both hemispheres.

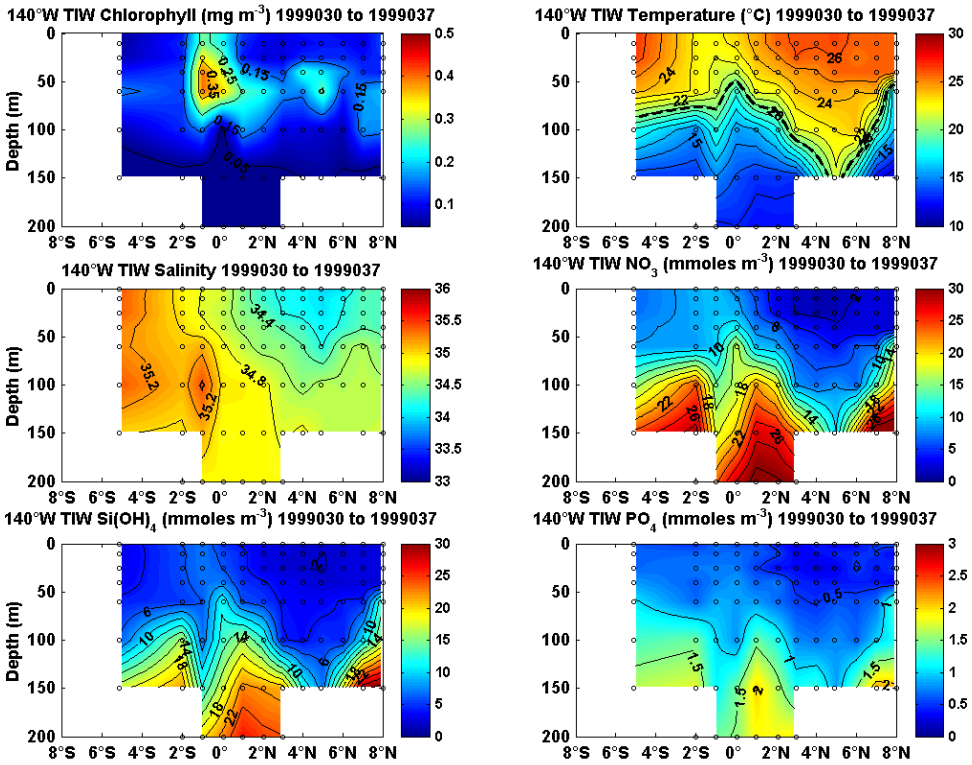

Figure 90: 140°W TAO cruise latitude/depth section for the January 1999 cruise identified crossing a TIW in the northern hemisphere.

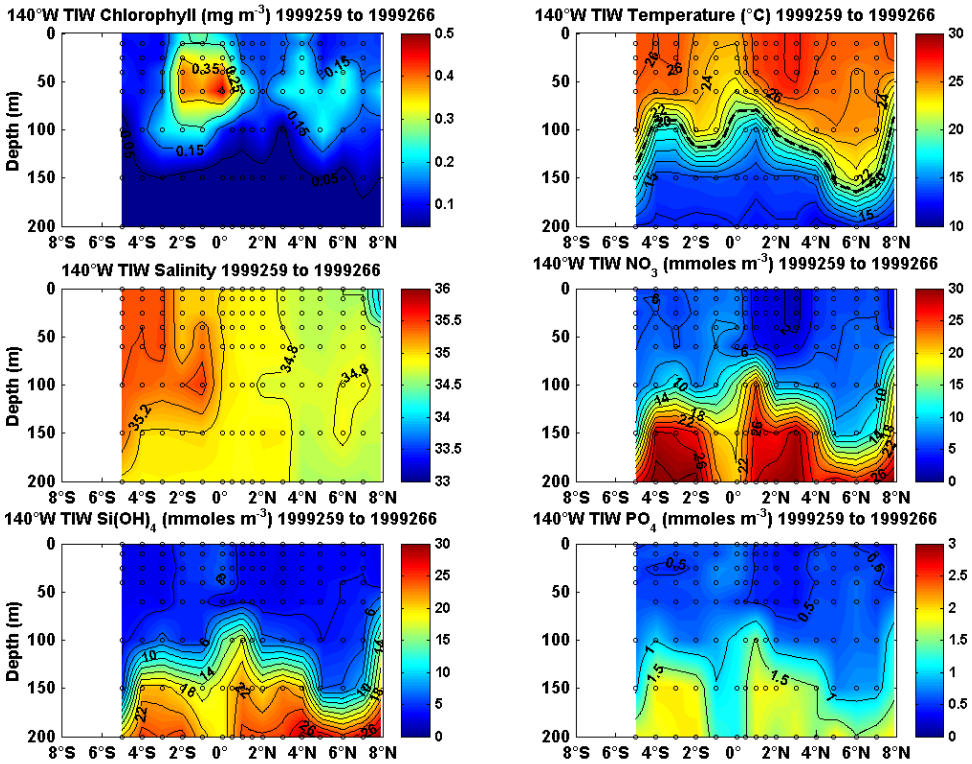

Figure 91: 140°W TAO cruise latitude/depth section for the September 1999 cruise identified crossing TIWs in both hemispheres.

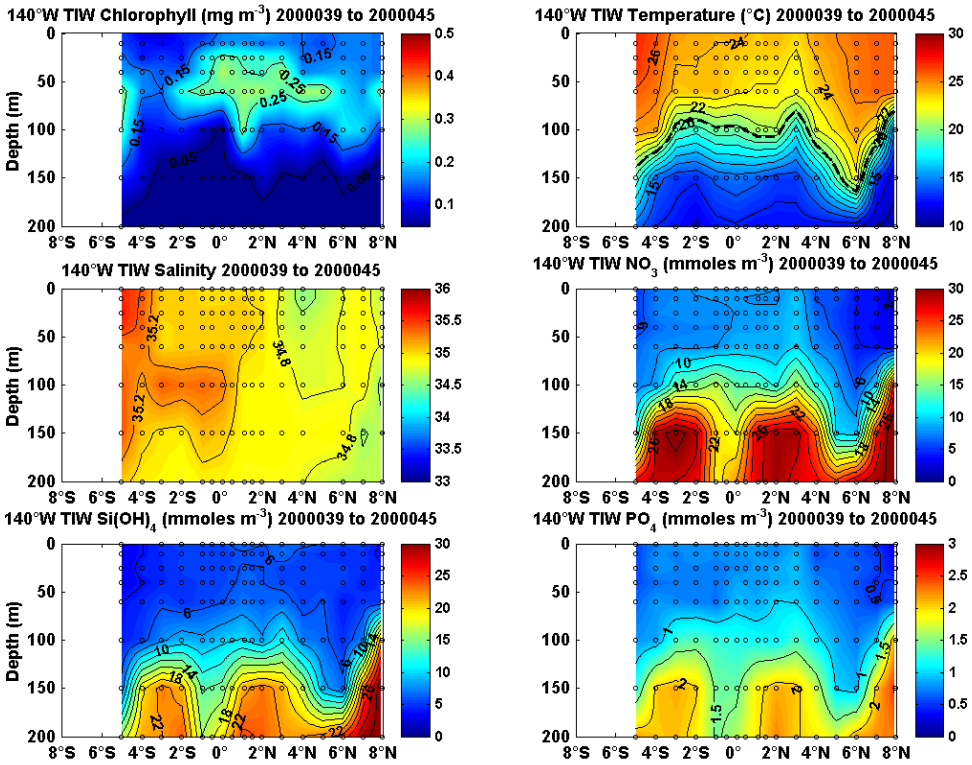

Figure 92: 140°W TAO cruise latitude/depth section for the February 2000 cruise identified crossing TIWs in both hemispheres.

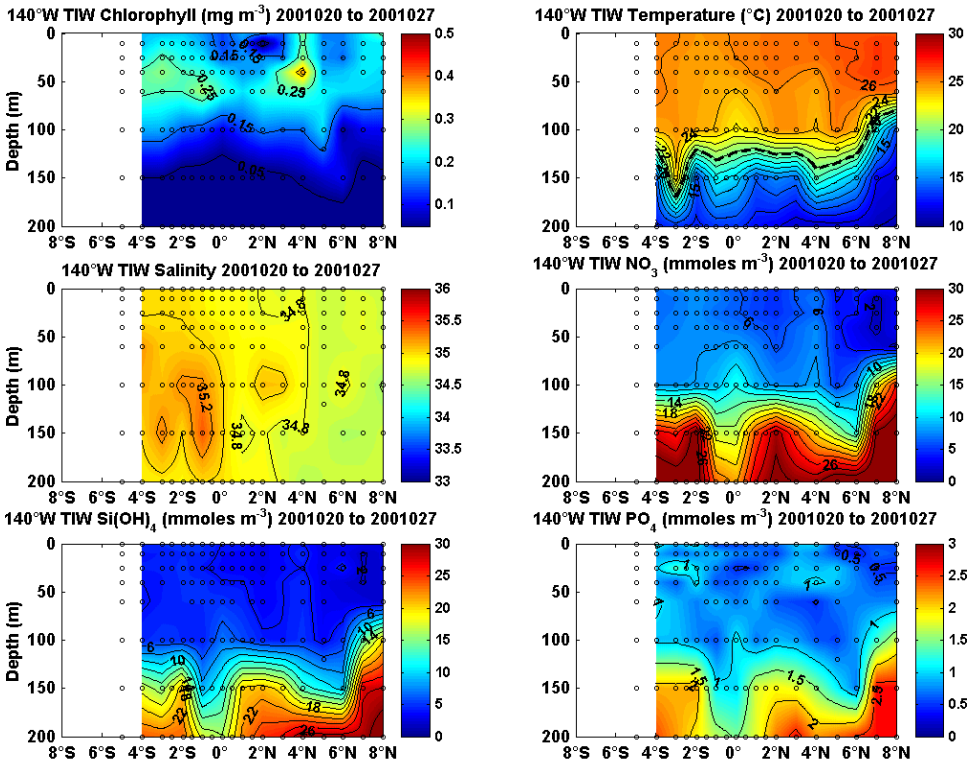

Figure 93: 140°W TAO cruise latitude/depth section for the January 2001 cruise identified crossing TIWs in both hemispheres.

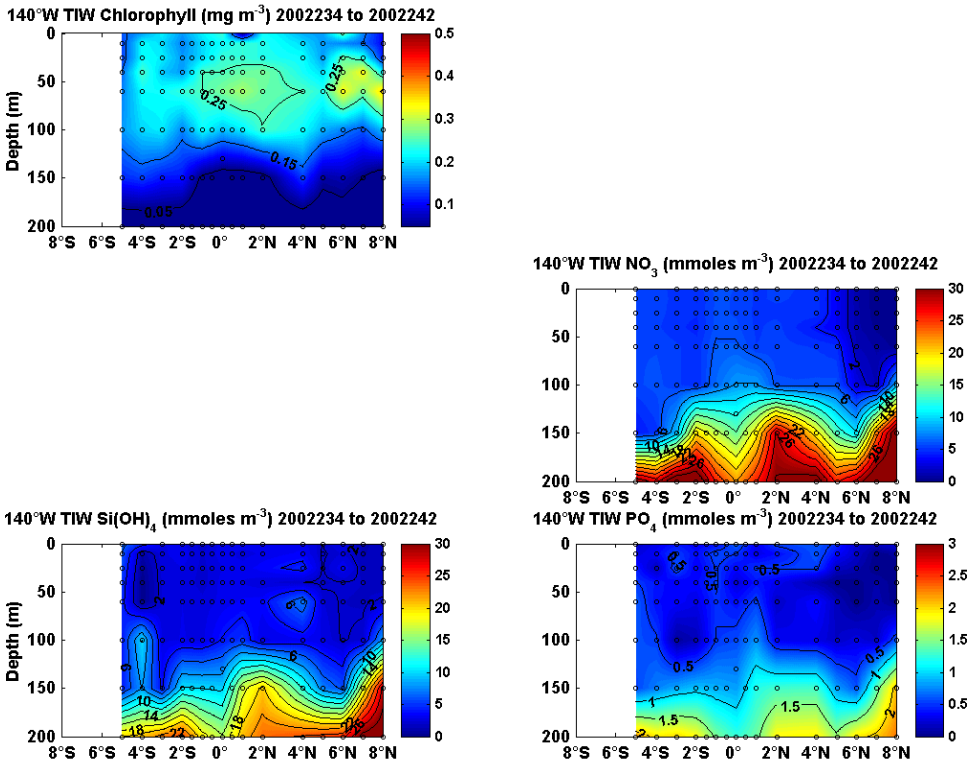

Figure 94: 140°W TAO cruise latitude/depth section for the August 2002 cruise identified crossing a TIW in the northern hemisphere.

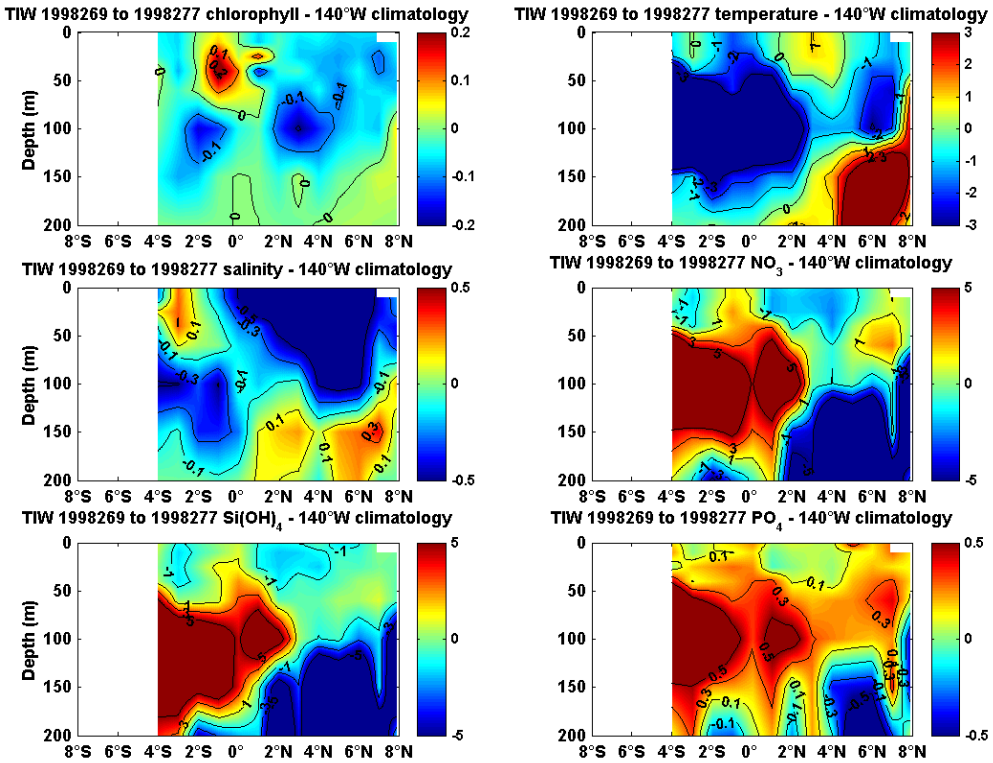

Figure 95: 140°W TAO cruise latitude/depth anomaly section for the September 1998 cruise identified crossing TIWs in both hemispheres.

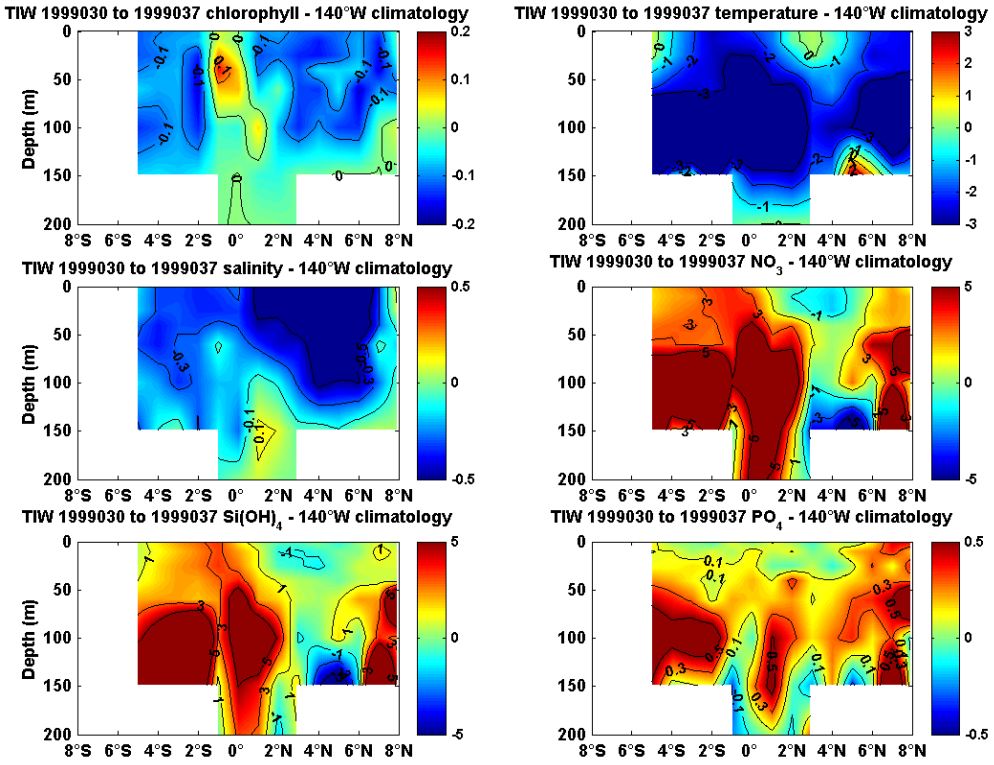

Figure 96: 140°W TAO cruise latitude/depth anomaly section for the January 1999 cruise identified crossing a TIW in the northern hemisphere.

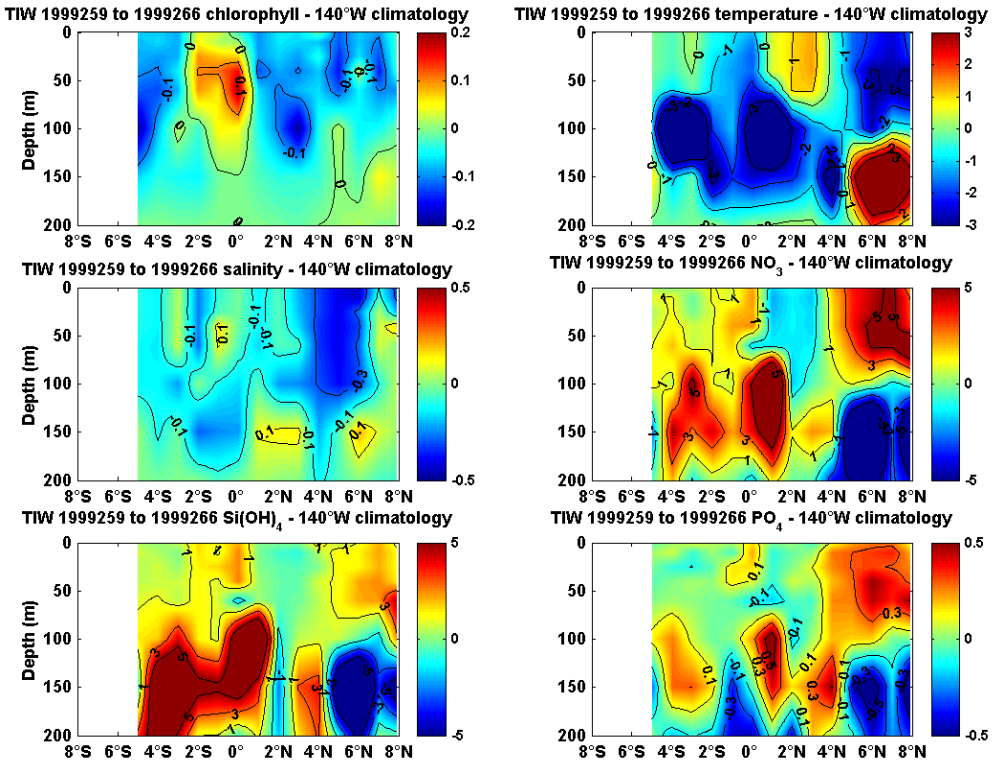

Figure 97: 140°W TAO cruise latitude/depth anomaly section for the September 1999 cruise identified crossing TIWs in both hemispheres.

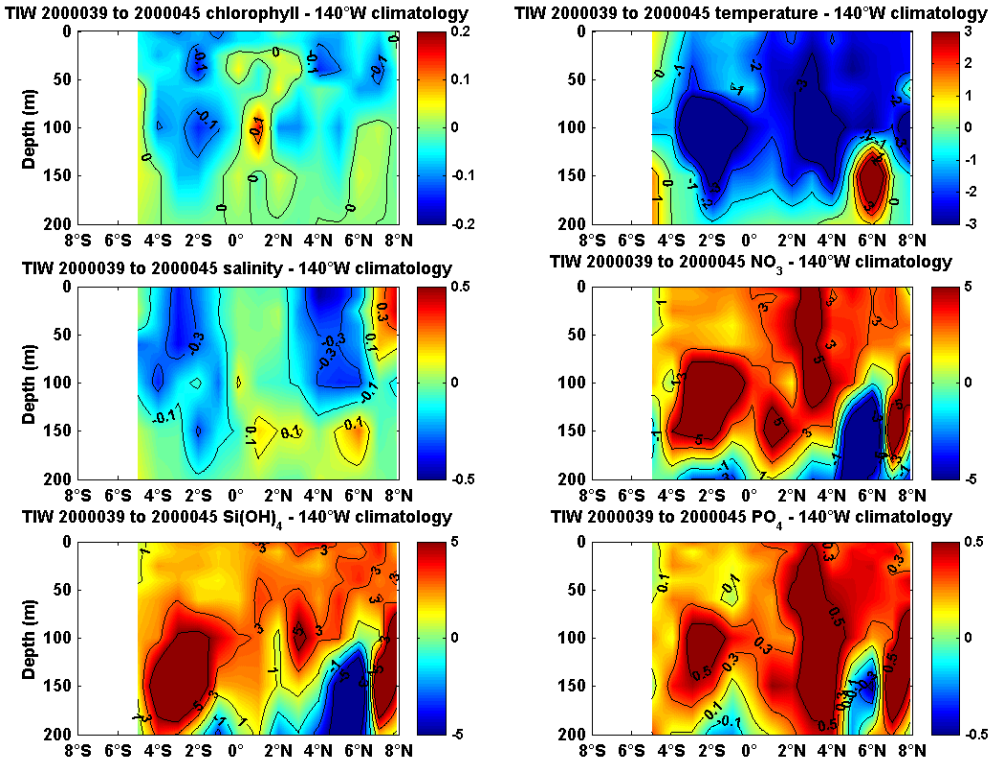

Figure 98: 140°W TAO cruise latitude/depth anomaly section for the February 2000 cruise identified crossing TIWs in both hemispheres.

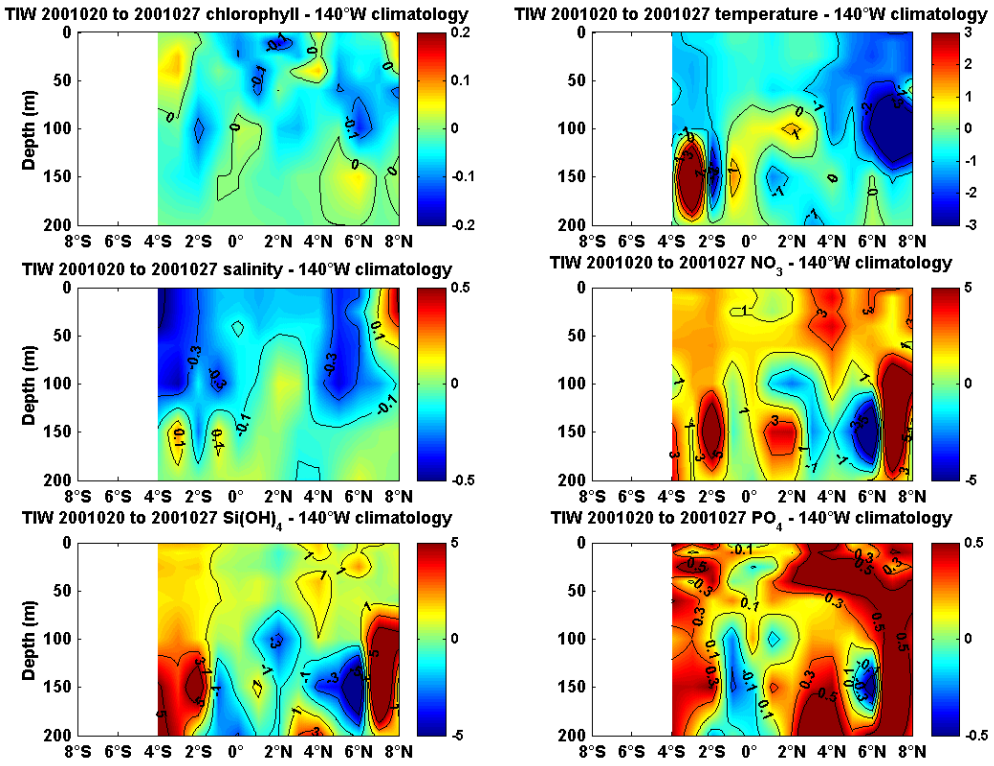

Figure 99: 140°W TAO cruise latitude/depth anomaly section for the January 2001 cruise identified crossing TIWs both hemispheres.

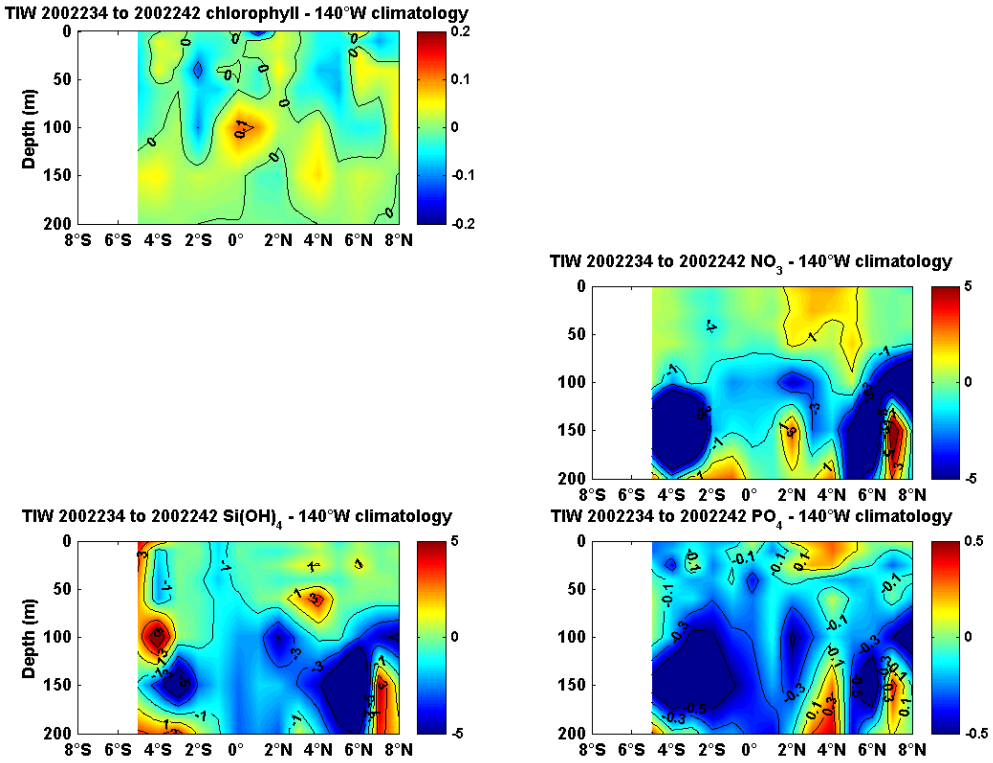

Figure 100: 140°W TAO cruise latitude/depth anomaly section for August 2002 cruise identified crossing a TIW in the northern hemisphere.

10.5 155°W TAO line

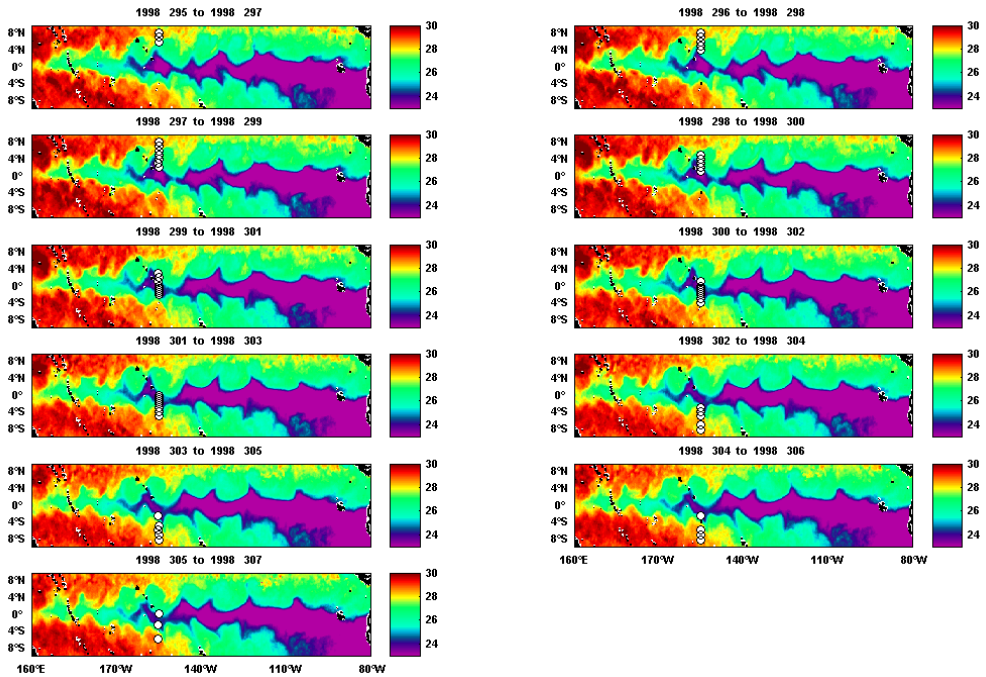

Figure 101: 155°W TAO cruise that crossed TIWs both hemispheres in October of 1998.

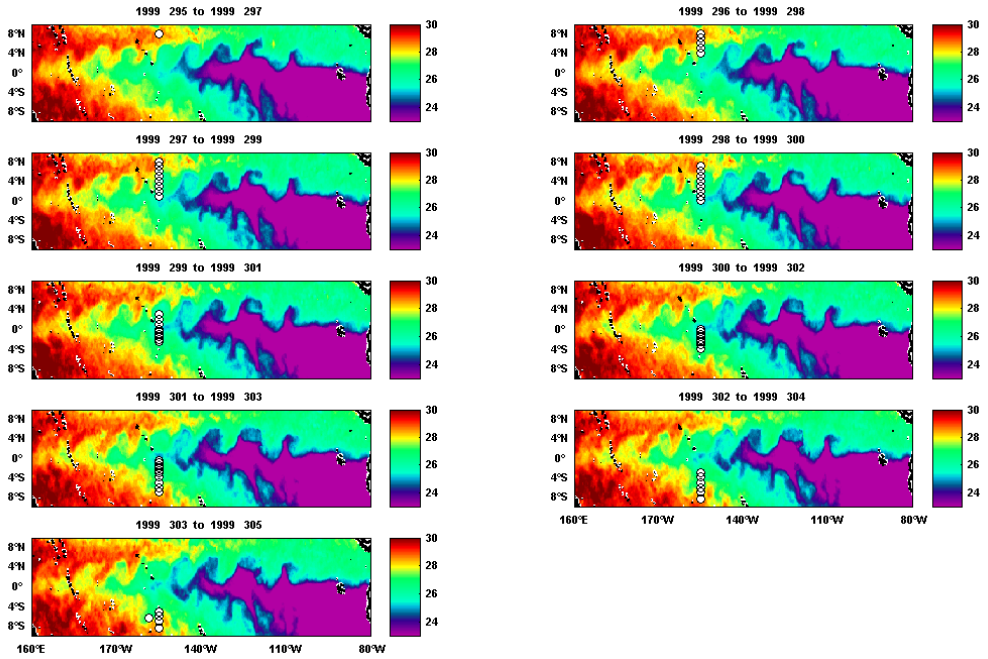

Figure 102: 155°W TAO cruise that crossed TIWs also in both hemispheres in October of 1999.

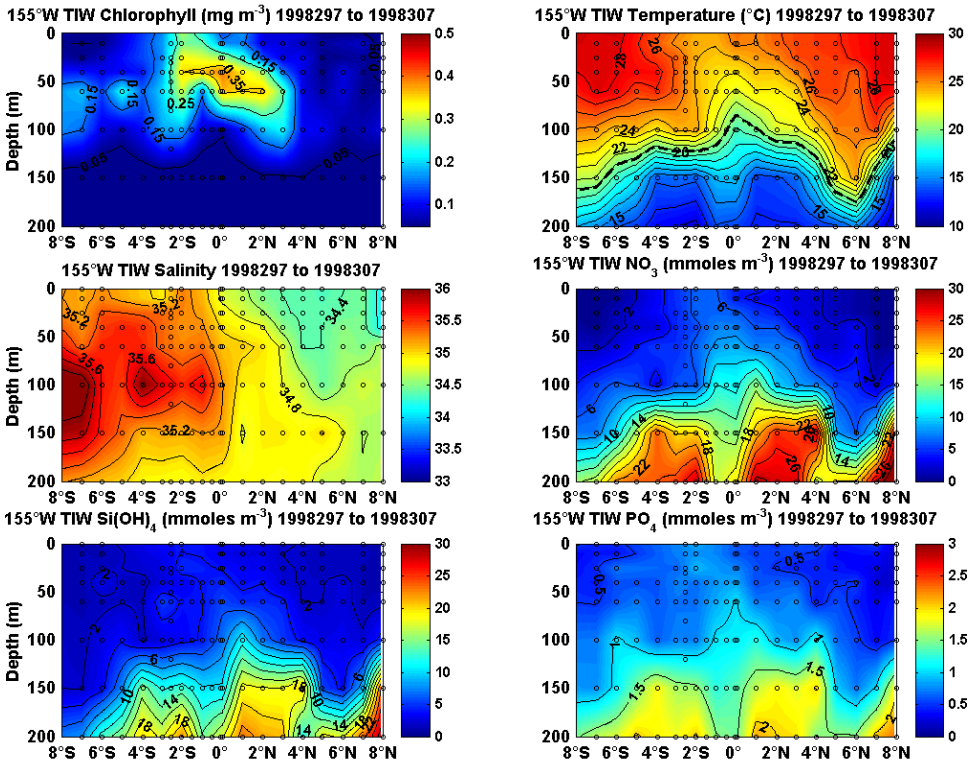

Figure 103: 155°W TAO cruise latitude/depth section for the October 1998 cruise identified crossing TIWs in both hemispheres.

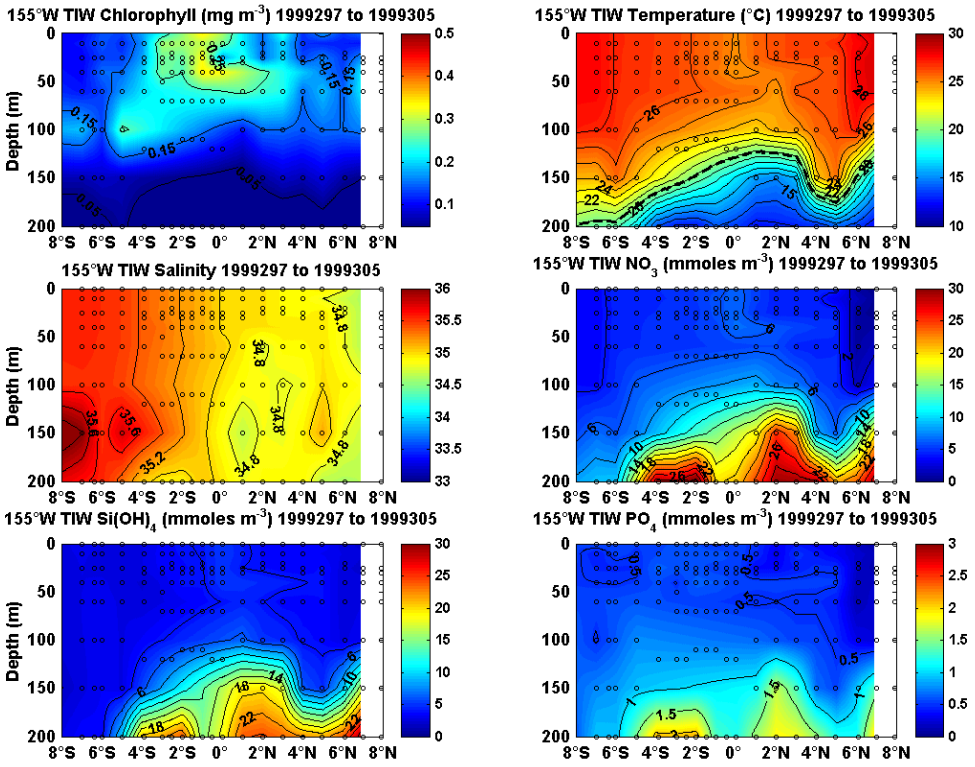

Figure 104: 155°W TAO cruise latitude/depth section for the October 1999 cruise identified crossing TIWs also in both hemispheres.

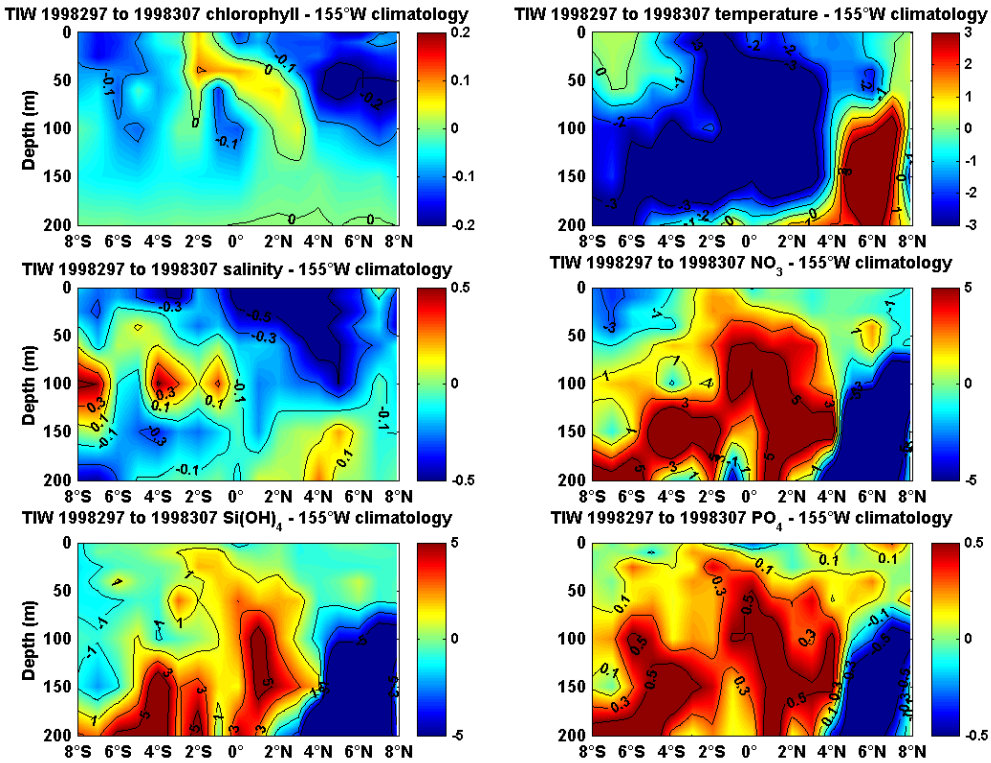

Figure 105: 155°W TAO cruise latitude/depth anomaly section for the October 1998 cruise identified crossing TIWs in both hemispheres.

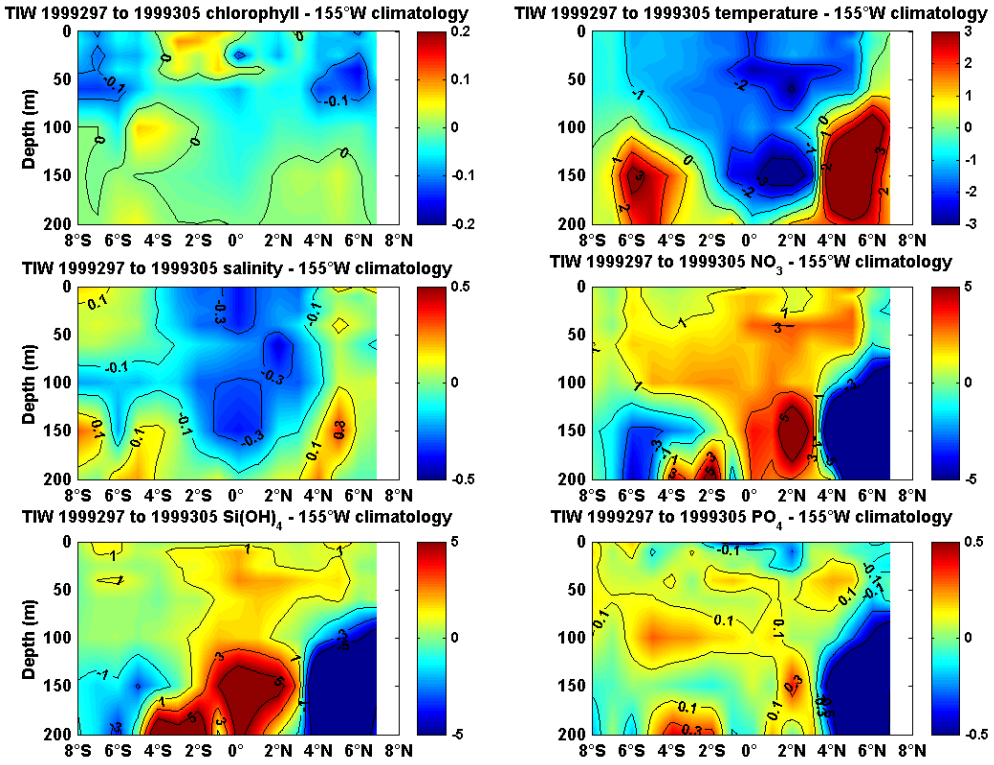

Figure 106: 155°W TAO cruise latitude/depth anomaly section for the October 1999 cruise identified crossing TIWs also in both hemispheres.

10.6 170°W TAO Line

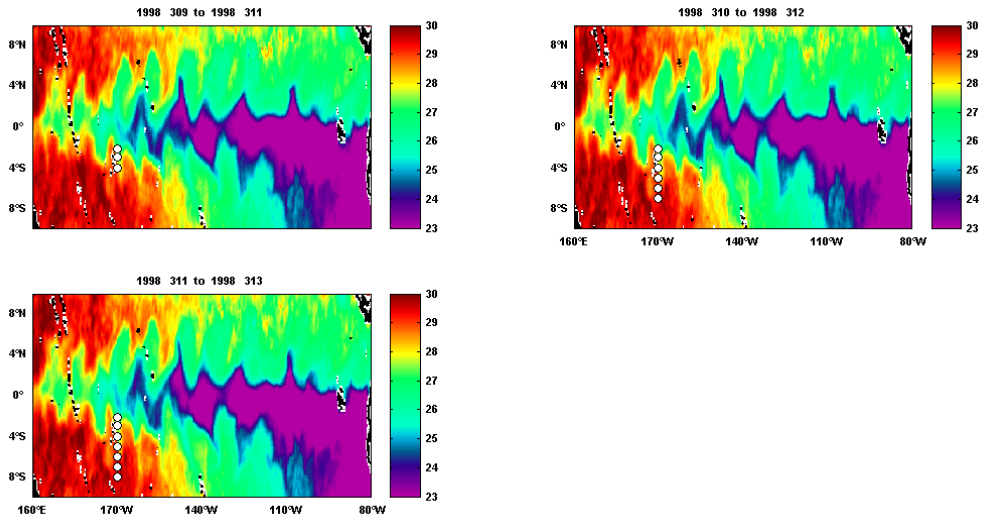

Figure 107: 170°W TAO cruise that crossed a TIW in the southern hemisphere in November of 1998.

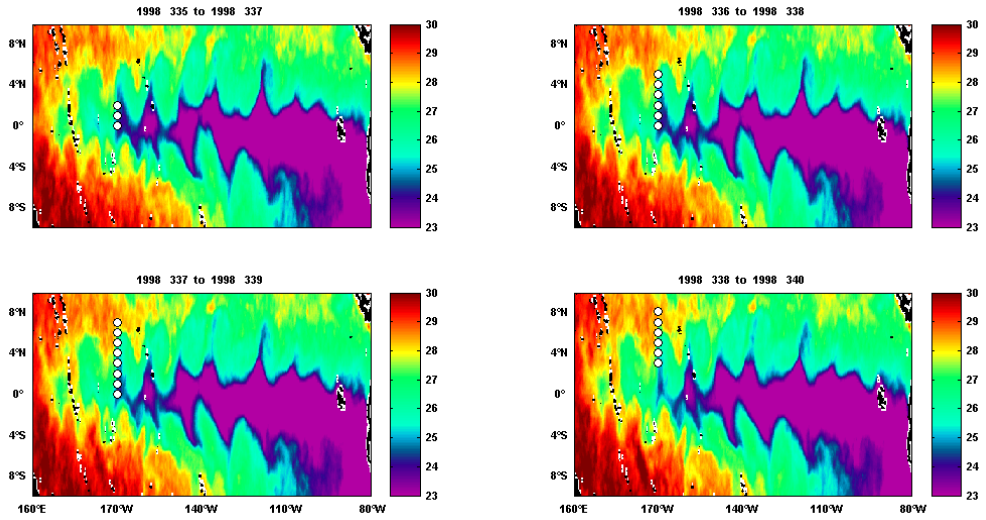

Figure 108: 170°W TAO cruise that crossed a TIW in the northern hemisphere in December of 1998.

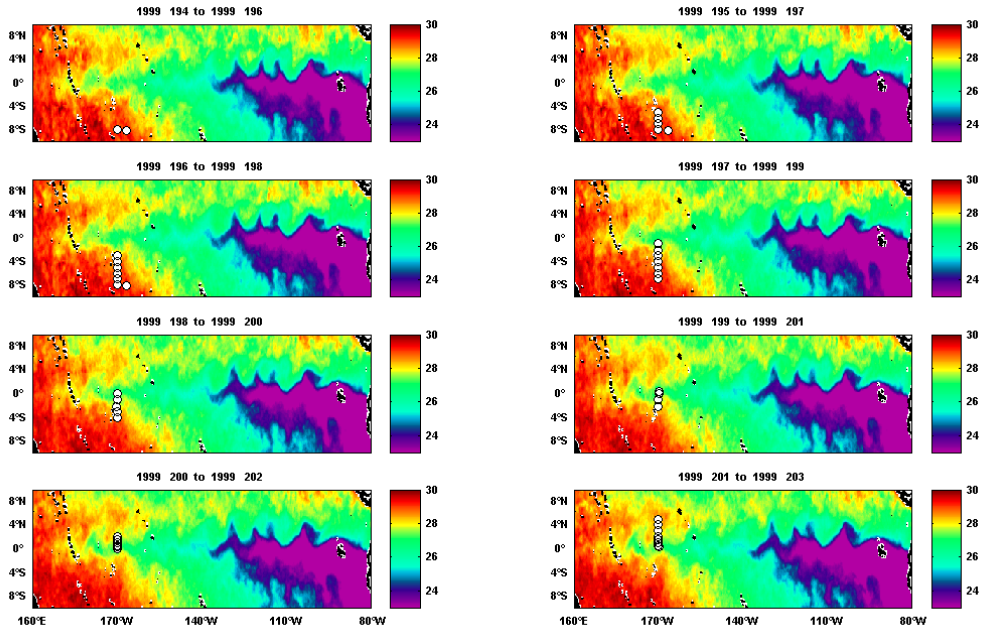

Figure 109: 170°W TAO cruise that crossed a TIW in the northern hemisphere in July of 1999.

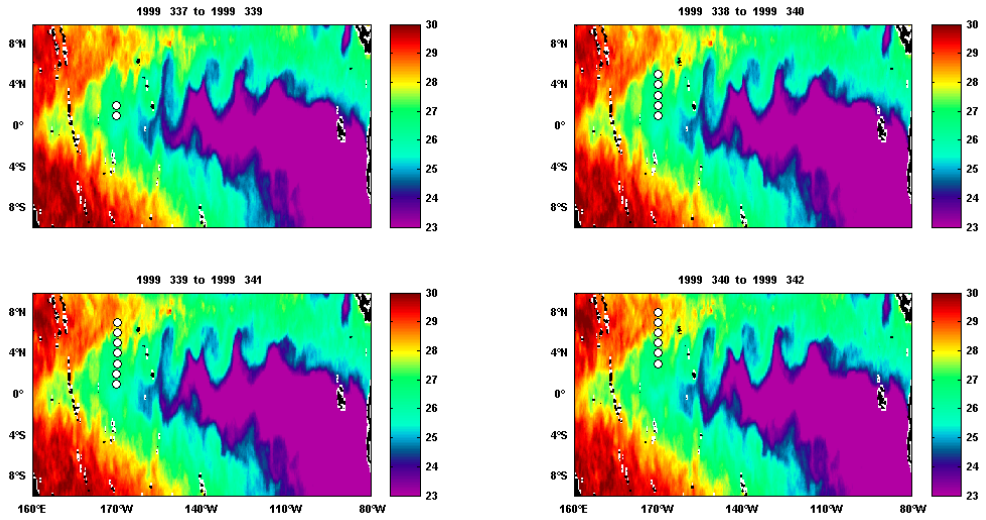

Figure 110: 170°W TAO cruise that crossed a TIW in the northern hemisphere in December of 1999.

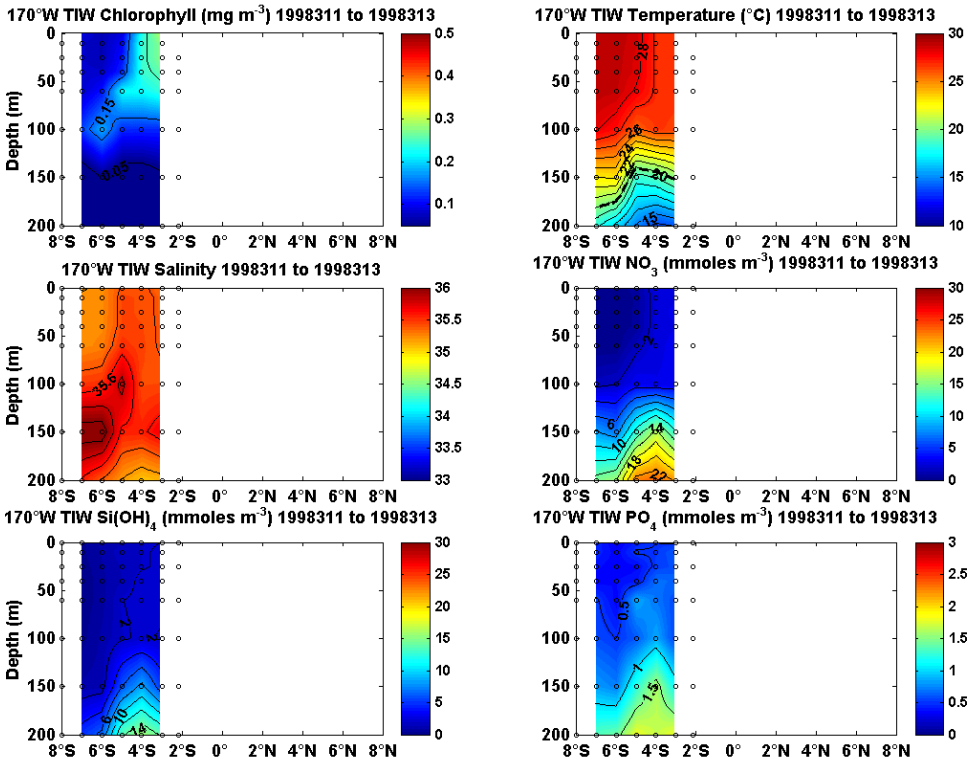

Figure 111: 170°W TAO cruise latitude/depth section for the November 1999 cruise identified crossing a TIW in the southern hemisphere.

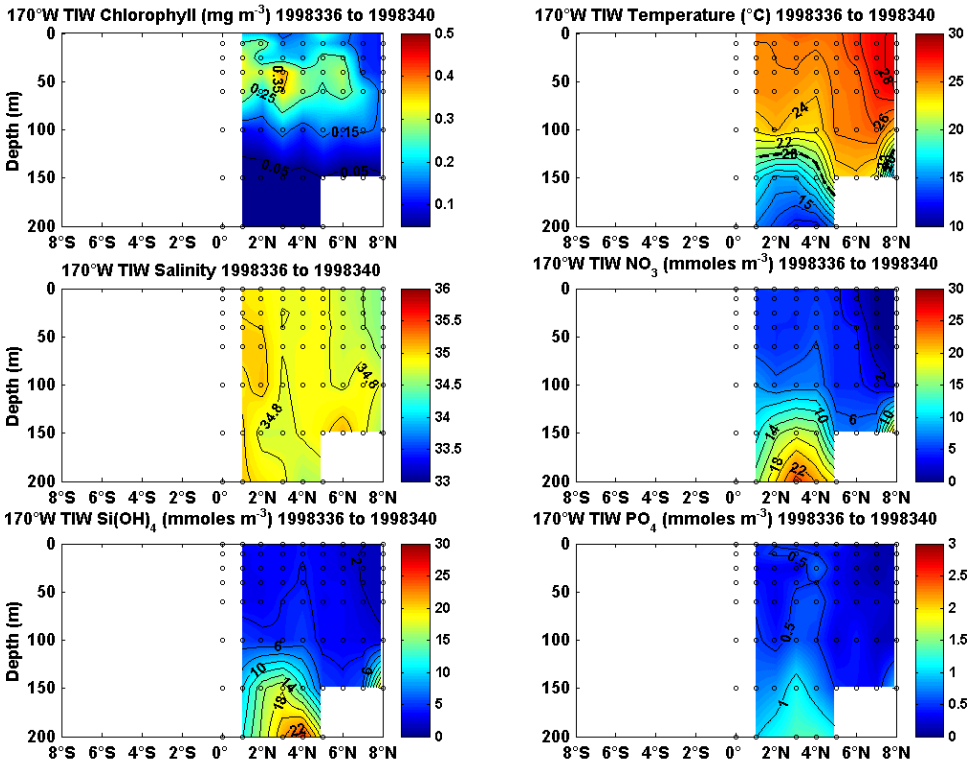

Figure 112: 170°W TAO cruise latitude/depth section for the December 1998 cruise identified crossing a TIW in the northern hemisphere.

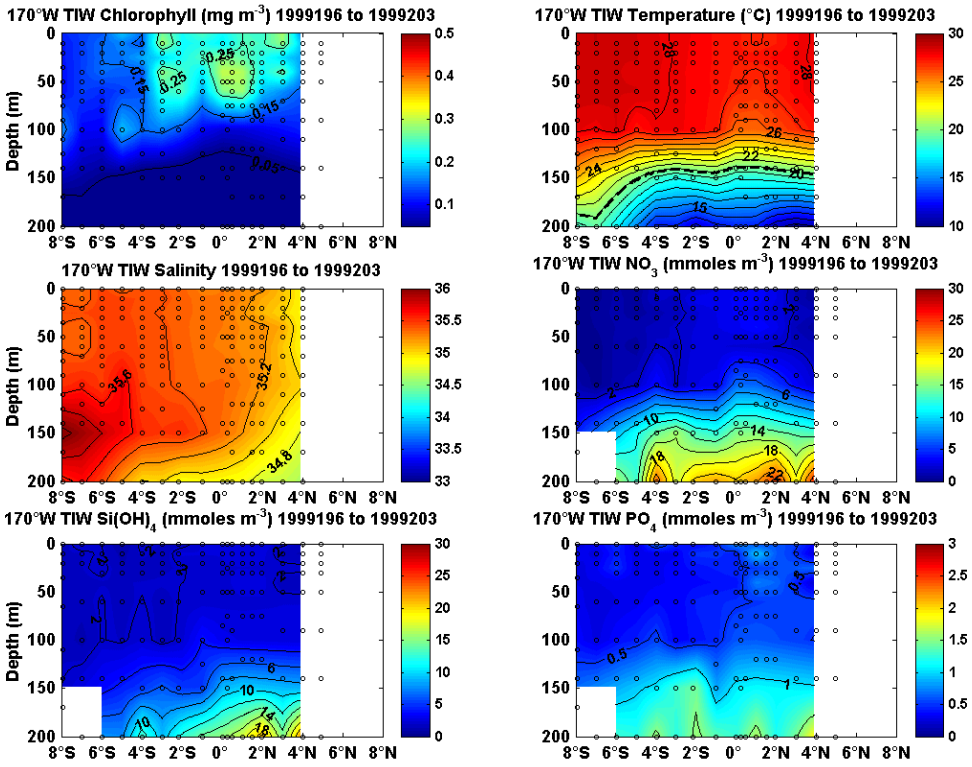

Figure 113: 170°W TAO cruise latitude/depth section for the July 1999 cruise identified crossing a TIW in the northern hemisphere.

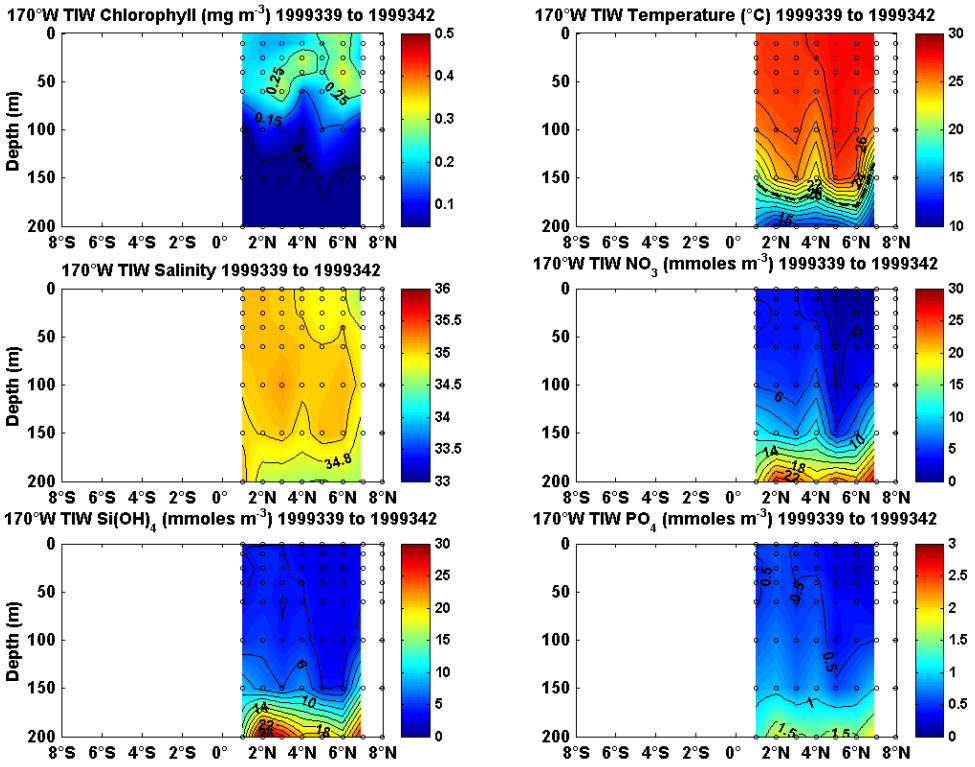

Figure 114: 170°W TAO cruise latitude/depth section for the December 1999 cruise identified crossing a TIW in the northern hemisphere.

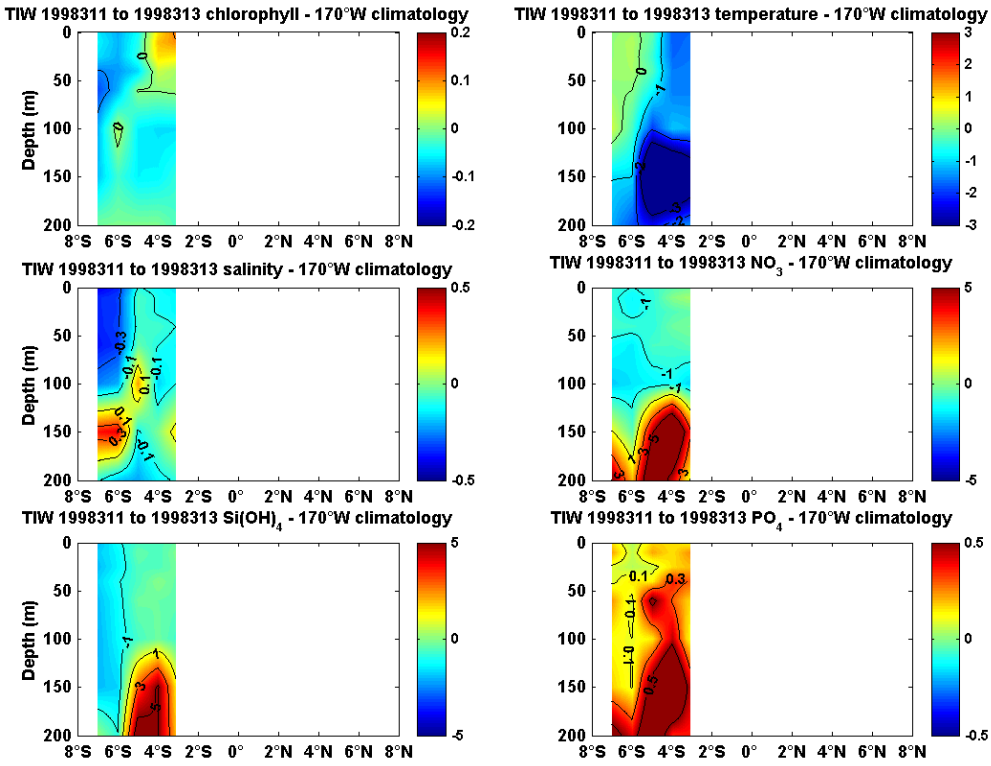

Figure 115: 170°W TAO cruise latitude/depth anomaly section for the November 1998 cruise identified crossing a TIW in the southern hemisphere.

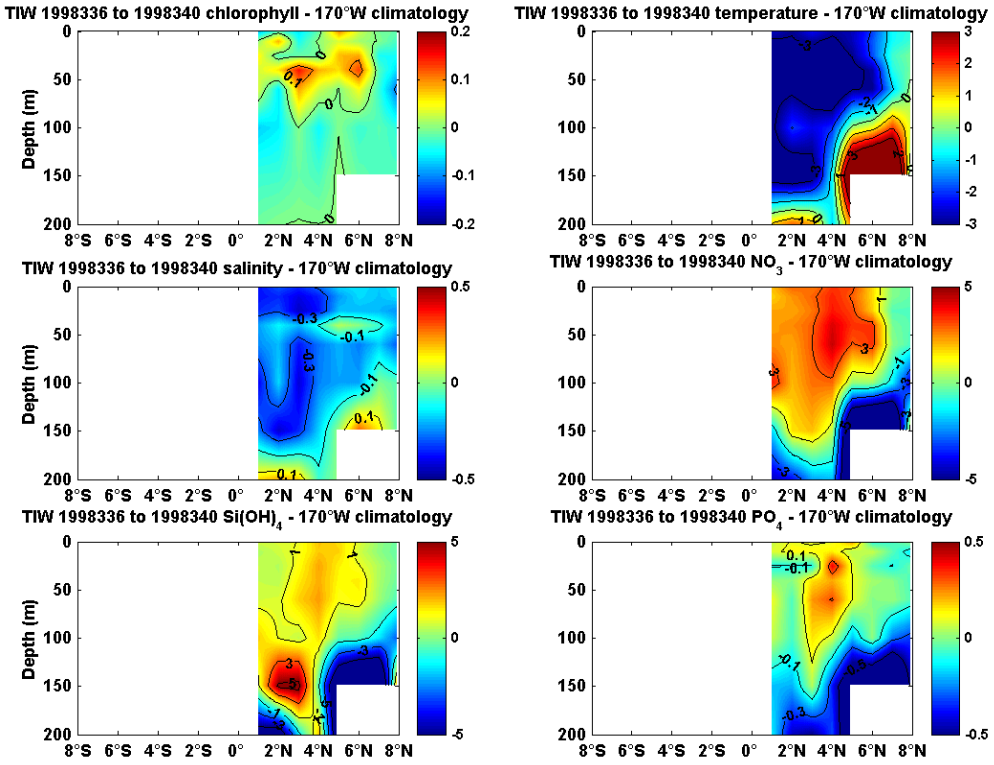

Figure 116: 170°W TAO cruise latitude/depth anomaly section for the December 1998 cruise identified crossing a TIW in the northern hemisphere.

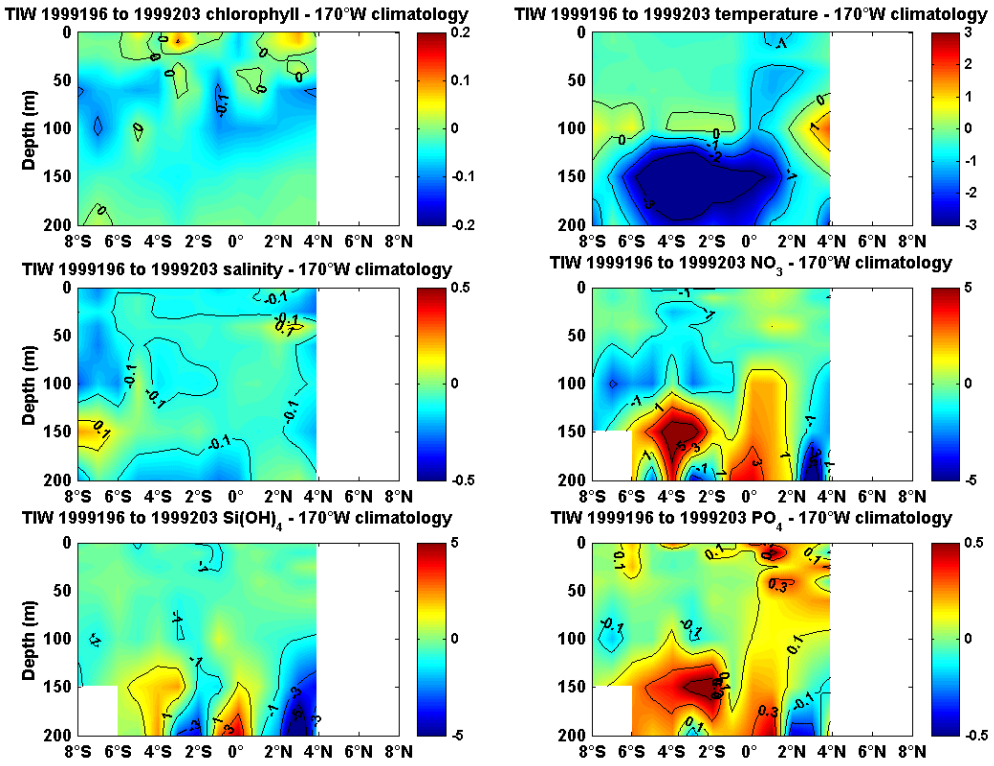

Figure 117: 170°W TAO cruise latitude/depth anomaly section for the July 1999 cruise identified crossing a TIW in the northern hemisphere.

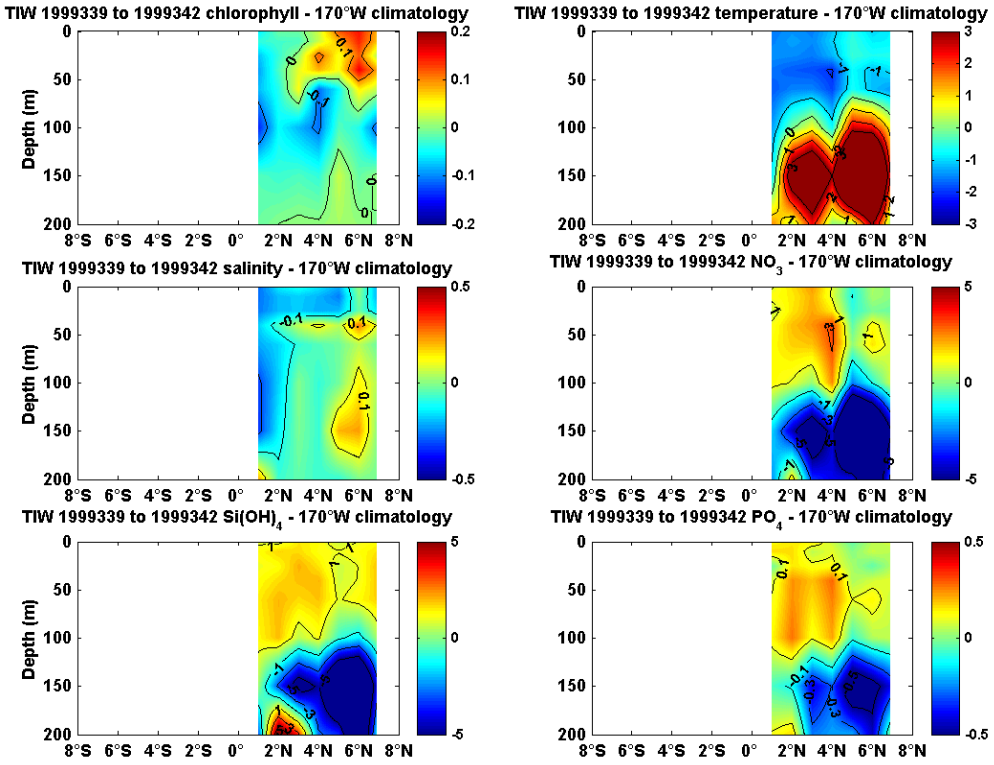

Figure 118: 170°W TAO cruise latitude/depth anomaly section for the December 1999 cruise identified crossing a TIW in the northern hemisphere.

10.7 180° TAO Line

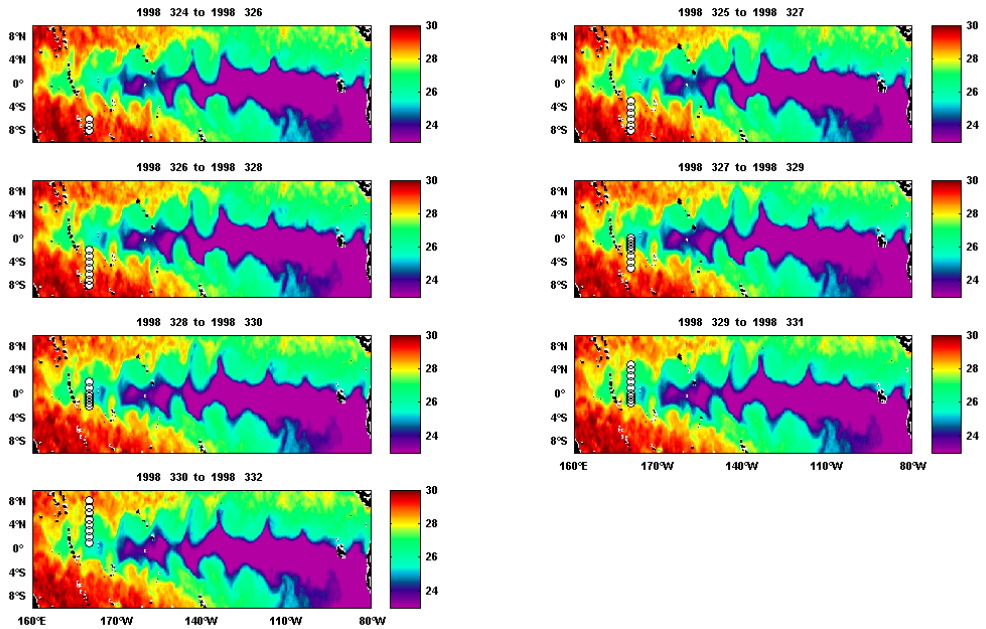

Figure 119: 180° TAO cruise that crossed TIWs in both hemispheres in November of 1998.

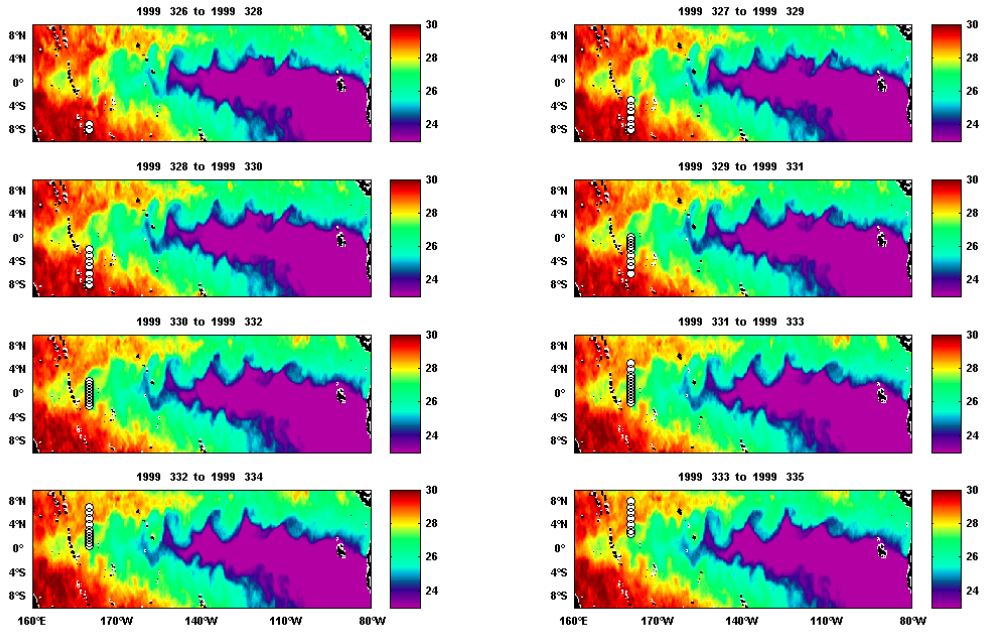

Figure 120: 180° TAO cruise that crossed TIWs also in both hemispheres in November of 1999.

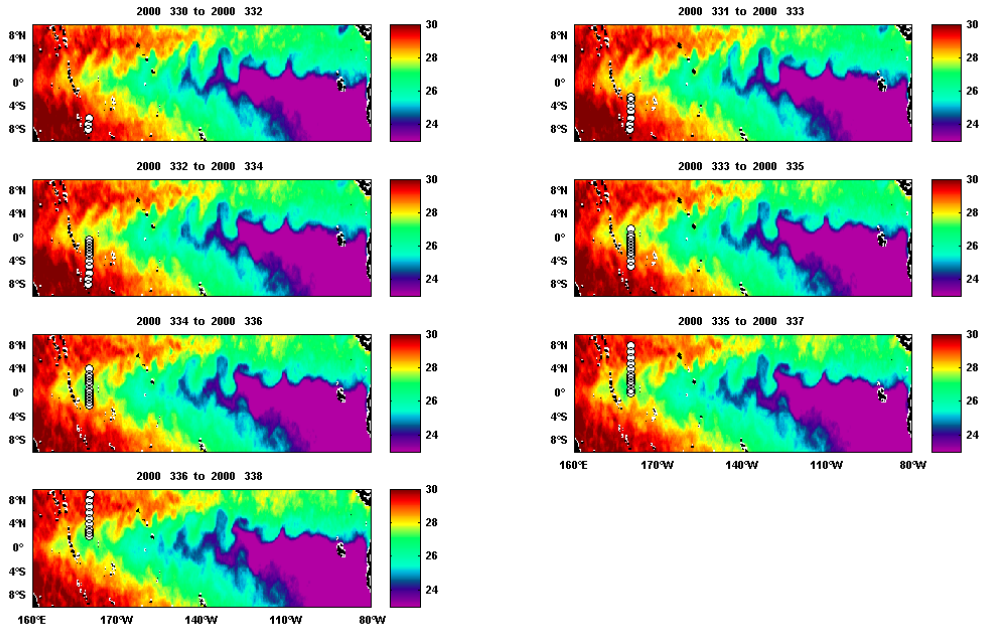

Figure 121: 180° TAO cruise that crossed a TIW in the northern hemisphere in November of 2000.

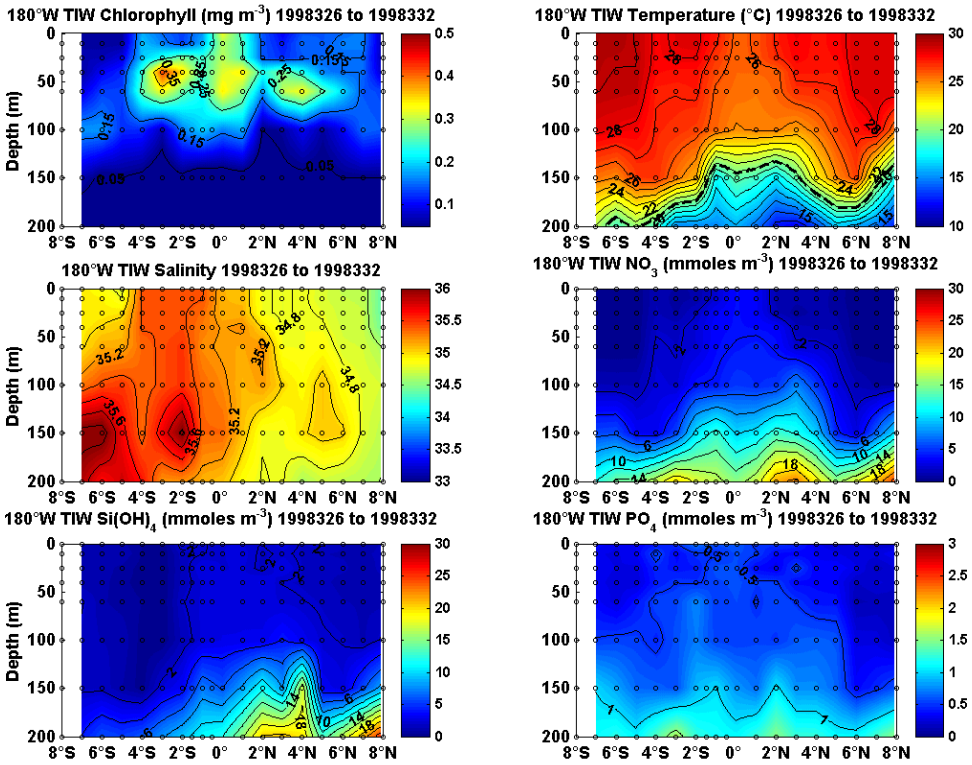

Figure 122: 180° TAO cruise latitude/depth section for the November 1998 cruise identified crossing TIWs in both hemispheres.

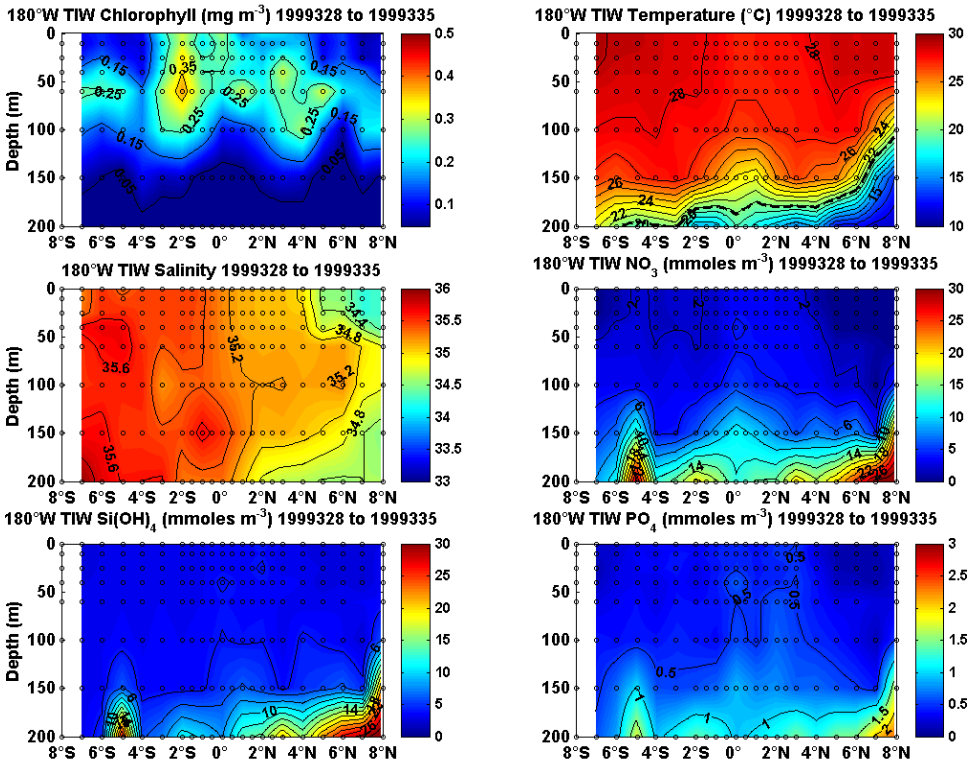

Figure 123: 180° TAO cruise latitude/depth section for the November 1999 cruise identified crossing TIWs in both hemispheres.

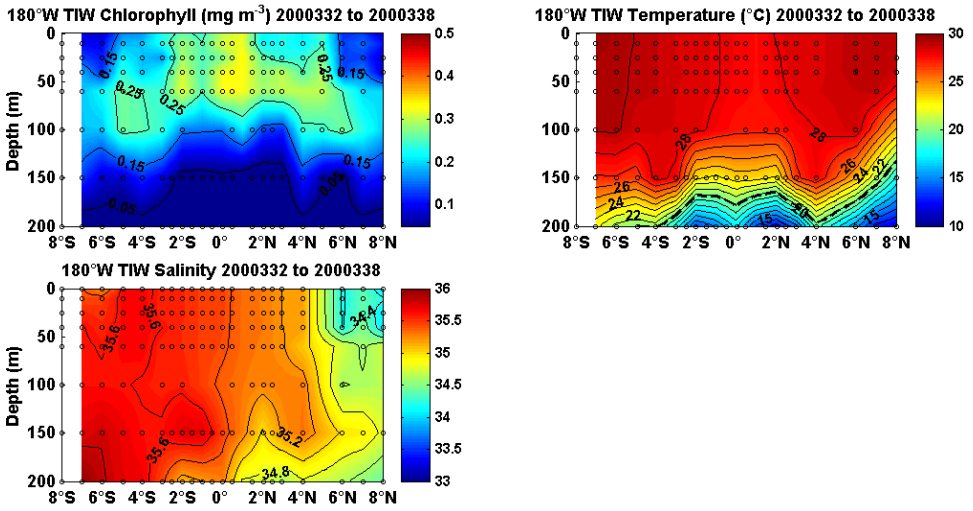

Figure 124: 180° TAO cruise latitude/depth section for the November 2000 cruise identified crossing a TIW in the northern hemisphere.

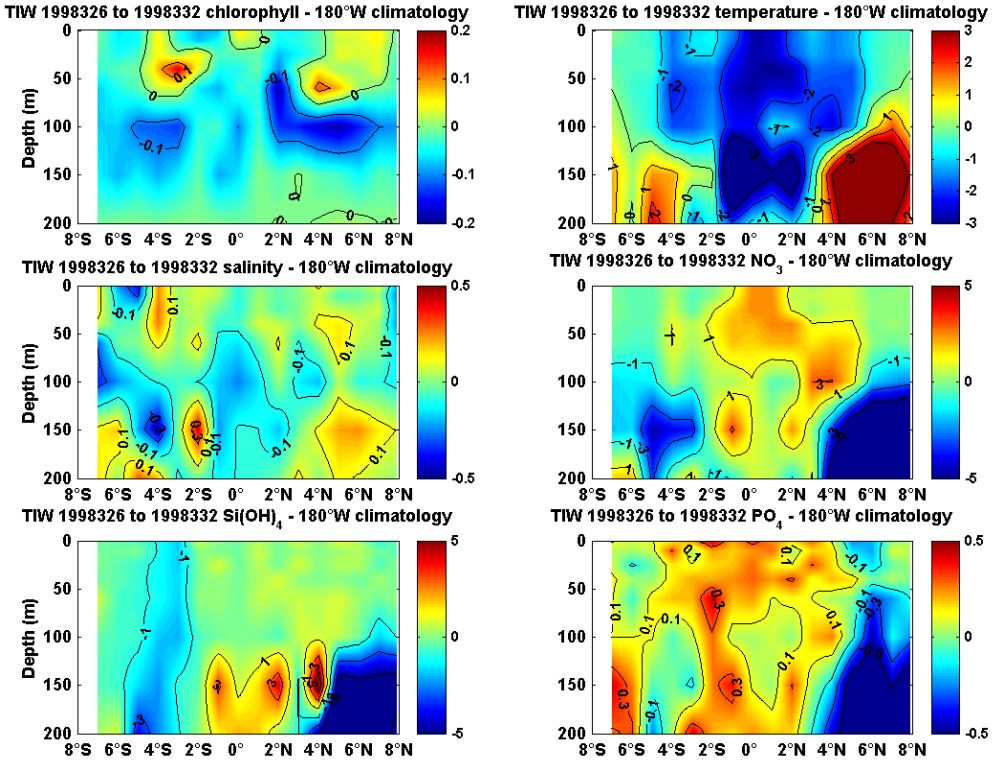

Figure 125: 180° TAO cruise latitude/depth anomaly section for the November 1998 cruise identified crossing TIWs in both hemispheres.

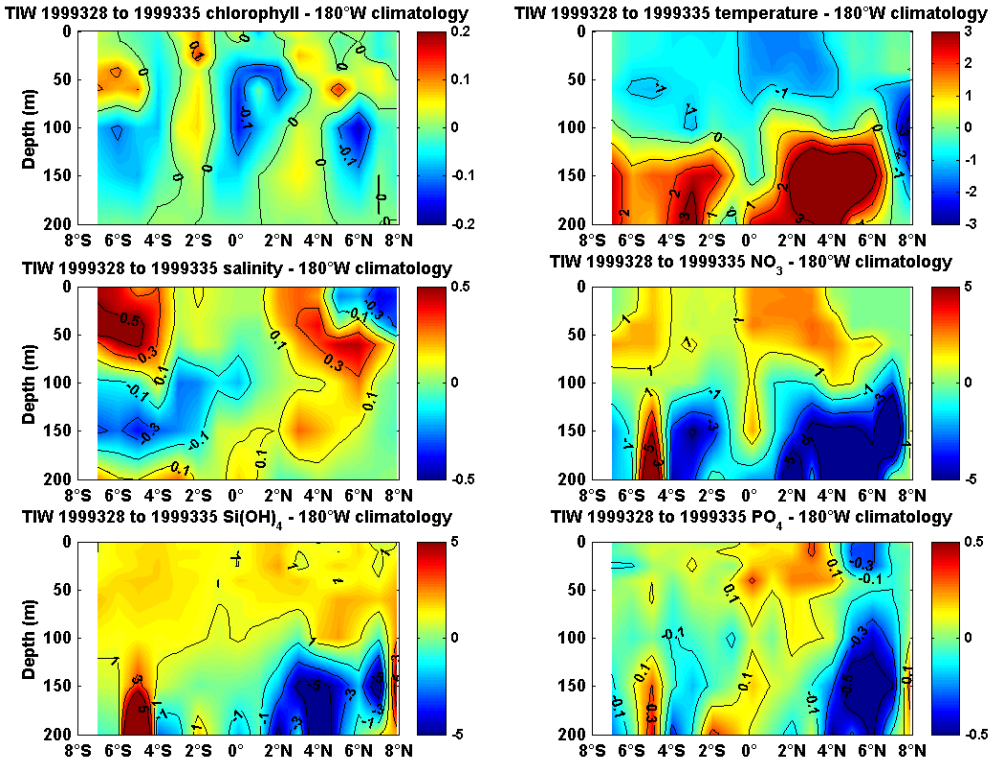

Figure 126: 180° TAO cruise latitude/depth anomaly section for the November 1999 cruise identified crossing TIWs also in both hemispheres.

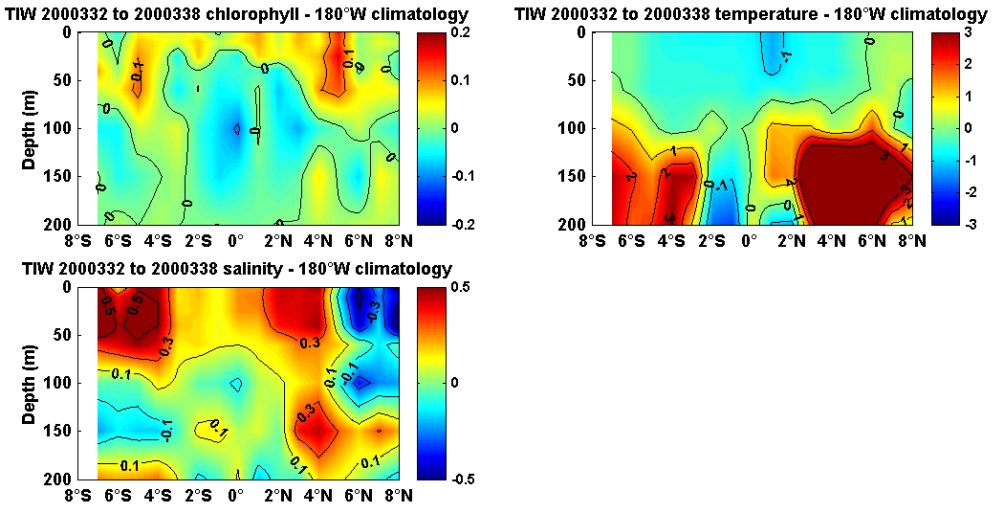

Figure 127: 180° TAO cruise latitude/depth anomaly section for the November 2000 cruise identified crossing a TIW in the northern hemisphere.